Scheme for constructing graphs associated with stabilizer quantum codes

Carlo Cafaro[1,2,3], Damian Markham[4], and Peter van Loock[2]

[1] Max-Planck Institute for the Science of Light, Gunther-Scharowsky-Str.1/Bau 26, 91058 Erlangen, Germany
[2] Institute of Physics, University of Mainz, Staudingerweg 7, 55128 Mainz, Germany
[3] Department of Mathematics, Clarkson University,
8 Clarkson Ave, Potsdam, NY 13699-5815, USA and
[4] CNRS LTCI, Département Informatique et Réseaux, Telecom ParisTech,
23 avenue d'Italie, CS 51327, 75214 Paris CEDEX 13, France

We propose a systematic scheme for the construction of graphs associated with binary stabilizer codes. The scheme is characterized by three main steps: first, the stabilizer code is realized as a codeword-stabilized (CWS) quantum code; second, the canonical form of the CWS code is uncovered; third, the input vertices are attached to the graphs. To check the effectiveness of the scheme, we discuss several graphical constructions of various useful stabilizer codes characterized by single and multi-qubit encoding operators. In particular, the error-correcting capabilities of such quantum codes are verified in graph-theoretic terms as originally advocated by Schlingemann and Werner. Finally, possible generalizations of our scheme for the graphical construction of both (stabilizer and nonadditive) nonbinary and continuous-variable quantum codes are briefly addressed.

PACS numbers: 03.67.-a (quantum information)

I. INTRODUCTION

Classical graphs [1–3] are closely related to quantum error correcting codes (QECCs) [4]. The first construction of QECCs based upon the use of graphs and finite Abelian groups appears in [5] and is provided by Schlingemann and Werner (SW-work). However, while in [5] it is proved that all codes constructed from graphs are stabilizer codes, it remains unclear how to embed the usual stabilizer code constructions into the proposed graphical scheme. Therefore, although necessary and sufficient conditions are uncovered for the graph such that the resulting code corrects a certain number of errors, the power of the graphical approach to quantum coding for stabilizer codes cannot be fully exploited unless this embedding issue is resolved. In [6], Schlingemann (S-work) clarifies this issue by establishing that each quantum stabilizer code (both binary and nonbinary) could be realized as a graph code and vice-versa. Almost at the same time, inspired by the work presented in [5], the equivalence of graphical quantum codes and stabilizer codes is also established by Grassl et al. in [7]. Despite being very important, the works in [6] and [7] still suffer from the fact that no systematic scheme for constructing a graph of a stabilizer code or the stabilizer of a graphical quantum code is available. The solution of this point is especially important in view of the fact that although any stabilizer code over a finite field has an equivalent representation as a graphical quantum code, unfortunately, this representation is not unique. Furthermore, the chosen representation does not reflect all the properties of the quantum code. A crucial step forward for the description and understanding of the interplay between properties of graphs and stabilizer codes is achieved thanks to the introduction of the notion of graph states (and cluster states, [8]) into the graphical construction of QECCs as presented by Hein et al. in [9]. In this last work, it is shown how graph states are in correspondence to graphs and special focus is devoted to the question of how the entanglement in a graph state is related to the topology of its underlying graph. In [9], it is also pointed out that codewords of various QECCs could be regarded as special instances of graph states and criteria for the equivalence of graph states under local unitary transformations entirely on the level of the underlying graphs are presented. Similar findings are uncovered by Van den Nest et al. in [10] (VdN-work) where a constructive scheme showing that each stabilizer state is equivalent to a graph state under local Clifford operations is discussed. Thus, the main finding of Schlingemann in [6] is re-obtained in [10] for the special case of binary quantum states. Most importantly, in [10], an algorithmic procedure for transforming any binary quantum stabilizer code into a graph code appears. However, to the best of our knowledge, nobody has fully and jointly exploited the results provided by either Schlingemann in [6] or Van den Nest et al. in [10] to provide a more systematic procedure for constructing graphs associated with arbitrary binary stabilizer codes with special emphasis on the verification of their error-correcting capabilities. We emphasize that this last point constitutes one of the original motivations for introducing the concept of a graph into quantum error correction (QEC) [5].

The CWS quantum code formalism presents a unifying approach for constructing both additive and nonadditive QECCs, for both binary [11] (CWS-work) and nonbinary states [12]. Furthermore, every CWS code in its canonical form can be fully characterized by a graph and a classical code. In particular, any CWS code is locally Clifford equivalent to a CWS code with a graph state stabilizer and word operators consistent only of Zs [11]. Since the notion of stabilizer codes, graph codes and graph states can be recast into the CWS formalism, it seems natural to investigate the graphical depiction of stabilizer codes as originally thought by Schlingemann and Werner within this

generalized framework where stabilizer codes are realized as CWS codes. Proceeding along this line of investigation, we shall observe that the notion of graph state in QEC as presented in [9] emerges naturally. Furthermore, the algorithmic procedure for transforming any (binary) quantum stabilizer code into a graph code advocated in [10] can be exploited and jointly used with the results in [6] where the notions of both coincidence and adjacency matrices of a classical graphs are introduced. For the sake of completeness, we point out that the CWS formalism has been already employed into the literature for the graphical construction of both binary [13] and nonbinary [14] (both additive/stabilizer and nonadditive) QECCs. For instance in [13], regarding stabilizer codes as CWS codes and employing a graphical approach to quantum coding, a classification of all the extremal stabilizer codes up to eight qubits and the construction of the optimal ((10, 24, 3)) code together with a family of 1-error detecting nonadditive codes with the highest encoding rate so far is presented. With a leap of imagination, in [13] it is also envisioned a graphical quantum computation based directly on graphical objects. Indeed, this vision became recently more realistic in the work of Beigi et *al.* [15]. Here, being essentially within the CWS framework, a systematic method for constructing both binary and nonbinary concatenated quantum codes based on graph concatenation is developed. Graphs representing the inner and the outer codes are concatenated via a simple graph operation (the so-called generalized local complementation, [15]). Despite their very illuminating findings, in [15] it is emphasized that the elusive role played by graphs in QEC is still not well-understood. In neither [13] nor [15], the Authors are concerned with the joint exploitation of the results provided by either Van den Nest et *al.* in [10] (algorithmic procedure for transforming any binary quantum stabilizer code into a graph code) or Schlingemann in [6] (use of both the coincidence and adjacency matrices of a classical graphs in QEC) in order to provide a more systematic procedure for constructing graphs associated with arbitrary binary stabilizer codes with special emphasis on the verification of their error correcting capabilities which, as pointed out earlier, constituted a major driving motivation for the introduction of graphs in QEC [5]. Instead, we aim here at investigating such unexplored topics and hope to further advance our understanding of the role played by classical graphs in quantum coding.

In this article, we propose a systematic scheme for the construction of graphs with both input and output vertices associated with arbitrary binary stabilizer codes. The scheme is characterized by three main steps: first, the stabilizer code is realized as a CWS quantum code; second, the canonical form of the CWS code is uncovered; third, the input vertices are attached to the graphs with only output vertices. To check the effectiveness of the scheme, we discuss several graphical constructions of various useful stabilizer codes characterized by single and multi-qubit encoding operators. In particular, the error-correcting capabilities of such quantum codes are verified in graph-theoretic terms as originally advocated by Schlingemann and Werner. Finally, possible generalizations of our scheme for the graphical construction of both (stabilizer and nonadditive) nonbinary and continuous variables quantum codes is briefly addressed.

The layout of the article is as follows. In Section II, we introduce some preliminary material. First, the notions of graphs, graph states and graph codes are presented. Second, local Clifford transformations on graph states and local complementations on graphs are briefly described. Third, the CWS quantum codes formalism is briefly explained. In Section III, we re-examine some basic ingredients of the Schlingemann-Werner work (SW-work, [5]), the Schlingemann work (S-work, [6]) and, finally, the Van den Nest et al. work (VdN-work, [10]). We focus on those aspects of these works that are especially important for our systematic scheme. In this Section IV, we formally describe our scheme and, for the sake of clarity, apply it to the graphical construction of the Leung et al. four-qubit quantum code for the error correction of single amplitude damping errors [16]. Finally, concluding remarks and a brief discussion on possible extensions of our schematic graphical construction to both (stabilizer and nonadditive) nonbinary and continuous variables quantum codes appear in Section V.

Several explicit constructions of graphs for various stabilizer codes characterized by either single or multi-qubit encoding operators are worked out in the Appendices. Specifically, we discuss the graphical construction of the following quantum codes: the three-qubit repetition code, the perfect 1-erasure correcting four-qubit code, the perfect 1-error correcting five-qubit code, 1-error correcting six-qubit quantum degenerate codes, the CSS seven-qubit stabilizer code, the Shor nine-qubit stabilizer code, the Gottesman 2-error correcting eleven-qubit code, [[4, 2, 2]] stabilizer codes, and, finally, the Gottesman [[8, 3, 3]] stabilizer code.

II. FROM GRAPH THEORY TO THE CWS FORMALISM

In this section, we present some preliminary material. First, the notions of graphs, graph states and graph codes are introduced. Second, local Clifford transformations on graph states and local complementations on graphs are briefly presented. Third, the CWS quantum codes formalism is briefly discussed.

A. Graphs, graph states, and graph codes

A graph $G = G(V, E)$ is characterized by a set V of n vertices and a set of edges E specified by the adjacency matrix Γ [1–3]. This matrix is a $n \times n$ symmetric matrix with vanishing diagonal elements and $\Gamma_{ij} = 1$ if vertices i, j are connected and $\Gamma_{ij} = 0$ otherwise. The neighborhood of a vertex i is the set of all vertices $v \in V$ that are connected to i and is defined by $N_i \overset{\text{def}}{=} \{v \in V : \Gamma_{iv} = 1\}$. When the vertices a, $b \in V$ are the end points of an edge, they are referred to as being adjacent. An $\{a, c\}$ path is an ordered list of vertices $a = a_1, a_2,..., a_{n-1}, a_n = c$, such that for all i, a_i and a_{i+1} are adjacent. A connected graph is a graph that has an $\{a, c\}$ path for any two a, $c \in V$. Otherwise it is referred to as disconnected. A vertex represents a physical system, e.g., a qubit (two-dimensional Hilbert space), qudit (d-dimensional Hilbert space), or continuous variables (CV) (continuous Hilbert space). An edge between two vertices represents the physical interaction between the corresponding systems. In what follows, we shall take into consideration simple graphs only. These are graphs that contain neither loops (edges connecting vertices with itself) nor multiple edges. Furthermore, for the time being, we do not make a distinction between different types of vertices. However, later on we will assign some vertices as inputs, and some as outputs.

Graph states [8] are multipartite entangled states that play a key-role in graphical constructions of QECCs codes and, in addition, are very important in quantum secret sharing [17] which is, to a certain extent, equivalent to error correction [18]. For a very recent experimental demonstration of a graph state quantum error correcting code, we refer to [19].

Consider a system of n qubits that are labeled by those n vertices in V and denote by I^i, X^i, Y^i, Z^i (or, equivalently, $X^i \equiv \sigma_x^i$, $Y^i \equiv \sigma_y^i$, $Z^i \equiv \sigma_z^i$) the identity matrix and the three Pauli operators acting on the qubit $i \in V$. The n-qubit graph state $|G\rangle$ associated with the graph G is defined by [9],

$$|G\rangle \overset{\text{def}}{=} \prod_{\Gamma_{ij}=1} \mathcal{U}_{ij} |+\rangle_x^V = \frac{1}{\sqrt{2^n}} \sum_{\vec{\mu}=\mathbf{0}}^{\mathbf{1}} (-1)^{\frac{1}{2}\vec{\mu}\cdot\Gamma\cdot\vec{\mu}} |\vec{\mu}\rangle_z, \tag{1}$$

where $|+\rangle_x^V$ is the joint $+1$ eigenstate of X^i with $i \in V$, $\mathcal{U}_{ij}$ is the controlled phase gate between qubits i and j given by,

$$\mathcal{U}_{ij} \overset{\text{def}}{=} \frac{1}{2} [I + Z_i + Z_j - Z_i Z_j], \tag{2}$$

and $|\vec{\mu}\rangle_z$ is the joint eigenstate of Z^i with $i \in V$ and $(-1)^{\mu_i}$ as eigenvalues. The graph-state basis of the n-qubit Hilbert space $\mathcal{H}_2^n$ is given by $\left\{ |G^C\rangle \overset{\text{def}}{=} Z^C |G\rangle \right\}$ where C is an element of the set of all the subsets of V denoted by 2^V. A collection of subsets $\{C_1,..., C_K\}$ specifies a K-dimensional subspace of $\mathcal{H}_2^n$ that is spanned by the graph-state basis $\left\{ |G^{C_i}\rangle \right\}$ with $i = 1,..., K$. The graph state $|G\rangle$ is the unique joint $+1$ eigenstate of the n-vertex stabilizers $\mathcal{G}_i$ with $i \in V$ defined as [9],

$$\mathcal{G}_i \overset{\text{def}}{=} X^i Z^{N_i} \overset{\text{def}}{=} X^i \prod_{j \in N_i} Z^j. \tag{3}$$

A graph code, first introduced into the realm of QEC in [5] and later reformulated into the graph state formalism in [9], is defined to be one in which a graph G is given and the codespace (or, coding space) is spanned by a subset of the graph state basis. These states are regarded as codewords, although we recall that what is significant from the point of view of the QEC properties is the subspace they span, not the codewords themselves [20].

B. Local Clifford transformations and local complementations

1. Transformations on quantum states

The Clifford group $\mathcal{C}_n$ is the normalizer of the Pauli group $\mathcal{P}_{\mathcal{H}_2^n}$ in $\mathcal{U}(2^n)$, i.e., it is the group of unitary operators U satisfying $U\mathcal{P}_{\mathcal{H}_2^n} U^\dagger = \mathcal{P}_{\mathcal{H}_2^n}$. The local Clifford group $\mathcal{C}_n^l$ is the subgroup of $\mathcal{C}_n$ and consists of all n-fold tensor products of elements in $\mathcal{C}_1$. The Clifford group is generated by a simple set of quantum gates: the Hadamard gate H, the phase gate P and the CNOT gate U_{CNOT} [21]. Using the well-known representations of the Pauli matrices in the computational basis, it is straightforward to show that the action of H on such matrices reads

$$\sigma_x \to H\sigma_x H^\dagger = \sigma_z, \ \sigma_y \to H\sigma_y H^\dagger = -\sigma_y, \ \sigma_z \to H\sigma_z H^\dagger = \sigma_x. \tag{4}$$

The action of the phase gate P on σ_x, σ_y and σ_z is given by,

$$\sigma_x \to P\sigma_x^\dagger P = \sigma_y,\ \sigma_y \to P\sigma_y^\dagger P = -\sigma_x,\ \sigma_z \to P\sigma_z^\dagger P = \sigma_z. \tag{5}$$

Finally, the CNOT gate leads to the following transformations rules,

$$\sigma_x \otimes I \to U_{\text{CNOT}}\left(\sigma_x \otimes I\right)U_{\text{CNOT}}^\dagger = \sigma_x \otimes \sigma_x,\ I \otimes \sigma_x \to U_{\text{CNOT}}\left(I \otimes \sigma_x\right)U_{\text{CNOT}}^\dagger = I \otimes \sigma_x,$$

$$\sigma_z \otimes I \to U_{\text{CNOT}}\left(\sigma_z \otimes I\right)U_{\text{CNOT}}^\dagger = \sigma_z \otimes I,\ I \otimes \sigma_z \to U_{\text{CNOT}}\left(I \otimes \sigma_z\right)U_{\text{CNOT}}^\dagger = \sigma_z \otimes \sigma_z. \tag{6}$$

Observe that the CNOT gate propagates bit flip errors from the control to the target, and phase errors from the target to the control. As a side remark, we stress that another useful two-qubit gate is the controlled-phase gate $U_{\text{CP}} \overset{\text{def}}{=} \left(I \otimes H\right)U_{\text{CNOT}}\left(I \otimes H\right)$. The controlled-phase gate has the following action on the generators of $\mathcal{P}_{\mathcal{H}_2^2}$,

$$\sigma_x \otimes I \to U_{\text{CP}}\left(\sigma_x \otimes I\right)U_{\text{CP}}^\dagger = \sigma_x \otimes \sigma_z,\ I \otimes \sigma_x \to U_{\text{CP}}\left(I \otimes \sigma_x\right)U_{\text{CP}}^\dagger = \sigma_z \otimes \sigma_x,$$

$$\sigma_z \otimes I \to U_{\text{CP}}\left(\sigma_z \otimes I\right)U_{\text{CP}}^\dagger = \sigma_z \otimes I,\ I \otimes \sigma_z \to U_{\text{CP}}\left(I \otimes \sigma_z\right)U_{\text{CP}}^\dagger = I \otimes \sigma_z. \tag{7}$$

We observe that a controlled-phase gate does not propagate phase errors, though a bit-flip error on one qubit spreads to a phase error on the other qubit.

We also point out that a unitary operator U that fixes the stabilizer group $S_{\text{stabilizer}}$ (we refer to [22] for a detailed characterization of the quantum stabilizer formalism in QEC) of a quantum stabilizer code $\mathcal{C}_{\text{stabilizer}}$ under conjugation is an encoded operation. In other words, U is an encoded operation that maps codewords to codewords whenever $US_{\text{stabilizer}}U^\dagger = S_{\text{stabilizer}}$. In particular, if $S' \overset{\text{def}}{=} USU^\dagger$ (every element of S' can be written as $UsU^\dagger$ for some $s \in S$) and $|c\rangle$ is a codeword stabilized by every element in S, then $|c'\rangle = U|c\rangle$ is stabilized by every stabilizer element in S'.

2. Transformations on graphs

If there exists a local unitary (LU) transformation U such that $U|G\rangle = |G'\rangle$, the states $|G\rangle$ and $|G'\rangle$ will have the same entanglement properties. If $|G\rangle$ and $|G'\rangle$ are graph states, we say that their corresponding graphs G and G' will then represent equivalent quantum codes, with the same distance, weight distribution, and other properties. Determining whether two graphs are LU-equivalent is a difficult task, but a sufficient condition for equivalence was given in [9]. Let the graphs $G = (V, E)$ and $G' = (V, E')$ on n vertices correspond to the n-qubit graph states $|G\rangle$ and $|G'\rangle$. We define the two 2×2 unitary matrices,

$$\tau_x \overset{\text{def}}{=} \sqrt{-i\sigma_x} = \frac{1}{\sqrt{2}}\begin{pmatrix} -1 & i \\ i & -1 \end{pmatrix} \text{ and, } \tau_z \overset{\text{def}}{=} \sqrt{i\sigma_z} = \begin{pmatrix} \omega & 0 \\ 0 & \omega^3 \end{pmatrix}, \tag{8}$$

where $\omega^4 = i^2 = -1$, and σ_x and σ_z are Pauli matrices. Given a graph $G = (V = \{0,..., n-1\}, E)$, corresponding to the graph state $|G\rangle$, we define a local unitary transformation U_a,

$$U_a \overset{\text{def}}{=} \bigotimes_{i \in N_a} \tau_x^{(i)} \bigotimes_{i \notin N_a} \tau_z^{(i)}, \tag{9}$$

where $a \in V$ is any vertex, $N_a \subset V$ is the neighborhood of a, and $\tau_x^{(i)}$ means that the transform τ_x should be applied to the qubit corresponding to vertex i. Given a graph G, if there exists a finite sequence of vertices $(u_0,..., u_{k-1})$ such that $U_{u_{k-1}}...U_{u_0}|G\rangle = |G'\rangle$, then G and G' are LU-equivalent [9]. It was discovered by Hein et al. and by Van den Nest et al. that the sequence of transformations taking $|G\rangle$ to $|G'\rangle$ can equivalently be expressed as a sequence of simple graph operations taking G to G'. In particular, it was shown in [10] that a graph G determines uniquely a graph state $|G\rangle$ and two graph states ($|G_1\rangle$ and $|G_2\rangle$) determined by two graphs (G_1 and G_2) are equivalent up to some local Clifford transformations iff these two graphs are related to each other by local complementations (LCs). The concept of LC was originally introduced by Bouchet in [23]. A LC of a graph on a vertex v refers to the operation that in the neighborhood of v we connect all the disconnected vertices and disconnect all the connected vertices. All the graphs on up to 12 vertices have been classified under LCs and graph isomorphisms [24]. In summary, the relation between graphs and quantum codes can be rather complicated since one graph may provide inequivalent codes and

different graphs may provide equivalent codes. However, it has been established that the family of codes given by a graph is equivalent to the family of codes given by a local complementation of that graph.

As pointed out earlier, unitary operations U in the local Clifford group $\mathcal{C}_n^l$ act on graph states $|G\rangle$. However, there exists also graph theoretical rules, transformations acting on graphs, which correspond to local Clifford operations. These operations generate the orbit of any graph state under local Clifford operations. The LC orbit of a graph G is the set of all non-isomorphic graphs, including G itself, that can be transformed into G by any sequence of local complementations and vertex permutations. The transformation laws for a graph state $|G\rangle$ and a graph stabilizer under local unitary transformations U read,

$$|G\rangle \to |G'\rangle = U |G\rangle \text{ and, } S_\Gamma \to S_{\Gamma'} = U S_\Gamma U^\dagger, \tag{10}$$

respectively. Neglecting overall phases, it turns out that local Clifford operations $U \in \mathcal{C}_n^l$ are just the symplectic transformations Q of $\mathbb{Z}_2^{2n}$ which preserve the symplectic inner product [25]. Therefore, the $(2n \times 2n)$-matrices Q satisfy the relation $Q^\mathrm{T} P Q = P$ where T denotes the transpose operation and P is the $(2n \times 2n)$-matrix that defines a symplectic inner product in $\mathbb{Z}_2^{2n}$,

$$P \stackrel{\mathrm{def}}{=} \begin{pmatrix} 0 & I \\ I & 0 \end{pmatrix}. \tag{11}$$

Furthermore, since local Clifford operations act on each qubit separately, they have the additional block structure

$$Q \stackrel{\mathrm{def}}{=} \begin{pmatrix} A & B \\ C & D \end{pmatrix}, \tag{12}$$

where the $(n \times n)$-blocks A, B, C, D are diagonal. It was shown in [10] that each binary stabilizer code is equivalent to a graph code. In particular, each graph code characterized by the adjacency matrix Γ corresponds to a stabilizer matrix $\mathcal{S}_b \stackrel{\mathrm{def}}{=} (\Gamma | I)$ and transpose stabilizer (generator matrix) $\mathcal{T} \stackrel{\mathrm{def}}{=} \mathcal{S}_b^T = \binom{\Gamma}{I}$. The generator matrix $\binom{\Gamma'}{I}$ for a graph state with adjacency matrix Γ' reads,

$$\begin{pmatrix} \Gamma \\ I \end{pmatrix} \to \begin{pmatrix} \Gamma' \\ I \end{pmatrix} = \begin{pmatrix} A & B \\ C & D \end{pmatrix} \begin{pmatrix} \Gamma \\ I \end{pmatrix} (C\Gamma + D)^{-1}, \tag{13}$$

where,

$$\Gamma' \stackrel{\mathrm{def}}{=} Q(\Gamma) = (A\Gamma + B)(C\Gamma + D)^{-1}. \tag{14}$$

Observe that in order to have properly defined generators matrices in Eq. (13), $C\Gamma + D$ must be nonsingular and Γ' must have vanishing diagonal elements. The graphical analog of the transformation law in Eq. (14) was provided in [10]. Before stating this result, some additional terminology awaits to be introduced.

Two vertices i and j of a graph $G = (V, E)$ are called adjacent vertices, or neighbors, if $\{i, j\} \in E$. The neighborhood $N(i) \subseteq V$ of a vertex i is the set of all neighbors of i. A graph $G' = (V', E')$ which satisfies $V' \subseteq V$ and $E' \subseteq E$ is a subgraph of G and one writes $G' \subseteq G$. For a subset $A \subseteq V$ of vertices, the induced subgraph $G[A] \subseteq G$ is the graph with vertex set A and edge set $\{\{i, j\} \in E : i, j \in A\}$. If G has an adjacency matrix Γ, its complement G^c is the graph with adjacency matrix $\Gamma + \mathbf{I}$, where $\mathbf{I}$ is the $(n \times n)$-matrix which has all ones, except for the diagonal entries which are zero. For each vertex $i = 1,..., n$, a local complementation g_i sends the n-vertex graph G to the graph $g_i(G)$ which is obtained by replacing the induced subgraph $G[N(i)]$ by its complement. In other words,

$$\Gamma \to \Gamma' \equiv g_i(\Gamma) \stackrel{\mathrm{def}}{=} \Gamma + \Gamma \Lambda_i \Gamma + \Lambda^{(i)}, \tag{15}$$

where Λ_i has a 1 on the ith diagonal entry and zeros elsewhere and $\Lambda^{(i)}$ is a diagonal matrix such that yields zeros on the diagonal of $g_i(\Gamma)$. Finally, the graphical analog of Eq. (14) becomes,

$$Q_i(\Gamma) = g_i(\Gamma), \tag{16}$$

with,

$$Q_i \stackrel{\mathrm{def}}{=} \begin{pmatrix} I & \mathrm{diag}(\Gamma_i) \\ \Lambda_i & I \end{pmatrix}, \tag{17}$$

and $\mathrm{diag}(\Gamma_i) \overset{\mathrm{def}}{=} \mathrm{diag}(\Gamma_{i1},..., \Gamma_{in})$. Observe that substituting (17) in (14) and using (15), Eq. (16) gives

$$Q_i(\Gamma) = g_i(\Gamma) \Leftrightarrow \Gamma + \Gamma\Lambda_i\Gamma + \Lambda^{(i)} = \Gamma + \Gamma\Lambda_i\Gamma + [\mathrm{diag}(\Gamma_i) + \mathrm{diag}(\Gamma_i)\Lambda_i\Gamma], \tag{18}$$

that is,

$$\Lambda^{(i)} = \mathrm{diag}(\Gamma_i) + \mathrm{diag}(\Gamma_i)\Lambda_i\Gamma. \tag{19}$$

The translation of the action of local Clifford operations on graph states into the action of local complementations on graphs as presented in Eq. (16) is a major achievement of [10].

C. The CWS-work

CWS codes include all stabilizer codes as well as several nonadditive codes. However, for the sake of completeness, we point out that there are indeed quantum codes that cannot be recast within the CWS framework as pointed out in [11] and shown in [26]. CWS codes in standard form can be specified by a graph G and a (nonadditive, in general) classical binary code $\mathcal{C}_{\mathrm{classical}}$. The n vertices of the graph G correspond to the n qubits of the code and its adjacency matrix is Γ. Given the graph state $|G\rangle$ and the binary code $\mathcal{C}_{\mathrm{classical}}$, a unique base state $|S\rangle$ and a set of word operators $\{w_k\}$ are specified. The base state $|S\rangle$ is a single stabilizer state stabilized by the word stabilizer $\mathcal{S}_{\mathrm{CWS}}$, a maximal Abelian subgroup of the Pauli group $\mathcal{P}_{\mathcal{H}_2^n}$.

Let $((n, K, d))$ denote a quantum code on n qubits that encodes K dimensions with distance d. Following [11], it can be shown that a $((n, K, d))$ codeword stabilized code with word operators $\mathcal{W} = \{w_l\}$ with $l \in \{1,..., K\}$ and codeword stabilizer $\mathcal{S}_{\mathrm{CWS}}$ is locally Clifford equivalent to a codeword stabilized code with word operators $\mathcal{W}'$,

$$\mathcal{W}' \overset{\mathrm{def}}{=} \{w'_l = Z^{\mathbf{c}_l}\}, \tag{20}$$

and codeword stabilizer $\mathcal{S}'_{\mathrm{CWS}}$,

$$\mathcal{S}'_{\mathrm{CWS}} \overset{\mathrm{def}}{=} \langle S'_l \rangle = \langle X_l Z^{\mathbf{r}_l} \rangle, \tag{21}$$

where $\mathbf{c}_l$s are codewords defining the classical binary code $\mathcal{C}_{\mathrm{classical}}$ and $\mathbf{r}_l$ is the lth row vector of the adjacency matrix Γ of the graph G. For the sake of clarity, we stress that $Z^{\mathbf{v}}$ in Eq. (21) is the notational shorthand for

$$Z^{\mathbf{v}} \overset{\mathrm{def}}{=} Z^{v_1} \otimes ... \otimes Z^{v_n}, \tag{22}$$

where $\mathbf{v} = (v_1,..., v_n) \in F_2^n$ is a binary n-vector. Thus, any CWS code is locally Clifford equivalent to a CWS code with a graph-state stabilizer and word operators consisting only of Zs. Moreover, the word operators can always be chosen to include the identity. Eqs. (20) and (21) characterize the so-called standard form of a CWS quantum code. For a CWS code in standard form, the base state $|S\rangle$ is a graph state. Furthermore, the codespace of a CWS code is spanned by a set of basis vectors which result from applying the word operators w_k on the base state $|S\rangle$,

$$\mathcal{C}_{\mathrm{CWS}} \overset{\mathrm{def}}{=} \mathrm{Span}\{|w_l\rangle\} \text{ with, } |w_l\rangle \overset{\mathrm{def}}{=} w_l |S\rangle. \tag{23}$$

Therefore, the dimension of the codespace equals the number of word operators. These operators are Pauli operators in $\mathcal{P}_{\mathcal{H}_2^n}$ that anticommute with one or more of the stabilizer generators for the base state. Thus, word operators map the base state onto an orthogonal state. The only exception is that in general the set of word operators also includes the identity operator so that the base state is a codeword of the quantum code as well. These basis states are also eigenstates of the stabilizer generators, but with some of the eigenvalues differing from $+1$. In addition, it turns out that a single qubit Pauli error X, Z or ZX acting on a codeword $\omega |S\rangle$ of a CWS code in standard form is equivalent up to a sign to another multi-qubit error consisting of Zs. Therefore, since all errors become Zs, the original quantum error model is transformed into a classical (induced by the CWS formalism) error model characterized, in general, by multi-qubit errors. The map $Cl_{\mathcal{S}_{\mathrm{CWS}}}$ that defines this transformation reads,

$$Cl_{\mathcal{S}_{\mathrm{CWS}}} : \mathcal{E} \ni E \equiv \pm Z^{\mathbf{v}} X^{\mathbf{u}} \mapsto Cl_{\mathcal{S}_{\mathrm{CWS}}}(\pm Z^{\mathbf{v}} X^{\mathbf{u}}) \overset{\mathrm{def}}{=} \mathbf{v} \oplus \bigoplus_{l=1}^{n} u_l \mathbf{r}_l \in \{0, 1\}^n, \tag{24}$$

where $\mathcal{E}$ denotes the set of Pauli errors E, $\mathbf{r}_l$ is the lth row of the adjacency matrix Γ for the graph G and u_l is the lth bit of the vector $\mathbf{u}$. Finally, it was shown in [11] that any stabilizer code is a CWS code. Specifically, a

quantum stabilizer code $[[n, k, d]]$ (where the parameters n, k, d denote the length, the dimension and the distance of the quantum code, respectively) with stabilizer $\mathcal{S} \overset{\text{def}}{=} \langle S_1,..., S_{n-k} \rangle$ where S_j with $j \in \{1,..., n-k\}$ denote the stabilizer generators and logical operations $\bar{X}_1,..., \bar{X}_k$ and $\bar{Z}_1,..., \bar{Z}_k$ is equivalent to a CWS code defined by,

$$\mathcal{S}_{\text{CWS}} \overset{\text{def}}{=} \langle S_1, ..., S_{n-k}, \bar{Z}_1,..., \bar{Z}_k \rangle, \tag{25}$$

and word operators $\omega_{\mathbf{v}}$,

$$\omega_{\mathbf{v}} = \bar{X}_1^{(\mathbf{v})_1} \otimes ... \otimes \bar{X}_k^{(\mathbf{v})_k}. \tag{26}$$

The vector $\mathbf{v}$ denotes a k-bit string and $(\mathbf{v})_l \equiv v_l$ with $l \in \{1,..., k\}$ is the lth bit of the vector $\mathbf{v}$. For further details on binary CWS quantum codes, we refer to [11]. Finally, for a very recent investigation on the symmetries of CWS codes, we refer to [27].

III. FROM GRAPHS TO STABILIZER CODES AND VICE-VERSA

In this section, we revisit some basic ingredients of the Schlingemann-Werner work (SW-work, [5]), the Schlingemann work (S-work, [6]) and, finally, the Van den Nest et al. work (VdN-work, [10]). We focus on those aspects of these works that will be especially relevant for our proposed scheme.

A. The Schlingemann-Werner work

The basic graphical construction of quantum codes within the SW-work [5] can be described as follows. Quantum codes are completely characterized by a unidirected graph $G = G(V, E)$ characterized by a set V of n vertices and a set of edges E specified by the coincidence matrix Ξ with both input and output vertices and a finite Abelian group $\mathcal{G}$ with a nondegenerate symmetric bicharacter χ. We remark that there are various types of matrices that can be used to specify a given graph (for instance, incidence and adjacency matrices [1]). The coincidence matrix introduced in [5] is simply the adjacency matrix of a graph with both input and output vertices (and, it should not be confused with the so-called incidence matrix of a graph). The sets of input and output vertices will be denoted by X and Y, respectively. Let $\mathcal{G}$ be any finite additive Abelian group of cardinality $|\mathcal{G}| = n$ with the addition operation denoted by $+$ and null element 0. A nondegenerate symmetric bicharacter is a map $\chi : \mathcal{G} \times \mathcal{G} \ni (g, h) \mapsto \chi(g, h) \equiv \langle g, h \rangle \in \mathbb{C}$ satisfying the following properties [28]: (i) $\langle g, h \rangle = \langle h, g \rangle, \forall g, h \in \mathcal{G}$; (ii) $\langle g, h_1 + h_2 \rangle = \langle g, h_1 \rangle \langle g, h_2 \rangle, \forall g, h_1, h_2 \in \mathcal{G}$; (iii) $\langle g, h \rangle = 1 \, \forall h \in \mathcal{G} \Leftrightarrow g = 0$. If $\mathcal{G} = \mathbb{Z}_n \overset{\text{def}}{=} \{0,..., n-1\}$ (the cyclic group of order n) with addition modulo n as the group operation, the bicharacter χ can be chosen as

$$\chi(g, h) \equiv \langle g, h \rangle \overset{\text{def}}{=} e^{i\frac{2\pi}{n}gh}, \tag{27}$$

with $g, h \in \mathbb{Z}_n$. The encoding operator $\mathbf{v}_G$ of an error correcting code is an isometry (a bijective map between two metric spaces that preserve distances),

$$\mathbf{v}_G : L^2\left(\mathcal{G}^X\right) \to L^2\left(\mathcal{G}^Y\right), \tag{28}$$

where $L^2\left(\mathcal{G}^X\right)$ is the $|X|$-fold tensor product $\mathcal{H}^{\otimes X}$ with $\mathcal{H} = L^2(\mathcal{G})$ (the Hilbert space $\mathcal{H}$ is realized as the space of integrable functions over $\mathcal{G}$) and $\mathcal{G} \overset{\text{def}}{=} \mathbb{Z}_2$ in the qubit case. Similarly, $L^2\left(\mathcal{G}^Y\right)$ is the $|Y|$-fold tensor product $\mathcal{H}^{\otimes Y}$. The Hilbert space $L^2(\mathcal{G})$ is defined as,

$$L^2(\mathcal{G}) \overset{\text{def}}{=} \{\psi \,|\, \psi : \mathcal{G} \to \mathbb{C}\}, \tag{29}$$

with scalar product between two elements ψ_1 and ψ_2 in $L^2(\mathcal{G})$ given by,

$$\langle \psi_1, \psi_2 \rangle \overset{\text{def}}{=} \frac{1}{|\mathcal{G}|} \sum_g \bar{\psi}_1(g) \psi_2(g). \tag{30}$$

The action of $\mathbf{v}_G$ on $L^2\left(\mathcal{G}^X\right)$ is defined as [5],

$$(\mathbf{v}_G \psi)\left(g^Y\right) \overset{\text{def}}{=} \int dg^X \mathbf{v}_G \left[g^{X \cup Y}\right] \psi\left(g^X\right), \tag{31}$$

where $\mathbf{v}_G\left[g^{X\cup Y}\right]$, the integral kernel of the isometry $\mathbf{v}_G$, is given by [5],

$$\mathbf{v}_G\left[g^{X\cup Y}\right] = |\mathcal{G}|^{\frac{|X|}{2}} \prod_{\{z,\,z'\}} \chi\left(g_z, g_{z'}\right)^{\Xi\left(z,\,z'\right)} = |\mathcal{G}|^{\frac{|X|}{2}} \prod_{\{z,\,z'\}} \left[\exp\left(\frac{2\pi i}{p}g_z g_{z'}\right)\right]^{\Xi\left(z,\,z'\right)}$$

$$= |\mathcal{G}|^{\frac{|X|}{2}} \prod_{\{z,\,z'\}} \left[\exp\left(\frac{2\pi i}{p}g_z \Xi\left(z, z'\right) g_{z'}\right)\right] = |\mathcal{G}|^{\frac{|X|}{2}} \exp\left(\frac{\pi i}{p}g^{X\cup Y}\cdot\Xi\cdot g^{X\cup Y}\right). \tag{32}$$

The product in Eq. (32) must be taken over each two elementary subsets $\{z, z'\}$ in $X\cup Y$. Substituting Eq. (32) into Eq. (31), the action of $\mathbf{v}_G$ on $L^2\left(\mathcal{G}^X\right)$ finally becomes,

$$\left(\mathbf{v}_G\psi\right)\left(g^Y\right) = \int dg^X |\mathcal{G}|^{\frac{|X|}{2}} \exp\left(\frac{\pi i}{p}g^{X\cup Y}\cdot\Xi\cdot g^{X\cup Y}\right)\psi\left(g^X\right). \tag{33}$$

We recall that the sequential steps of a QEC cycle can be described as follows,

$$\rho \xrightarrow{\text{coding}} \mathbf{v}\rho\mathbf{v}^* \equiv \rho', \ \rho' \xrightarrow{\text{noise}} \mathbf{T}\left(\rho'\right) = \sum_\alpha F_\alpha \rho' F_\alpha^* \equiv \rho'', \ \rho'' \xrightarrow{\text{recovery}} \mathbf{R}\left(\rho''\right) = \rho, \tag{34}$$

that is,

$$\mathbf{R}\left(\mathbf{T}\left(\mathbf{v}\rho\mathbf{v}^*\right)\right) = \rho. \tag{35}$$

Furthermore, the traditional Knill-Laflamme error-correction conditions read,

$$\langle\mathbf{v}\psi_1, F_\alpha^* F_\beta\mathbf{v}\psi_2\rangle = \omega\left(F_\alpha^* F_\beta\right)\langle\psi_1, \psi_2\rangle, \tag{36}$$

where the multiplicative factor $\omega\left(F_\alpha^* F_\beta\right)$ does not depend on the states ψ_1 and ψ_2. The graphical analog of Eq. (36) is given by,

$$\langle\mathbf{v}\psi_1, F\mathbf{v}\psi_2\rangle = \omega\left(F\right)\langle\psi_1, \psi_2\rangle, \tag{37}$$

for all operators in $\mathcal{U}(E)$, the set of all operators in $L^2(\mathcal{G}^Y)$ which are localized in $E\subset Y$. Thus, operators in $\mathcal{U}(E)$ are given by the tensor product of an arbitrary operator on $\mathcal{H}^{\otimes E}$ with the identity on $\mathcal{H}^{\otimes Y\backslash E}$. A graph code corrects e errors if and only if it detects all error configurations $E\subset Y$ with $|E|\leq 2e$. Given this graphical construction of the encoding operator $\mathbf{v}_G$ in Eq. (33) and the graphical quantum error-correction conditions in Eq. (37), the main finding provided by Schlingemann and Werner can be restated as follows: given a finite Abelian group $\mathcal{G}$ and a weighted graph G, an error configuration $E\subset Y$ is detected by the quantum code $\mathbf{v}_G$ if and only if given that

$$d^X = 0 \text{ and, } \Xi_E^X d^E = 0, \tag{38}$$

then,

$$\Xi_{X\cup E}^I d^{X\cup E} = 0 \Rightarrow d^{X\cup E} = 0, \tag{39}$$

with $I = Y\backslash E$. In general, the condition $\Xi_B^A d^B = 0$ is a set of equations, one for each integration vertex $a\in A$: for each vertex $a\in A$, we have to sum the d_b for all vertices $b\in B$ connected to a, and equate it to zero. Furthermore, we underline that the fact that v_G is an isometry is equivalent to the detection of zero errors. In graph-theoretic terms, the detection of zero errors requires that $\Xi_X^Y d^X = 0$ implies $d^X = 0$. A code that satisfies Eq. (39) given Eq. (38) can be either nondegenerate or degenerate. We shall assume that Eq. (39) with the additional constraints in Eq. (38) denotes the weak version (necessary and sufficient conditions) of the graph-theoretic error detection conditions. However, sufficient graph-theoretic error detection conditions can be introduced as well. Specifically, an error configuration E is detectable by a quantum code if,

$$\Xi_{X\cup E}^I d^{X\cup E} = 0 \Rightarrow d^{X\cup E} = 0. \tag{40}$$

We shall denote conditions in Eq. (40) without any additional set of graph-theoretic constraints (like the ones provided in Eq. (38)) the strong version (sufficient conditions) of the graph-theoretic error detection conditions. We finally emphasize, as originally pointed out in [5], that a code that satisfies Eq. (40) is nondegenerate.

B. The Schlingemann-work

Schlingemann was able to show that stabilizer codes, either binary or nonbinary, are equivalent to graph codes (and vice-versa). However, as far as our proposed scheme concerns, the main finding uncovered in the S-work [6] may be stated as follows. Consider a graph code with only one input and $(n-1)$-output vertices. Its corresponding coincidence matrix $\Xi_{n\times n}$ can be written as,

$$\Xi_{n\times n} \overset{\text{def}}{=} \begin{pmatrix} 0_{1\times 1} & B^{\dagger}_{1\times(n-1)} \\ B_{(n-1)\times(1)} & A_{(n-1)\times(n-1)} \end{pmatrix}, \tag{41}$$

where $A_{(n-1)\times(n-1)}$ denotes the $(n-1)\times(n-1)$-symmetric adjacency matrix $\Gamma_{(n-1)\times(n-1)}$. Then, the graph code with symmetric coincidence matrix $\Xi_{n\times n}$ in Eq. (41) is equivalent to stabilizer codes being associated with the isotropic subspace $\mathcal{S}_{\text{isotropic}}$ defined as,

$$\mathcal{S}_{\text{isotropic}} \overset{\text{def}}{=} \left\{ (Ak\,|k\,) : k \in \ker B^{\dagger} \right\}, \tag{42}$$

that is, omitting unimportant phase factors, with the binary stabilizer group $\mathcal{S}_{\text{binary}}$,

$$\mathcal{S}_{\text{binary}} \overset{\text{def}}{=} \left\{ g_k = X^k Z^{Ak} : k \in \ker B^{\dagger} \right\}. \tag{43}$$

Observe that a stabilizer operator $g_k \in \mathcal{S}_{\text{binary}}$ for an n-vertex graph has a $2n$-dimensional binary vector space representation such that $g_k \leftrightarrow v_{g_k} \overset{\text{def}}{=} (Ak\,|k\,)$.

More generally, consider a $[[n,k,d]]$ binary quantum stabilizer code associated with a graph $G = (V, E)$ characterized by the $(n+k)\times(n+k)$ symmetric coincidence matrix $\Xi_{(n+k)\times(n+k)}$,

$$\Xi_{(n+k)\times(n+k)} \overset{\text{def}}{=} \begin{pmatrix} 0_{k\times k} & B^{\dagger}_{k\times n} \\ B_{n\times k} & \Gamma_{n\times n} \end{pmatrix}. \tag{44}$$

To attach the input vertices, Ξ has to be constructed in such a manner that the following conditions are satisfied: i) first, $\det\Gamma_{n\times n} = 0 \pmod 2$; ii) second, the matrix $B^{\dagger}_{k\times n}$ must define a k-dimensional subspace in $\mathbf{F}_2^n$ spanned by k linearly independent binary vectors of length n not included in the Span of the raw-vectors defining the symmetric adjacency matrix $\Gamma_{n\times n}$,

$$\text{Span}\{\vec{v}_1,..., \vec{v}_k\} \cap \text{Span}\left\{\vec{v}_{\Gamma}^{(1)},..., \vec{v}_{\Gamma}^{(n)}\right\} = \{\emptyset\}, \tag{45}$$

where $\vec{v}_j \in \mathbf{F}_2^n$ for $j \in \{1,..., k\}$ and $\vec{v}_{\Gamma}^{(i)} \in \mathbf{F}_2^n$ for $i \in \{1,..., n\}$; iii) third, $\text{Span}\{\vec{v}_1,..., \vec{v}_k\}$ contains a vector $\vec{v}_B \in \mathbf{F}_2^n$ such that $\vec{v}_B \cdot \vec{v}_{\Gamma}^{(i)} = 0$ for any $i \in \{1,..., n\}$. Condition i) is needed to avoid disconnected graphs. Condition ii) is required to have a properly defined isometry capable of detecting zero errors. Finally, condition iii) is needed to generate an isotropic subspace (or, in other words, an Abelian subgroup of the Pauli group, the so-called stabilizer group) with,

$$\left(\Gamma\vec{v}_{\Gamma}^{(l)},\ \vec{v}_{\Gamma}^{(l)}\right) \odot \left(\Gamma\vec{v}_{\Gamma}^{(m)},\ \vec{v}_{\Gamma}^{(m)}\right) = 0, \tag{46}$$

for any pair $\left(\vec{v}_{\Gamma}^{(l)},\ \vec{v}_{\Gamma}^{(m)}\right)$ in $\left\{\vec{v}_{\Gamma}^{(1)},..., \vec{v}_{\Gamma}^{(n)}\right\}$ where the symbol $\odot$ denotes the symplectic product [21].

As a final remark, we point out that in a more general framework like the one presented in [6], we could consider three types of vertices: input, auxiliary and output vertices. The input vertices label the input systems and are used for encoding. The auxiliary vertices are inputs used as auxiliary degrees of freedom for implementing additional constraints for the protected code subspace. Finally, output vertices simply label the output quantum systems.

C. The Van den Nest-work

The main achievement of the VdN-work in [10] is the construction of a very useful algorithmic procedure for transforming any binary quantum stabilizer code into a graph code. Before describing this procedure, we remark that it is straightforward to check that a graph code given by the adjacency matrix Γ corresponds to a stabilizer matrix

$\mathcal{S}_b \stackrel{\text{def}}{=} (\Gamma \,|\, I)$ and transpose stabilizer $\mathcal{T} \stackrel{\text{def}}{=} \mathcal{S}_b^{\mathrm{T}} = \binom{\Gamma}{I}$. That said, consider a quantum stabilizer code with stabilizer matrix,

$$\mathcal{S}_b \stackrel{\text{def}}{=} (Z \,|\, X)\,, \tag{47}$$

and transpose stabilizer $\mathcal{T}$ given by,

$$\mathcal{T} \stackrel{\text{def}}{=} \mathcal{S}_b^{\mathrm{T}} = \begin{pmatrix} Z^{\mathrm{T}} \\ X^{\mathrm{T}} \end{pmatrix} \equiv \begin{pmatrix} A \\ B \end{pmatrix}. \tag{48}$$

Let us define $\mathcal{S}_b$ in Eq. (47). Given a set of generators of the stabilizer, the stabilizer matrix $\mathcal{S}_b$ is constructed by assembling the binary representations of the generators as the rows of a full rank $(n \times 2n)$-matrix. The transpose of the binary stabilizer matrix (i.e., the transpose stabilizer) $\mathcal{T}$ is simply the full rank $(2n \times n)$-matrix obtained from $\mathcal{S}_b$ after exchanging rows with columns. The goal of the algorithmic procedure is to convert the transpose stabilizer $\mathcal{T}$ in Eq. (48) of a given stabilizer code into the transpose stabilizer $\mathcal{T}' = \binom{A'}{B'}$ of an equivalent graph code. Then, the matrix A' will represent the adjacency matrix of the corresponding graph. Two scenarios may occur: i) B is a $n \times n$ invertible matrix; ii) B is not an invertible matrix. In the first scenario where B is invertible, a right-multiplication of the transpose stabilizer $\mathcal{T} = \binom{A}{B}$ by B^{-1} will perform a basis change, an operation that provides us with an equivalent stabilizer code,

$$\mathcal{T} B^{-1} = \begin{pmatrix} A \\ B \end{pmatrix} B^{-1} = \begin{pmatrix} A B^{-1} \\ I \end{pmatrix}. \tag{49}$$

Then, the matrix AB^{-1} will denote the resulting adjacency matrix of the corresponding graph. Furthermore, if the matrix AB^{-1} has nonzero diagonal elements, we can simply set these elements to zero in order to satisfy the standard requirements for a correct definition of an adjacency matrix of simple graphs. In the second scenario where B is not invertible, we can always find a suitable local Clifford unitary transformation U such that [10],

$$\mathcal{S}_b \stackrel{\text{def}}{=} (Z \,|\, X) \xrightarrow{U} \mathcal{S}_b' \stackrel{\text{def}}{=} (Z' \,|\, X')\,, \tag{50}$$

and,

$$\mathcal{T} \stackrel{\text{def}}{=} \mathcal{S}_b^{\mathrm{T}} = \begin{pmatrix} Z^{\mathrm{T}} \\ X^{\mathrm{T}} \end{pmatrix} \equiv \begin{pmatrix} A \\ B \end{pmatrix} \xrightarrow{U} \mathcal{T}' \stackrel{\text{def}}{=} \mathcal{S}_b'^{\mathrm{T}} = \begin{pmatrix} Z'^{\mathrm{T}} \\ X'^{\mathrm{T}} \end{pmatrix} \equiv \begin{pmatrix} A' \\ B' \end{pmatrix}, \tag{51}$$

with $\det B' \neq 0$. Therefore, right-multiplying $\mathcal{T}'$ with B'^{-1}, we get

$$\mathcal{T}' B'^{-1} = \begin{pmatrix} A' \\ B' \end{pmatrix} B'^{-1} = \begin{pmatrix} A' B'^{-1} \\ I \end{pmatrix}. \tag{52}$$

Thus, the adjacency matrix of the corresponding graph becomes $A' B'^{-1}$.

The above-described algorithmic procedure for transforming any binary quantum stabilizer code into a graph code is very important for our proposed scheme as it will become clear in the next section.

IV.   THE SCHEME

In this section, we formally describe our scheme and apply it to the graphical construction of the Leung et al. four-qubit quantum code for the error correction of single amplitude damping errors.

A.   Description of the scheme

We emphasize that our ultimate goal is the construction of classical graphs $G(V, E)$ with both input and output vertices defined by the coincidence matrix Ξ in order to verify the error-correcting capabilities of the corresponding quantum stabilizer codes via the graph-theoretic error correction conditions advocated in the SW-work. To achieve this goal, we propose a systematic scheme based on a very simple idea. The CWS-, VdN- and S-works must be combined in such a manner that, with respect to our ultimate goal, the weak-points of one method should be compensated by the strong-points of another method.

1. Step one

The CWS formalism offers a very general framework where both binary/nonbinary and/or additive/nonadditive quantum codes can be described. For this reason, the starting point of our scheme is the realization of binary stabilizer codes as CWS quantum codes. Although this is a relatively straightforward step, the CWS code that one obtains is not, in general, in the standard canonical form. From the CWS-work in [11], it is known that there does exist a local (unitary) Clifford operations that allows in principle to write down the CWS code that realizes the binary stabilizer code in standard form. However, the CWS-work does not suggest any algorithmic procedure to achieve this standard form. In the absence of a systematic procedure, uncovering a local Clifford unitary U such that $\mathcal{S}'_{\mathrm{CWS}} \stackrel{\mathrm{def}}{=} U\mathcal{S}_{\mathrm{CWS}}U^{\dagger}$ (every element $s' \in \mathcal{S}'_{\mathrm{CWS}}$ can be written as $UsU^{\dagger}$ for some $s \in \mathcal{S}_{\mathrm{CWS}}$) may constitute a very tedious challenge. Fortunately, we can avoid this. Before explaining how, let us introduce the codeword stabilizer matrix $\mathcal{H}_{\mathcal{S}_{\mathrm{CWS}}} \stackrel{\mathrm{def}}{=} (Z\,|X\,)$ corresponding to the codeword stabilizer $\mathcal{S}_{\mathrm{CWS}}$.

2. Step two

Two main achievements of the VdN-work in [10] are the following: first, each stabilizer state is equivalent to a graph state under local Clifford operations; second, an algorithmic procedure for transforming any binary quantum stabilizer code into a graph code is provided. Observe that a stabilizer state can be regarded as a quantum code with parameters $[[n, 0, d]]$. Our idea is to exploit the algorithmic procedure provided by the VdN-work by translating the starting point of the algorithmic procedure in the CWS language. To achieve this, we replace the generator matrix of the stabilizer state with the codeword stabilizer matrix $\mathcal{H}_{\mathcal{S}_{\mathrm{CWS}}}$ corresponding to the codeword stabilizer $\mathcal{S}_{\mathrm{CWS}}$ of the CWS code that realizes the binary stabilizer code whose graphical depiction is being sought. This way, we can simply apply the VdN algorithmic procedure to uncover the standard form of the CWS code and, if necessary, the explicit expression for the local (unitary) Clifford operation that links the non-standard to the standard forms of the CWS code. After applying this VdN algorithmic procedure adapted to the CWS formalism, we can construct a graph characterized by a symmetric adjacency matrix Γ with only output vertices. How do we attach possible input vertices to this graph associated with the $[[n, k, d]]$ binary stabilizer codes with $k \neq 0$?

3. Step three

Unlike the VdN-work whose findings are limited to the binary quantum states, the S-work extends its applicability to both binary and nonbinary quantum codes. In particular, in [6] it was shown that any stabilizer code is a graph code and vice-versa. However, in the S-work an analog of the algorithmic procedure for transforming any binary quantum stabilizer code into a graph code is missing. Despite this fact, the S-work does provide a very useful result for our proposed scheme. Namely, it is shown that a graph code with associated graph $G(V, E)$ with both input and output vertices and corresponding symmetric coincidence matrix Ξ is equivalent to stabilizer codes being associated with a suitable isotropic subspace space $\mathcal{S}_{\mathrm{isotropic}}$. Recall that at the end of the above-mentioned step two, we are basically given both the isotropic subspace and the graph without input vertices, that is the symmetric adjacency matrix Γ embedded in the more general coincidence matrix Ξ. Therefore, by exploiting the just mentioned very useful specific finding of the S-work in a reverse direction (we are allowed to do so since a graph code is equivalent to a stabilizer code and vice-versa), in some sense, we can construct the full coincidence matrix Ξ and finally attach the input vertices to the graph. What can we do with a graphical depiction of a binary stabilizer code?

4. Step three+one

In the SW-work, outstanding graphical QEC conditions were introduced [5]. However, these conditions were only partially employed for quantum codes associated with graphs and the codes needed not be necessarily stabilizer codes. By logically combining the CWS-, VdN- and S-works, the power of the graphical QEC conditions in [5] can be fully exploited in a systematic manner in both directions: from graph codes to stabilizer codes and vice-versa.

In summary, given a binary quantum stabilizer code $\mathcal{C}_{\mathrm{stabilizer}}$, the systematic procedure that we propose can be described in $3 + 1 = 4$ points as follows:

- Realize the stabilizer code $\mathcal{C}_{\mathrm{stabilizer}}$ as a CWS quantum code $\mathcal{C}_{\mathrm{CWS}}$;

- Apply the VdN-work adapted to the CWS formalism to identify the standard form of the CWS code that realizes the stabilizer code whose graphical depiction is being sought. In other words, find the graph G with only output vertices characterized by the symmetric adjacency matrix Γ associated with $\mathcal{C}_{\mathrm{CWS}}$ in the standard form;

- Exploit the S-work as explained to identify the extended graph with both input and output vertices characterized by the symmetric coincidence matrix Ξ associated with the isometric encoding map that defines $\mathcal{C}_{\mathrm{CWS}}$;

- Use the SW-work to apply the graph-theoretic error-correction conditions to the extended graph in order to explicitly verify the error-correcting capabilities of the corresponding $\mathcal{C}_{\mathrm{stabilizer}}$ realized as a $\mathcal{C}_{\mathrm{CWS}}$ quantum code.

B. Application of the scheme

We think there is no better way to describe and understand the effectiveness of our proposed scheme than by simply working out in detail a simple illustrative example. In what follows, we wish to uncover the graph associated with the Leung et *al.* [[4,1]] four-qubit stabilizer (nondegenerate) quantum code [16]. Several explicit constructions of graphs for various stabilizer codes characterized by either single or multi-qubit encoding operators are added in the Appendices: the three-qubit repetition code, the perfect 1-erasure correcting four-qubit code, the perfect 1-error correcting five-qubit code, 1-error correcting six-qubit quantum degenerate codes, the CSS seven-qubit stabilizer code, the Shor nine-qubit stabilizer code, the Gottesman 2-error correcting eleven-qubit code, [[4, 2, 2]] stabilizer codes, and, finally, the Gottesman [[8, 3, 3]] stabilizer code.

1. Step one

Recall that the stabilizer $\mathcal{S}_{\mathrm{b}}^{\mathrm{Leung}}$ of the Leung et *al.* [[4, 1]] code is given by [29],

$$\mathcal{S}_{\mathrm{b}}^{\mathrm{Leung}} \overset{\mathrm{def}}{=} \left\langle X^1 X^2 X^3 X^4,\, Z^1 Z^2,\, Z^3 Z^4 \right\rangle, \tag{53}$$

with a suitable logical $\bar{Z}$ operation given by $\bar{Z} = Z^1 Z^3$. Therefore, when regarded within the CWS framework [11], the Leung et *al.* code is equivalent to a CWS code defined with codeword stabilizer,

$$\mathcal{S}_{\mathrm{CWS}}^{\mathrm{Leung}} \overset{\mathrm{def}}{=} \left\langle X^1 X^2 X^3 X^4,\, Z^1 Z^2,\, Z^3 Z^4,\, Z^1 Z^3 \right\rangle. \tag{54}$$

2. Step two

Taking into consideration Eq. (54), we observe that $\mathcal{S}_{\mathrm{Leung}}^{\mathrm{CWS}}$ is local Clifford equivalent to $S_{\mathrm{Leung}}'^{\mathrm{CWS}}$ given by,

$$\mathcal{S}_{\mathrm{CWS}}'^{\mathrm{Leung}} \overset{\mathrm{def}}{=} U \mathcal{S}_{\mathrm{CWS}}^{\mathrm{Leung}} U^\dagger, \tag{55}$$

with $U \overset{\mathrm{def}}{=} I^1 \otimes H^2 \otimes H^3 \otimes H^4$ where H denotes the Hadamard transformation. We notice that the codeword stabilizer matrix $\mathcal{H}_{\mathcal{S}_{\mathrm{CWS}}'^{\mathrm{Leung}}}$ associated with the codeword stabilizer $\mathcal{S}_{\mathrm{CWS}}'^{\mathrm{Leung}}$ reads,

$$\mathcal{H}_{\mathcal{S}_{\mathrm{CWS}}'^{\mathrm{Leung}}} \overset{\mathrm{def}}{=} (Z' \,|\, X') = \begin{pmatrix} 0 & 1 & 1 & 1 & 1 & 0 & 0 & 0 \\ 1 & 0 & 0 & 0 & 0 & 1 & 0 & 0 \\ 0 & 0 & 0 & 0 & 0 & 0 & 1 & 1 \\ 1 & 0 & 0 & 0 & 0 & 0 & 1 & 0 \end{pmatrix}, \tag{56}$$

with $\det X' \neq 0$. Therefore, we can find a suitable graph with output vertices only that is associated with the Leung et *al.* code by applying the VdN algorithmic procedure. The transpose of $\mathcal{H}_{\mathcal{S}_{\mathrm{CWS}}'^{\mathrm{Leung}}}$ becomes,

$$\mathcal{T}' \overset{\mathrm{def}}{=} \mathcal{H}_{\mathcal{S}_{\mathrm{CWS}}'^{\mathrm{Leung}}}^{\mathrm{T}} \equiv \begin{pmatrix} A' \\ B' \end{pmatrix} = \left(\begin{array}{cccc} 0 & 1 & 0 & 1 \\ 1 & 0 & 0 & 0 \\ 1 & 0 & 0 & 0 \\ 1 & 0 & 0 & 0 \\ \hline 1 & 0 & 0 & 0 \\ 0 & 1 & 0 & 0 \\ 0 & 0 & 1 & 1 \\ 0 & 0 & 1 & 0 \end{array} \right). \tag{57}$$

From Eq. (57) it turns out that B' is a 4×4 invertible matrix with inverse given by,

$$B'^{-1} = \begin{pmatrix} 1 & 0 & 0 & 0 \\ 0 & 1 & 0 & 0 \\ 0 & 0 & 0 & 1 \\ 0 & 0 & 1 & 1 \end{pmatrix}. \tag{58}$$

Finally, the adjacency matrix Γ of a graph that realizes the Leung et *al.* code is given by $\Gamma = A'B'^{-1}$, that is

$$\Gamma = A'B'^{-1} = \begin{pmatrix} 0 & 1 & 0 & 1 \\ 1 & 0 & 0 & 0 \\ 1 & 0 & 0 & 0 \\ 1 & 0 & 0 & 0 \end{pmatrix} \begin{pmatrix} 1 & 0 & 0 & 0 \\ 0 & 1 & 0 & 0 \\ 0 & 0 & 0 & 1 \\ 0 & 0 & 1 & 1 \end{pmatrix} = \begin{pmatrix} 0 & 1 & 1 & 1 \\ 1 & 0 & 0 & 0 \\ 1 & 0 & 0 & 0 \\ 1 & 0 & 0 & 0 \end{pmatrix} \stackrel{\text{def}}{=} \Gamma_{\text{Leung}}. \tag{59}$$

As a side remark, we recall that a graph determines uniquely a graph state and two graph states determined by two graphs are equivalent up to some local Clifford transformations if and only if these two graphs are related to each other via local complementations (LC) [10]. Avoiding unnecessary formalities, we recall that a local complementation of a graph on a vertex v can be regarded as the the operation where in the neighborhood of v we connect all the disconnected vertices and disconnect all the connected vertices. For instance, applying a local complementation on vertex $v = 1$ on the graph with adjacency matrix Γ in Eq. (59), we obtain

$$\Gamma_{\text{Leung}} \stackrel{\text{def}}{=} \begin{pmatrix} 0 & 1 & 1 & 1 \\ 1 & 0 & 0 & 0 \\ 1 & 0 & 0 & 0 \\ 1 & 0 & 0 & 0 \end{pmatrix} \stackrel{\text{LC}_{v=1}}{\longrightarrow} \Gamma'_{\text{Leung}} \stackrel{\text{def}}{=} \begin{pmatrix} 0 & 1 & 1 & 1 \\ 1 & 0 & 1 & 1 \\ 1 & 1 & 0 & 1 \\ 1 & 1 & 1 & 0 \end{pmatrix}. \tag{60}$$

It turns out that Γ_{Leung} and Γ'_{Leung} are the only two adjacency matrices corresponding to the only two connected graphs, up to graph isomorphisms, that realize the Leung et *al.* [[4, 1]] code. As a matter of fact, recall that the LC orbit $\mathbf{L} = [G]$ of a graph G is the set of all non-isomorphic graphs, including G itself, that can be transformed into G by any sequence of local complementations and vertex permutations. Let $\mathcal{G}_n$ denote the set of all non-isomorphic simple unidirected connected graphs on n vertices. Let $\mathcal{L}_n \stackrel{\text{def}}{=} \{\mathbf{L}_1,..., \mathbf{L}_k\}$ be the set of all distinct orbits of graphs in $\mathcal{G}_n$. All $\mathbf{L} \in \mathcal{L}_n$ are disjoint and $\mathcal{L}_n$ constitutes a partitioning of $\mathcal{G}_n$, that is to say

$$\mathcal{G}_n \stackrel{\text{def}}{=} \bigcup_{i=1}^{k} \mathbf{L}_i. \tag{61}$$

Two graphs, G_1 and G_2, are equivalent with respect to local complementations and vertex permutations if one of the graphs is in the LC orbit of the other, for instance $G_2 \in [G_1]$. In [30], the set $\mathcal{L}_4$ of all LC orbits on 4 vertices was generated. It was shown that despite the fact that there are $2^{\binom{4}{2}} = 64$ unidirected simple graphs on 4 vertices, the number of non-isomorphic connected graphs is only $|\mathcal{G}_4| = 6$. Furthermore, it was shown that there are only $|\mathcal{L}_4| = 2$ distinct LC orbits on 4 vertices, $\mathcal{L}_4 = \{\mathbf{L}_1, \mathbf{L}_2\}$ with,

$$\Gamma_{\mathbf{L}_1}^{(1)} \stackrel{\text{def}}{=} \begin{pmatrix} 0 & 1 & 1 & 1 \\ 1 & 0 & 0 & 1 \\ 1 & 0 & 0 & 1 \\ 1 & 1 & 1 & 0 \end{pmatrix}, \Gamma_{\mathbf{L}_1}^{(2)} \stackrel{\text{def}}{=} \begin{pmatrix} 0 & 1 & 1 & 1 \\ 1 & 0 & 1 & 0 \\ 1 & 1 & 0 & 0 \\ 1 & 0 & 0 & 0 \end{pmatrix}, \Gamma_{\mathbf{L}_1}^{(3)} \stackrel{\text{def}}{=} \begin{pmatrix} 0 & 1 & 0 & 1 \\ 1 & 0 & 1 & 0 \\ 0 & 1 & 0 & 0 \\ 1 & 0 & 0 & 0 \end{pmatrix}, \Gamma_{\mathbf{L}_1}^{(4)} \stackrel{\text{def}}{=} \begin{pmatrix} 0 & 1 & 0 & 1 \\ 1 & 0 & 1 & 0 \\ 0 & 1 & 0 & 1 \\ 1 & 0 & 1 & 0 \end{pmatrix}, \tag{62}$$

and,

$$\Gamma_{\mathbf{L}_2}^{(5)} \stackrel{\text{def}}{=} \begin{pmatrix} 0 & 1 & 1 & 1 \\ 1 & 0 & 1 & 1 \\ 1 & 1 & 0 & 1 \\ 1 & 1 & 1 & 0 \end{pmatrix}, \Gamma_{\mathbf{L}_2}^{(6)} \stackrel{\text{def}}{=} \begin{pmatrix} 0 & 1 & 1 & 1 \\ 1 & 0 & 0 & 0 \\ 1 & 0 & 0 & 0 \\ 1 & 0 & 0 & 0 \end{pmatrix}. \tag{63}$$

We stress that $\Gamma_{\mathbf{L}_2}^{(5)}$ and $\Gamma_{\mathbf{L}_2}^{(6)}$ correspond to Γ'_{Leung} and Γ_{Leung}, respectively. Therefore, we have uncovered that the Leung et *al.* [[4, 1]] code can be realized by graphs that belong to the orbit $\mathbf{L}_2$ of $\mathcal{L}_4$ in $\mathcal{G}_4 = \mathbf{L}_1 \cup \mathbf{L}_2$, the set of all non-isomorphic unidirected connected graphs on 4 vertices.

For the sake of completeness, we also point out that all graphs on up to 12 vertices have been classified under LCs and graph isomorphisms [24]. Furthermore, the number of graphs on n unlabeled vertices or the number of connected graphs with n vertices can be found in [31]. Finally, a very recent database of interesting graphs appears in [32].

3. Step three

Let us consider the symmetric adjacency matrix Γ_{Leung} as given in Eq. (60). How do we find the enlarged **graph** with corresponding symmetric coincidence matrix Ξ_{Leung} given Γ_{Leung}? Recall that the graph related to Γ_{Leung} realizes a stabilizer code which is locally Clifford equivalent to the Leung et *al.* code with standard binary stabilizer matrix $\mathcal{S}'_{\text{b}}$ given by

$$\mathcal{S}'_{\text{b}} \overset{\text{def}}{=} \left\langle X^1 Z^2 Z^3 Z^4,\ Z^1 X^2,\ X^3 X^4 \right\rangle. \tag{64}$$

Putting $g_1 \overset{\text{def}}{=} X^1 Z^2 Z^3 Z^4$, $g_2 \overset{\text{def}}{=} Z^1 X^2$ and $g_3 \overset{\text{def}}{=} X^3 X^4$, we have

$$\mathcal{S}'_b = \langle g_1, g_2, g_3 \rangle = \{ I,\ g_1,\ g_2,\ g_3,\ g_1 g_2,\ g_1 g_3,\ g_2 g_3,\ g_1 g_2 g_3 \}. \tag{65}$$

The 8-dimensional binary vector representation of these stabilizer operators is given by,

$$I \leftrightarrow v_I = (0000\,|0000)\,,\ g_1 \leftrightarrow v_{g_1} = (0111\,|1000)\,,\ g_2 \leftrightarrow v_{g_2} = (1000\,|0100)\,,$$

$$g_3 \leftrightarrow v_{g_3} = (0000\,|0011)\,,\ g_1 g_2 \leftrightarrow v_{g_1 g_2} = (1111\,|1100)\,,\ g_1 g_3 \leftrightarrow v_{g_1 g_3} = (0111\,|1011)\,,$$

$$g_2 g_3 \leftrightarrow v_{g_2 g_3} = (1000\,|0111)\,,\ g_1 g_2 g_3 \leftrightarrow v_{g_1 g_2 g_3} = (1111\,|1111)\,. \tag{66}$$

Recall that for a graph code with both 1-input and n-output vertices, its corresponding coincidence matrix $\Xi_{(n+1)\times(n+1)}$ has the form expressed in Eq. (44). The graph code with symmetric coincidence matrix $\Xi_{(n+1)\times(n+1)}$ is equivalent to stabilizer codes being associated with the isotropic subspace $\mathcal{S}_{\text{isotropic}}$ defined as,

$$\mathcal{S}_{\text{isotropic}} \overset{\text{def}}{=} \left\{ (Ak\,|k) : k \in \ker B^\dagger \right\}, \tag{67}$$

that is, omitting unimportant phase factors, with the binary stabilizer group $\mathcal{S}_b$,

$$\mathcal{S}_b \overset{\text{def}}{=} \left\{ g_k = X^k Z^{Ak} : k \in \ker B^\dagger \right\}. \tag{68}$$

In our case, in agreement with the four conditions for attaching input vertices as outlined in the S-work paragraph, it turns out that

$$B_{4\times 1} \overset{\text{def}}{=} \begin{pmatrix} 0 \\ 0 \\ 1 \\ 1 \end{pmatrix} \text{ and, } A \overset{\text{def}}{=} \begin{pmatrix} 0 & 1 & 1 & 1 \\ 1 & 0 & 0 & 0 \\ 1 & 0 & 0 & 0 \\ 1 & 0 & 0 & 0 \end{pmatrix} \equiv \Gamma_{\text{Leung}}. \tag{69}$$

Finally, the enlarged graph is defined by the following symmetric coincidence matrix Ξ_{Leung},

$$\Xi_{\text{Leung}} \overset{\text{def}}{=} \begin{pmatrix} 0 & 0 & 0 & 1 & 1 \\ 0 & 0 & 1 & 1 & 1 \\ 0 & 1 & 0 & 0 & 0 \\ 1 & 1 & 0 & 0 & 0 \\ 1 & 1 & 0 & 0 & 0 \end{pmatrix}. \tag{70}$$

An additional self-consistency check that substantiates the correctness of Ξ_{Leung} in Eq. (70) is represented by the fact that any g_k in $\mathcal{S}'_b$ in Eq. (65) has a 8-dimensional binary vector representation of the form v_{g_k} with $v_{g_k} \overset{\text{def}}{=} (\Gamma_{\text{Leung}} k_{g_k}\,|k_{g_k})$ with $k_{g_k} \in \ker B^\dagger$ with B given in Eq. (69).

V. FINAL REMARKS

In this article, we proposed a systematic scheme for the construction of graphs with both input and output vertices associated with arbitrary binary stabilizer codes. The scheme is characterized by three main steps: first, the stabilizer code is realized as a codeword-stabilized (CWS) quantum code; second, the canonical form of the CWS code is uncovered; third, the input vertices are attached to the graphs. To check the effectiveness of the scheme, we discussed

several graphical constructions of various useful stabilizer codes characterized by single and multi-qubit encoding operators (for details, see appendices). In particular, the error correction capabilities of such quantum codes are verified in graph-theoretic terms as originally advocated by Schlingemann and Werner (for details, see appendices).

Finally, in what follows, possible generalizations of our scheme for the graphical construction of both (stabilizer and nonadditive) nonbinary and continuous-variable quantum codes will be briefly addressed.

The scheme proposed is limited to binary stabilizer codes. How about nonbinary and continuous-variable (CV) codes? How about nonadditive codes? We point out the following three points:

- *From additive to nonadditive case.* The codeword-stabilized quantum code formalism presents a unifying approach to both additive and nonadditive quantum error-correcting codes, for both binary and nonbinary states [12].

- *From binary to nonbinary case.* The stabilizer formalism, graph states and quantum error correcting codes for d-dimensional quantum systems have been extensively considered in [33] and [34]. However, as pointed out in [35], no straightforward extension of the stabilizer formalism in terms of generators within the Pauli group is possible for d-level systems. As a consequence, it is possible that results obtained within the binary framework are no longer valid when taking into consideration weighted graph states. The generalizations of the Pauli group, the Clifford group, and the stabilizer states for qudits in a Hilbert space of arbitrary dimension d appears in [36]. When moving into the nonbinary case, new features emerge. For instance, the symmetric adjacency matrix does not contain any longer binary entries as in the case of a simple graph as in qubit systems. The generalization of the Pauli operators, the so-called Weyl operators, are no longer Hermitian. The finite field $\mathbf{F}_2$ is replaced by the finite field of prime order d and all arithmetic operations are defined modulo d. The dimension d can be naturally generalized to prime power dimension $d = p^r$ with p being prime and r being an integer. If, however, the underlying integer ring is no longer a field, one loses the vector space structure of $\mathbf{F}_d$, which demands some caution with respect to the concept of a basis. If d contains multiple prime factors, the stabilizer, consisting of d^N different elements, is in general no longer generated by a set of only N generators. For the minimal generating set, more elements $N \leq m \leq 2N$ of the stabilizer might be needed as pointed out in [36]. Furthermore, it is possible to show that the action of the local (generalized) Clifford group on nonbinary stabilizer states can be translated into operations on graphs. However, unlike the binary case, the single local complementation is replaced by a pair of two different graph-theoretic operations. Furthermore, an efficient polynomial time algorithm to verify whether two graph states, in the non-binary case, are locally Clifford equivalent is available [37]. Despite these challenges, new important advances have been recently achieved. For instance, an explicit method of going from qudit CSS codes to qudit graph codes, including all the encoding and decoding procedures, has been presented in [38].

- *From discrete to continuous case.* A remarkable difference between discrete and continuous variables (DV and CV, respectively) quantum information is that while quantum states and unitary transformations involved are described by integer-valued parameters in the DV case, they are characterized by *real*-valued parameters in the CV case. The continuous-variable analog of the Pauli and Clifford algebras and groups together with sets of gates that can efficiently simulate any arbitrary unitary transformation in these groups were defined in [39]. The standard Pauli group for CV quantum computation on n coupled oscillator is the Heisenberg-Weyl group $\mathcal{HW}(n)$ which consists of phase-space displacement operators for the n oscillators. Unlike the discrete Pauli group for qubits, the group $\mathcal{HW}(n)$ is a continuous Lie group, and can therefore only be generalized by a set of continuously parametrized operators. Furthermore, the Clifford group for CV is the semidirect product group of the symplectic group and Heisenberg-Weyl group, $Sp(2n, \mathbb{R}) \ltimes \mathcal{HW}(n)$, consisting of all phase-space translations along with all one-mode and two-mode squeezing transformations [39]. This group is generated by inhomogeneous quadratic polynomials in the canonical operators. For DV, it is possible to generate the Clifford group using only the CNOT, Hadamard and phase gates. However, in the CV case, the analog of these gates (namely, the SUM, the Fourier F and the phase $P(\eta)$ gates with $\eta \in \mathbb{R}$) are all elements of $Sp(2n, \mathbb{R})$. They are generated by homogeneous quadratic Hamiltonians only. Thus, they are in the subgroup of the Clifford group. In order to generate the entire Clifford group, one requires a continuous $\mathcal{HW}(1)$ transformation (i.e., a linear Hamiltonian that generates a one-parameter subgroup of $\mathcal{HW}(1)$) such as the Pauli operator $X(q)$ with $q \in \mathbb{R}$. Finally, the Clifford group in the CV case is generated by the set $\{SUM, F, P(\eta), X(q) : \eta, q \in \mathbb{R}\}$. Continuous-variable graph states were proposed in [40, 41]. It is of great relevance understanding the graph-theoretic transformation rules that describe both local unitary and local Clifford unitary equivalences of arbitrary CV graph states. For a particular class of CV graph states, the so-called CV four-mode unweighted graph states, such transformation rules have been uncovered in [42]. It turns out that even for such restricted class of states, the corresponding local Clifford unitary cannot exactly mirror that for the qubit case and a greater level of complexity arises in the CV framework. In addition, the complete implementation of local complementations

for CV weighted graphs (a weighted graph state is described by a graph $G = (V, E)$ in which every edge is specified by a factor Ω_{ab} corresponding to the strength of modes a and b; for unweighted graph states, all the interactions have the same strength) remains an open problem. In [43], the graphical description of local Clifford transformations for CV weighted graph states were considered. In particular, it was shown that unlike qubit weighted graph states, CV weighted graph states can be expressed by the stabilizer formalism in terms of generators in the Pauli group. The main reason for this difference is that the CZ gate for qubit is periodic as a function of the interaction strength while the CV CZ gate is not. We remark that in this context, the CV case is even more subtle, besides the fact that weighted CV graph states are still stabilizer states unlike weighted qubit graph states. In particular, the most general form of weighted CV graph states has a complex adjacency matrix. In fact, all real-valued (with real adjacency matrix) CV graph states (weighted or unweighted) are unphysical states (only defined in the limit of infinite squeezing). In order to represent physical CV graph states, corresponding to pure multi-mode Gaussian states, the weights become necessarily complex. All this is introduced and discussed in [44] where it is also described how such general, physical CV graph states transform under local and general Gaussian transformations. In particular, we emphasize that the general results presented in [44] include Zhang's results in [42, 43] as the limiting cases of infinite squeezing and real-weighted states. We recall that in the qubit-case a systematic classification of local Clifford equivalence of qubit graph states has been executed and an efficient algorithm with polynomial time complexity in the number of qubits to decide whether two given stabilizer states are local Clifford equivalent is known. In the CV framework, it can be proved that any CV stabilizer state is equivalent to a weighted graph state under local Clifford operations, the equivalence between two stabilizer states under local Clifford operations can be investigated by studying the equivalence between weighted graph states under local Clifford operations [45]. However, the existence of a universal method to determine whether two CV stabilizer states with finite modes are equivalent or not under local Clifford operation has been only partially addressed in [44]. In the CV case, the local-Clifford equivalence of stabilizer states translates into local-Gaussian unitary equivalence of (pure) Gaussian states. Furthermore, while a single unifying definition of complex-weighted CV graph states (Gaussian pure states) together with graph transformation rules for all local Gaussian unitary operations were presented in [44], no systematic algorithm for deciding on the local equivalence of two given CV (Gaussian) stabilizer states was discussed. This issue, however, was recently addressed in [46]. Specifically, necessary and sufficient conditions of Gaussian local unitary equivalence for arbitrary (mixed or pure) Gaussian states were derived. Despite such advances, several questions remain to be better understood. For instance, the relation between local equivalence of CV Gaussian states and Gaussian local equivalence deserves further investigation [46, 47]. A thorough analysis of this type of questions is not only important from a theoretical point of view, it can also be of practical use concerning which states are the most suitable for optical realizations of stabilizer quantum error correction codes in any dimension [48].

In view of these considerations, we conclude that the extension of our proposed scheme to arbitrary nonbinary/CV codes and/or additive/nonadditive codes might turn out to be nontrivial. However, in light of the recent advances, we are confident that its generalization could be achieved with a reasonable effort.

[1] R. Diestel, *Graph Theory*, Springer, Heildeberg (2000).
[2] D. B. West, *Introduction to Graph Theory*, Prentice Hall, Upper Saddle River, New Jersey (2001).
[3] R. J. Wilson and J. J. Watkins, *Graphs: An Introductory Approach*, John Wiley & Sons, Inc. (1990).
[4] D. Gottesman, *An introduction to quantum error correction and fault-tolerant quantum computation*, in Quantum Information Science and Its Contributions to Mathematics, Proceedings of Symposia in Applied Mathematics **68**, pp. 13-58, Amer. Math. Soc., Providence, Rhode Island, USA (2010).
[5] D. Schlingemann and R. F. Werner, *Quantum error-correcting codes associated with graphs*, Phys. Rev. **A65**, 012308 (2001).
[6] D. Schlingemann, *Stabilizer codes can be realized as graph codes*, Quant. Inf. Comput. **2**, 307 (2002).
[7] M. Grassl, A. Klappenecker and M. Rotteler, *Graphs, quadratic forms, and quantum codes*, in *Proceedings of the International Symposium on Information Theory*, Lausanne, Switzerland, 30 June- 5 July, p. 45 (2002).
[8] H. J. Briegel and R. Raussendorf, *Persistent entanglement in arrays of interacting particles*, Phys. Rev. Lett. **86**, 910 (2001).

[9] M. Hein, J. Eisert, and H. J. Briegel, *Multiparty entanglement in graph states*, Phys. Rev. **A69**, 062311 (2004).

[10] M. Van den Nest, J. Dehaene and B. De Moor, *Graphical description of the action of local Clifford transformations on graph states*, Phys. Rev. **A69**, 022316 (2004).

[11] A. Cross, G. Smith, J. A. Smolin and B. Zeng, *Codeword stabilized quantum codes*, IEEE Trans. Info. Theory **55**, 433 (2009).

[12] X. Chen, B. Zeng and I. L. Chuang, *Nonbinary codeword-stabilized quantum codes*, Phys. Rev. **A78**, 062315 (2008).

[13] S. Yu, Q. Chen and C. H. Oh, *Graphical quantum error-correcting codes*, arXiv:quant-ph/0709.1780 (2007).

[14] D. Hu, W. Tang, M. Zhao, and Q. Chen, *Graphical nonbinary quantum error-correcting codes*, Phys. Rev. **A78**, 012306 (2008).

[15] S. Beigi, I. Chuang, M. Grassl, P. Shor and B. Zeng, *Graph concatenation for quantum codes*, J. Math. Phys. **52**, 022201 (2011).

[16] D. W. Leung, M. A. Nielsen, I. L. Chuang, and Y. Yamamoto, *Approximate quantum error correction can lead to better codes*, Phys. Rev. **A56**, 2567 (1997).

[17] D. Markham and B. C. Sanders, *Graph states for quantum secret sharing*, Phys. Rev. **A78**, 042309 (2008).

[18] A. Marin and D. Markham, *On the equivalence between sharing quantum and classical secrets, and error correction*, Phys. Rev. **A88**, 042332 (2013).

[19] B. A. Bell, D. A. Herrera-Marti, M. S. Tame, D. Markham, W. J. Wadsworth, and J. G. Rarity, *Experimental demonstration of a graph state quantum error-correcting code*, Nature Comm. **5**, 3658 (2014).

[20] A. R. Calderbank, E. M. Rains, P. W. Shor and N. J. A. Sloane, *Quantum error correction via codes over GF*(4), IEEE Transactions on Information Theory **44**, 1369 (1998).

[21] F. Gaitan, *Quantum Error Correction and Fault Tolerant Quantum Computing*, CRC Press (2008).

[22] D. Gottesman, *Stabilizer codes and quantum error correction*, Ph. D. thesis, California Institute of Technology, Pasadena, CA, 1998.

[23] A. Bouchet, *Recognizing locally equivalent graphs*, Discrete Mathematics **114**, 75 (1993).

[24] L. E. Danielsen and M. G. Parker, *On the classification of all self-dual additive codes over GF(4) of length up to* 12, J. Combin. Theory **A113**, 1351 (2006).

[25] J. Dehaene and B. De Moor, *Clifford group, stabilizer states, and linear and quadratic operations over GF* (2), Phys. Rev. **A68**, 042318 (2003).

[26] H. Pollatsek and M. B. Ruskai, *Permutationally invariant codes for quantum error correction*, Lin. Alg. Appl. **392**, 255 (2004).

[27] S. Beigi, J. Chen, M. Grassl, Z. Ji, Q. Wang, and B. Zeng, *Symmetries of codeword stabilized quantum codes*, in TQC 2013, 8th Conference on Theory of Quantum Computation, Communication and Cryptography, 21-23 May, Guelph, Canada (2013).

[28] K. R. Parthasarathy, *Extremality and entanglement of states in coupled quantum systems*, AIP Conf. Proc. **864**, 54 (2006).

[29] A. S. Fletcher, P. W. Shor, and M. Z. Win, *Channel-adapted quantum error correction for the amplitude damping channel*, IEEE Transactions on Information Theory **54**, 5705 (2008).

[30] L. E. Danielsen, *On self-dual quantum codes, graphs, and boolean functions*, arXiv:quant-ph/0503236 (2005).

[31] N. J. A. Sloane, *The online encyclopedia of integer sequences*, https://oeis.org.

[32] G. Brinkmann, K. Coolsaet, J. Goedgebeur, H. Melot, *House of graphs: a database of interesting graphs*, Discrete Appl. Math. **161**, 311 (2013).

[33] D. Schlingemann, *Cluster states, algorithms and graphs*, Quant. Inf. Comput. **4**, 287 (2004).

[34] D. Schlingemann, *Error syndrome calculation for graph codes on a one way quantum computer: Towards a quantum memory*, J. Math. Phys. **45**, 4322 (2004).

[35] M. Hein, W. Dur, J. Eisert, R. Raussendorf, M. Van den Nest, H. J. Briegel, *Entanglement in graph states and its applications*, arXiv:quant-ph/0602096 (2006).

[36] E. Hostens, J. Dehaene and B. De Moor, *Stabilizer states and Clifford operations for systems of arbitrary dimensions and modular arithmetic*, Phys. Rev. **A71**, 042315 (2005).

[37] M. Bahramgiri and S. Beigi, *Graph states under the action of local Clifford group in non-binary case*, arXiv:quant-ph/0610267 (2007).

[38] A. Marin, *Entanglement in quantum information networks. Graph states for quantum secret sharing*, Ph. D. thesis, Telecom ParisTech, France (2013).

[39] S. D. Bartlett, B. C. Sanders, S. L. Braunstein and K. Nemoto, *Efficient classical simulation of continuous variable quantum information processes*, Phys. Rev. Lett. **88**, 097904 (2002).

[40] J. Zhang and S. L. Braunstein, *Continuous-variable Gaussian analog of cluster states*, Phys. Rev. **A73**, 032318 (2006).

[41] P. van Loock, C. Weedbrook, and M. Gu, *Building Gaussian cluster states by linear optics*, Phys. Rev. **A76**, 032321 (2007).

[42] J. Zhang, *Local complementation rule for continuous-variable four-mode unweighted graph states*, Phys. Rev. **A78**, 034301 (2008).

[43] J. Zhang, *Graphical description of local Gaussian operations for continuous-variable weighted graph states*, Phys. Rev. **A78**, 052307 (2008).

[44] N. C. Menicucci, S. T. Flammia, and P. van Loock, *Graphical calculus for Gaussian pure states*, Phys. Rev. **A83**, 042335 (2011).

[45] J. Zhang, G. He and G. Zeng, *Equivalence of continuous-variable stabilizer states under local Clifford operations*, Phys. Rev. **A80**, 052333 (2009).

[46] G. Giedke and B. Kraus, *Gaussian local unitary equivalence of n-mode Gaussian states and Gaussian transformations by*

local operations with classical communications, Phys. Rev. **A89**, 012335 (2014).

[47] O. Cernotic and J. Fiurasek, *Transformations of symmetric multipartite Gaussian states by Gaussian local operations and classical communication*, Phys. Rev. **A89**, 042331 (2014).

[48] P. van Loock and D. Markham, *Implementing stabilizer codes by linear optics*, AIP Conf. Proc. **1363**, 256 (2011).

[49] M. Grassl, Th. Beth and T. Pellizzari, *Codes for the quantum erasure channel*, Phys. Rev. **A56**, 33 (1997).

[50] R. Laflamme, C. Miquel, J. P. Paz, and W. H. Zurek, *Perfect quantum error correcting code*, Phys. Rev. Lett. **77**, 198 (1996).

[51] C. H. Bennett, D. P. Di Vincenzo, J. A. Smolin, and W. K. Wootters, *Mixed-state entanglement and quantum error correction*, Phys. Rev. **A54**, 3824 (1996).

[52] B. Shaw, M. M. Wilde, O. Oreshkov, I. Kremsky, and D. A. Lidar, *Encoding one logical qubit into six physical qubits*, Phys. Rev. **A78**, 012337 (2008).

[53] A. M. Steane, *Multiple-particle interference and quantum error correction*, Proc. R. Soc. Lond. **A452**, 2551 (1996).

[54] A. R. Calderbank and P. W. Shor, *Good quantum error correcting codes exist*, Phys. Rev. **A54**, 1098 (1996).

[55] P. W. Shor, *Scheme for reducing decoherence in quantum computer memory*, Phys. Rev. **A52**, 2493 (1995).

[56] D. Gottesman, *Class of quantum error correcting codes saturating the quantum Hamming bound*, Phys. Rev. **A54**, 1862 (1996).

Appendix A: Single qubit encoding

Before presenting our illustrative examples, we would like to make few remarks on graphs in quantum error correction.

The coincidence matrix of a graph characterizes the structural properties of a graph: number of vertices, number of edges, and, above all, the manner in which vertices are connected. The structure of graphs associated with stabilizer quantum codes hides essential information about the graphical error detection conditions in Eqs. (38) and (39). Such graphical conditions may not be necessarily visible in a direct manner as originally pointed out in [6]. This becomes especially evident when the number of vertices and edges in the graph increases in the presence of multi-qubit encodings and/or big code lengths. However, graphs do maintain part of their appeal in that they provide a *geometric* aid in identifying the explicit *algebraic* linear equations that characterize the graphical error detection conditions without taking into consideration the explicit form of their corresponding coincidence matrices. In our opinion, this is no negligible advantage of our graphical approach since identifying the algebraic equations directly from the coincidence matrices can become quite tedious without a visual aid provided by graphs. Clearly, the peculiar advantage of our scheme is that it allows to uncover the expression of the coincidence matrix of a graph associated with a binary stabilizer code. We shall further discuss some of these aspects in our illustrative examples that appear below.

As an additional side remark, we point out that there could be scenarios where one can exploit the high symmetry of the graph in an efficient manner in order to check the graphical conditions for error detection [5]. While symmetry arguments are elegant and powerful, they require some caution in the case of graphs in quantum error correction: symmetries of graphs are not necessarily the same as symmetries of the associated stabilizer codes [6, 7, 27]. For instance, graphs with different symmetries can lead to a class of codes that are equivalent to the CSS seven-qubit code as shown in Ref. [7]. As recently pointed out in [27], a clear understanding of the requirements under which a graph can exhibit the same symmetry as the quantum (CWS, in general) code is still missing. In this article, we do not address this issue. However, in agreement with the statement appeared in Ref. [27], we do think that this point is definitively worth further attention.

1. The $[[3, 1, 1]]$ stabilizer code

Before applying our scheme for the construction of the graph associated with a $[[3, 1, 1]]$ stabilizer code [21], we emphasize how intricate can be finding the explicit expression of unitary transformations that relate sets of vertex stabilizers of graphs. For the sake of reasoning, consider the following sets $\mathcal{S}_{|\Gamma_1\rangle}$, $\mathcal{S}_{|\Gamma_2\rangle}$ and $\mathcal{S}_{|\Gamma_3\rangle}$ defined as

$$\mathcal{S}_{|\Gamma_1\rangle} \overset{\text{def}}{=} \left\langle X^1,\, X^2,\, X^3 \right\rangle,\; \mathcal{S}_{|\Gamma_2\rangle} \overset{\text{def}}{=} \left\langle X^1 Z^2 Z^3,\, Z^1 X^2,\, Z^1 X^3 \right\rangle \text{ and, } \mathcal{S}_{|\Gamma_3\rangle} \overset{\text{def}}{=} \left\langle X^1 Z^2 Z^3,\, Z^1 X^2 Z^3,\, Z^1 Z^2 X^3 \right\rangle, \quad \text{(A1)}$$

respectively. In the canonical basis $\mathcal{B}_{\mathcal{H}_2^3}$ of the eight-dimensional *complex* Hilbert space $\mathcal{H}_2^3$,

$$\mathcal{B}_{\mathcal{H}_2^3} \overset{\text{def}}{=} \left\{ |000\rangle,\, |001\rangle,\, |010\rangle,\, |011\rangle,\, |100\rangle,\, |101\rangle,\, |110\rangle,\, |111\rangle \right\}, \quad \text{(A2)}$$

the graph states $|\Gamma_1\rangle$, $|\Gamma_2\rangle$ and $|\Gamma_3\rangle$ read,

$$|\Gamma_1\rangle \overset{\text{def}}{=} \frac{|000\rangle + |001\rangle + |010\rangle + |011\rangle + |100\rangle + |101\rangle + |110\rangle + |111\rangle}{\sqrt{8}},$$

$$|\Gamma_2\rangle \overset{\text{def}}{=} \frac{|000\rangle + |001\rangle + |010\rangle + |011\rangle + |100\rangle - |101\rangle - |110\rangle + |111\rangle}{\sqrt{8}},$$

$$|\Gamma_3\rangle \overset{\text{def}}{=} \frac{|000\rangle + |001\rangle + |010\rangle - |011\rangle + |100\rangle - |101\rangle - |110\rangle - |111\rangle}{\sqrt{8}}. \quad \text{(A3)}$$

We observe that,

$$\mathcal{S}_{|\Gamma_3\rangle} = \mathcal{U}_{|\Gamma_1\rangle \to |\Gamma_3\rangle} \mathcal{S}_{|\Gamma_1\rangle} \mathcal{U}_{|\Gamma_1\rangle \to |\Gamma_3\rangle}^\dagger, \quad \text{(A4)}$$

with,

$$\mathcal{U}_{|\Gamma_1\rangle \to |\Gamma_3\rangle} \overset{\text{def}}{=} \left(I^1 \otimes I^2 \otimes H^3 \right) \cdot \left(U_{CP}^{12} \otimes I^3 \right) \left(I^1 \otimes H^2 \otimes I^3 \right) \cdot \left(I^1 \otimes U_{CP}^{23} \right) \cdot \left(U_{CP}^{12} \otimes I^3 \right). \quad \text{(A5)}$$

Similarly, it can be shown that

$$\mathcal{S}_{|\Gamma_2\rangle} = \mathcal{U}_{|\Gamma_1\rangle\to|\Gamma_2\rangle}\mathcal{S}_{|\Gamma_1\rangle}\mathcal{U}^{\dagger}_{|\Gamma_1\rangle\to|\Gamma_2\rangle}, \tag{A6}$$

with,

$$\mathcal{U}_{|\Gamma_1\rangle\to|\Gamma_2\rangle} \overset{\text{def}}{=} \left(H^1\otimes I^2\otimes I^3\right)\cdot\left(I^1\otimes H^2\otimes I^3\right)\cdot\left(I^1\otimes U_{CP}^{23}\right)\cdot\left(U_{CP}^{12}\otimes I^3\right). \tag{A7}$$

Finally, combining (A4) and (A6), we get

$$\mathcal{S}_{|\Gamma_3\rangle} = \mathcal{U}_{|\Gamma_2\rangle\to|\Gamma_3\rangle}\mathcal{S}_{|\Gamma_2\rangle}\mathcal{U}^{\dagger}_{|\Gamma_2\rangle\to|\Gamma_3\rangle} = \mathcal{U}_{|\Gamma_1\rangle\to|\Gamma_3\rangle}\mathcal{S}_{|\Gamma_1\rangle}\mathcal{U}^{\dagger}_{|\Gamma_1\rangle\to|\Gamma_3\rangle} = \mathcal{U}_{|\Gamma_1\rangle\to|\Gamma_3\rangle}\mathcal{U}^{\dagger}_{|\Gamma_1\rangle\to|\Gamma_2\rangle}\mathcal{S}_{|\Gamma_2\rangle}\mathcal{U}_{|\Gamma_1\rangle\to|\Gamma_2\rangle}\mathcal{U}^{\dagger}_{|\Gamma_1\rangle\to|\Gamma_3\rangle}, \tag{A8}$$

that is,

$$\mathcal{U}_{|\Gamma_2\rangle\to|\Gamma_3\rangle} = \mathcal{U}_{|\Gamma_1\rangle\to|\Gamma_3\rangle}\mathcal{U}^{\dagger}_{|\Gamma_1\rangle\to|\Gamma_2\rangle}. \tag{A9}$$

After some algebra, we obtain that the explicit expressions for the Clifford unitary matrices $\mathcal{U}_{|\Gamma_1\rangle\to|\Gamma_3\rangle}$, $\mathcal{U}_{|\Gamma_1\rangle\to|\Gamma_2\rangle}$, and $\mathcal{U}_{|\Gamma_2\rangle\to|\Gamma_3\rangle}$ become,

$$\mathcal{U}_{|\Gamma_1\rangle\to|\Gamma_3\rangle} \overset{\text{def}}{=} \frac{1}{2}\begin{pmatrix} 1 & 1 & 1 & -1 & 0 & 0 & 0 & 0 \\ 1 & -1 & 1 & 1 & 0 & 0 & 0 & 0 \\ 1 & 1 & -1 & 1 & 0 & 0 & 0 & 0 \\ 1 & -1 & -1 & -1 & 0 & 0 & 0 & 0 \\ 0 & 0 & 0 & 0 & 1 & 1 & -1 & 1 \\ 0 & 0 & 0 & 0 & 1 & -1 & -1 & -1 \\ 0 & 0 & 0 & 0 & -1 & -1 & -1 & 1 \\ 0 & 0 & 0 & 0 & -1 & 1 & -1 & -1 \end{pmatrix}, \mathcal{U}_{|\Gamma_1\rangle\to|\Gamma_2\rangle} \overset{\text{def}}{=} \frac{1}{2}\begin{pmatrix} 1 & 0 & 1 & 0 & 1 & 0 & -1 & 0 \\ 0 & 1 & 0 & -1 & 0 & 1 & 0 & 1 \\ 1 & 0 & -1 & 0 & 1 & 0 & 1 & 0 \\ 0 & 1 & 0 & 1 & 0 & 1 & 0 & -1 \\ 1 & 0 & 1 & 0 & -1 & 0 & 1 & 0 \\ 0 & 1 & 0 & -1 & 0 & -1 & 0 & -1 \\ 1 & 0 & -1 & 0 & -1 & 0 & -1 & 0 \\ 0 & 1 & 0 & 1 & 0 & -1 & 0 & 1 \end{pmatrix},$$

$$\mathcal{U}_{|\Gamma_2\rangle\to|\Gamma_3\rangle} \overset{\text{def}}{=} \frac{1}{2}\begin{pmatrix} 1 & 1 & 0 & 0 & 1 & 1 & 0 & 0 \\ 1 & -1 & 0 & 0 & 1 & -1 & 0 & 0 \\ 0 & 0 & 1 & 1 & 0 & 0 & 1 & 1 \\ 0 & 0 & 1 & -1 & 0 & 0 & 1 & -1 \\ 1 & 1 & 0 & 0 & -1 & -1 & 0 & 0 \\ 1 & -1 & 0 & 0 & -1 & 1 & 0 & 0 \\ 0 & 0 & -1 & -1 & 0 & 0 & 1 & 1 \\ 0 & 0 & -1 & 1 & 0 & 0 & 1 & -1 \end{pmatrix}. \tag{A10}$$

A systematic strategy for finding the explicit expressions for the unitary transformations in Eqs. (A5), (A7) and (A9) would be very useful. The VdN-work is especially important in this regard, as we shall see.

Let us consider the three-qubit bit-flip repetition code with codespace spanned by the codewords $|0_L\rangle \overset{\text{def}}{=} |000\rangle$ and $|1_L\rangle \overset{\text{def}}{=} |111\rangle$. The two stabilizer generators of this code are $g_1 \overset{\text{def}}{=} Z^1Z^2$ and $g_2 \overset{\text{def}}{=} Z^1Z^3$ while the logical operations can read $\bar{Z} \overset{\text{def}}{=} Z^1Z^2Z^3$ and $\bar{X} \overset{\text{def}}{=} X^1X^2X^3$ with,

$$\bar{Z}|0_L\rangle = |0_L\rangle, \ \bar{Z}|1_L\rangle = -|1_L\rangle, \ \bar{X}|0_L\rangle = |1_L\rangle \ \text{and,} \ \bar{X}|1_L\rangle = |0_L\rangle. \tag{A11}$$

This stabilizer code can be regarded as a CWS code with codeword stabilizer given by,

$$\mathcal{S}_{\text{CWS}} \overset{\text{def}}{=} \left\langle g_1, g_2, \bar{Z} \right\rangle = \left\langle Z^1Z^2, Z^1Z^3, Z^1Z^2Z^3 \right\rangle = \left\langle Z^1, Z^2, Z^3 \right\rangle. \tag{A12}$$

Observe that $\mathcal{S}_{\text{CWS}} = U\mathcal{S}_{|\Gamma_1\rangle}U^{\dagger}$ with $\mathcal{S}_{|\Gamma_1\rangle}$ in Eq. (A1) and $U \overset{\text{def}}{=} H^1H^2H^3$. Therefore, the graph state associated with $\mathcal{S}_{\text{CWS}}$ is locally Clifford equivalent to the graph state $|\Gamma_1\rangle$ in Eq. (A3). Let us consider now an alternative graphical description of the three-qubit bit-flip repetition code that better fits into our scheme.

Let us consider the codespace of the code spanned by the following new codewords,

$$\mathcal{C} \overset{\text{def}}{=} \text{Span} \left\{|0_L\rangle \overset{\text{def}}{=} |000\rangle, \ |1_L\rangle \overset{\text{def}}{=} |111\rangle\right\} \to \mathcal{C}' \overset{\text{def}}{=} \text{Span} \left\{|0'_L\rangle \overset{\text{def}}{=} \frac{|0_L\rangle + |1_L\rangle}{\sqrt{2}}, \ |1'_L\rangle \overset{\text{def}}{=} \frac{|0_L\rangle - |1_L\rangle}{\sqrt{2}}\right\}. \tag{A13}$$

Notice that the codespace of the code does not change since $\mathcal{C}' = \mathcal{C}$ and we have simply chosen a different orthonormal basis to describe the code. However, with this alternative choice, the new codeword stabilizer reads

$$\mathcal{S}'_{\text{CWS}} \stackrel{\text{def}}{=} \langle g_1, g_2, \bar{Z}' \rangle = \langle Z^1 Z^2, Z^1 Z^3, X^1 X^2 X^3 \rangle, \tag{A14}$$

and the remaining logical operation is given by $\bar{X}' \stackrel{\text{def}}{=} Z^1 Z^2 Z^3$. Observe that $\mathcal{S}'_{\text{CWS}}$ is locally Clifford equivalent to $\mathcal{S}''_{\text{CWS}}$ with $\mathcal{S}''_{\text{CWS}} \stackrel{\text{def}}{=} U\mathcal{S}'_{\text{CWS}}U$ and $U \stackrel{\text{def}}{=} H^2 H^3$. The codeword stabilizer $\mathcal{S}''_{\text{CWS}}$ reads,

$$\mathcal{S}''_{\text{CWS}} = \langle Z^1 X^2, Z^1 X^3, X^1 Z^2 Z^3 \rangle. \tag{A15}$$

Observe that $\mathcal{S}''_{\text{CWS}}$ equals $\mathcal{S}_{|\Gamma_2\rangle}$ in Eq. (A1). Therefore, the graph state associated with $\mathcal{S}''_{\text{CWS}}$ is $|\Gamma_2\rangle$ in Eq. (A3). We notice that this is such a simple example that we really do not need to apply our scheme. The adjacency matrix Γ of the graph associated with the CWS code with codeword stabilizer $\mathcal{S}''_{\text{CWS}}$ reads,

$$\Gamma = \begin{pmatrix} 0 & 1 & 1 \\ 1 & 0 & 0 \\ 1 & 0 & 0 \end{pmatrix}. \tag{A16}$$

However, acting with a local complementation on the vertex 1 of the graph with adjacency matrix Γ in (A16), we get

$$\Gamma \to \Gamma' = \begin{pmatrix} 0 & 1 & 1 \\ 1 & 0 & 1 \\ 1 & 1 & 0 \end{pmatrix}. \tag{A17}$$

Furthermore, the new codeword stabilizer becomes $\left[\mathcal{S}''_{\text{CWS}} \right]_{\text{new}}$,

$$\mathcal{S}''_{\text{CWS}} \to \left[\mathcal{S}''_{\text{CWS}} \right]_{\text{new}} \stackrel{\text{def}}{=} \langle X^1 Z^2 Z^3, Z^1 X^2 Z^3, Z^1 Z^2 X^3 \rangle. \tag{A18}$$

Note that the graph state associated with $\left[\mathcal{S}''_{\text{CWS}} \right]_{\text{new}}$ is $|\Gamma_3\rangle$ in Eq. (A3). We also point out that following the VdN-work, it turns out that the 6×6 local unitary Clifford transformation Q that links the six-dimensional binary vector representation of the operators in $\mathcal{S}''_{\text{CWS}}$ and $\left[\mathcal{S}''_{\text{CWS}} \right]_{\text{new}}$ is given by,

$$Q \stackrel{\text{def}}{=} \begin{pmatrix} 1 & 0 & 0 & 0 & 0 & 0 \\ 0 & 1 & 0 & 0 & 1 & 0 \\ 0 & 0 & 1 & 0 & 0 & 1 \\ 1 & 0 & 0 & 1 & 0 & 0 \\ 0 & 0 & 0 & 0 & 1 & 0 \\ 0 & 0 & 0 & 0 & 0 & 1 \end{pmatrix}. \tag{A19}$$

For the sake of clarity, consider

$$\left[\mathcal{S}''_{\text{CWS}} \right]_{\text{new}} \stackrel{\text{def}}{=} \{I, g'_1, g'_2, g'_3, g'_1 g'_2, g'_1 g'_3, g'_2 g'_3, g'_1 g'_2 g'_3\}, \tag{A20}$$

with $g'_1 \stackrel{\text{def}}{=} X^1 Z^2 Z^3$, $g'_2 \stackrel{\text{def}}{=} Z^1 X^2 Z^3$, $g'_3 \stackrel{\text{def}}{=} Z^1 Z^2 X^3$ and,

$$v_I = (000\,|000)\,,\ v_{g'_1} = (011\,|100)\,,\ v_{g'_2} = (101\,|010)\,,\ v_{g'_3} = (110\,|001)\,,\ v_{g'_1 g'_2} = (110\,|110)\,,$$

$$v_{g'_1 g'_3} = (101\,|101)\,,\ v_{g'_2 g'_3} = (011\,|011)\,,\ v_{g'_1 g'_2 g'_3} = (000\,|111)\,, \tag{A21}$$

where $v_{g'}$ denotes the binary vectorial representation of the Pauli operators. Furthermore,

$$\mathcal{S}''_{\text{CWS}} \stackrel{\text{def}}{=} \{I, g_1, g_2, g_3, g_1 g_2, g_1 g_3, g_2 g_3, g_1 g_2 g_3\}, \tag{A22}$$
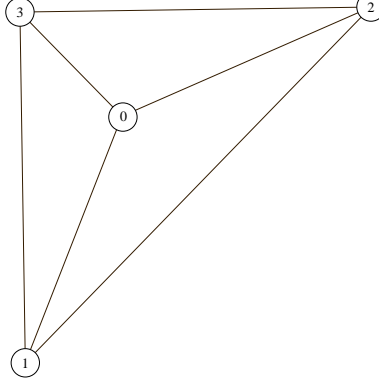
FIG. 1: Graph for a quantum code that is locally Clifford equivalent to the [[3,1,1]]-code.

with $g_1 \stackrel{\text{def}}{=} Z^1 X^2$, $g_2 \stackrel{\text{def}}{=} Z^1 X^3$, $g_3 \stackrel{\text{def}}{=} X^1 Z^2 Z^3$. Using Q in Eq. (A19), we have

$$I \to v_{QI} = (000\,|000)\,, \ g_1 \to v_{Qg_1} = (110\,|110)\,, \ g_2 \to v_{Qg_2} = (101\,|101)\,,$$

$$g_3 \to v_{Qg_3} = (011\,|100)\,, \ g_1 g_2 \to v_{Qg_1 g_2} = (011\,|011)\,, \ g_1 g_3 \to v_{Qg_1 g_3} = (101\,|010)\,,$$

$$g_2 g_3 \to v_{Qg_2 g_3} = (110\,|001)\,, \ g_1 g_2 g_3 \to v_{Qg_1 g_2 g_3} = (000\,|111)\,. \tag{A23}$$

From Eqs. (A21) and (A23), we arrive at

$$v_I = v_{QI}, \ v_{g_1'} = v_{Qg_3}, \ v_{g_2'} = v_{Qg_1 g_3}, \ v_{g_3'} = v_{Qg_2 g_3},$$

$$v_{g_1' g_2'} = v_{Qg_1}, \ v_{g_1' g_3'} = v_{Qg_2}, \ v_{g_2' g_3'} = v_{Qg_1 g_2}, \ v_{g_1' g_2' g_3'} = v_{Qg_1 g_2 g_3}. \tag{A24}$$

Finally, given Γ' in Eq. (A17) and applying the S-work, the coincidence matrix for a graph associated with a $[[3, 1, 1]]$ stabilizer code becomes,

$$\Xi_{[[3,1,1]]} \stackrel{\text{def}}{=} \begin{pmatrix} 0 & 1 & 1 & 1 \\ 1 & 0 & 1 & 1 \\ 1 & 1 & 0 & 1 \\ 1 & 1 & 1 & 0 \end{pmatrix}. \tag{A25}$$

It is not that difficult to use the graphical quantum error correction conditions presented in the SW-work and verify that the $[[3, 1, 1]]$ code with associated coincidence matrix in Eq. (A25) is not a 1-error correcting quantum code.

2.   The $[[4, 1]]$ stabilizer code

Let us consider the Grassl et *al.* perfect 1-erasure correcting four-qubit code with codespace spanned by the following codewords [49],

$$|0_L\rangle \stackrel{\text{def}}{=} \frac{|0000\rangle + |1111\rangle}{\sqrt{2}} \ \text{and,} \ |1_L\rangle \stackrel{\text{def}}{=} \frac{|1001\rangle + |0110\rangle}{\sqrt{2}}. \tag{A26}$$

The three stabilizer generators of such a code are given by $g_1 \stackrel{\text{def}}{=} X^1 X^2 X^3 X^4$, $g_2 \stackrel{\text{def}}{=} Z^1 Z^4$ and $g_3 \stackrel{\text{def}}{=} Z^2 Z^3$. Furthermore, the logical operations are $\bar{X} \stackrel{\text{def}}{=} X^1 X^4$ and $\bar{Z} \stackrel{\text{def}}{=} Z^1 Z^3$. We notice that such a code, just like the four-qubit code provided by Leung et *al.*, is also a 1-error detecting code and can be used for the error correction of single amplitude damping errors. When viewed as a CWS code, the codeword stabilizer reads

$$\mathcal{S}_{\text{CWS}} \stackrel{\text{def}}{=} \langle g_1, g_2, g_3, \bar{Z} \rangle = \langle X^1 X^2 X^3 X^4, Z^1 Z^4, Z^2 Z^3, Z^1 Z^3 \rangle. \tag{A27}$$

Observe that $\mathcal{S}_{\mathrm{CWS}}$ is local Clifford equivalent to $\mathcal{S}'_{\mathrm{CWS}}$ with $\mathcal{S}'_{\mathrm{CWS}} \overset{\text{def}}{=} U\mathcal{S}_{\mathrm{CWS}}U^\dagger$ and $U \overset{\text{def}}{=} H^2 H^3 H^4$. Therefore, $\mathcal{S}'_{\mathrm{CWS}}$ is given by

$$\mathcal{S}'_{\mathrm{CWS}} = \left\langle X^1 Z^2 Z^3 Z^4,\, Z^1 X^4,\, X^2 X^3,\, Z^1 X^3 \right\rangle. \tag{A28}$$

The codeword stabilizer matrix $\mathcal{H}_{\mathcal{S}'_{\mathrm{CWS}}}$ associated with $\mathcal{S}'_{\mathrm{CWS}}$ is given by,

$$\mathcal{H}_{\mathcal{S}'_{\mathrm{CWS}}} \overset{\text{def}}{=} (Z'\,|\,X') = \left(\begin{array}{cccc|cccc} 0 & 1 & 1 & 1 & 1 & 0 & 0 & 0 \\ 1 & 0 & 0 & 0 & 0 & 0 & 0 & 1 \\ 0 & 0 & 0 & 0 & 0 & 1 & 1 & 0 \\ 1 & 0 & 0 & 0 & 0 & 0 & 1 & 0 \end{array} \right). \tag{A29}$$

We observe that $\det X'^{\mathrm{T}} \neq 0$ and, applying the VdN-work, the symmetric adjacency matrix Γ reads,

$$\Gamma \overset{\text{def}}{=} Z'^{\mathrm{T}} \cdot \left(X'^{\mathrm{T}}\right)^{-1} = \begin{pmatrix} 0 & 1 & 1 & 1 \\ 1 & 0 & 0 & 0 \\ 1 & 0 & 0 & 0 \\ 1 & 0 & 0 & 0 \end{pmatrix}. \tag{A30}$$

Therefore, applying now the S-work, the 5×5 symmetric coincidence matrix $\Xi_{[[4,1]]}$ that characterizes the graph with both input and output vertices becomes,

$$\Xi_{[[4,1]]} \overset{\text{def}}{=} \begin{pmatrix} 0 & 0 & 0 & 1 & 1 \\ 0 & 0 & 1 & 1 & 1 \\ 0 & 1 & 0 & 0 & 0 \\ 1 & 1 & 0 & 0 & 0 \\ 1 & 1 & 0 & 0 & 0 \end{pmatrix}. \tag{A31}$$

For the sake of completeness, we also remark that acting with a local complementation with respect to the vertex 1 of the graph with adjacency matrix Γ in Eq. (A30), we obtain the fully connected graph with adjacency matrix Γ',

$$\Gamma \to \Gamma' \equiv g_1(\Gamma) \overset{\text{def}}{=} \Gamma + \Gamma\Lambda_1\Gamma + \Lambda^{(1)} = \begin{pmatrix} 0 & 1 & 1 & 1 \\ 1 & 0 & 1 & 1 \\ 1 & 1 & 0 & 1 \\ 1 & 1 & 1 & 0 \end{pmatrix}, \tag{A32}$$

where,

$$\Lambda_1 \overset{\text{def}}{=} \begin{pmatrix} 1 & 0 & 0 & 0 \\ 0 & 0 & 0 & 0 \\ 0 & 0 & 0 & 0 \\ 0 & 0 & 0 & 0 \end{pmatrix} \text{ and, } \Lambda^{(1)} \overset{\text{def}}{=} \begin{pmatrix} 0 & 0 & 0 & 0 \\ 0 & 1 & 0 & 0 \\ 0 & 0 & 1 & 0 \\ 0 & 0 & 0 & 1 \end{pmatrix}. \tag{A33}$$

We also point out that following the VdN-work, it turns out that the 8×8 local unitary Clifford transformation Q that links the eight-dimensional binary vector representation of the operators in $\mathcal{S}'_{\mathrm{CWS}}$ and $\left[\mathcal{S}'_{\mathrm{CWS}}\right]_{\text{new}}$ (associated with the graph with adjacency matrix Γ' in Eq. (A32)) with,

$$\mathcal{S}'_{\mathrm{CWS}} \to \left[\mathcal{S}'_{\mathrm{CWS}}\right]_{\text{new}} \overset{\text{def}}{=} \left\langle X^1 Z^2 Z^3 Z^4,\, Z^1 X^2 Z^3 Z^4,\, Z^1 Z^2 X^3 Z^4,\, Z^1 Z^2 Z^3 X^4 \right\rangle, \tag{A34}$$

reads,

$$Q \overset{\text{def}}{=} \begin{pmatrix} 1 & 0 & 0 & 0 & 0 & 0 & 0 & 0 \\ 0 & 1 & 0 & 0 & 0 & 1 & 0 & 0 \\ 0 & 0 & 1 & 0 & 0 & 0 & 1 & 0 \\ 0 & 0 & 0 & 1 & 0 & 0 & 0 & 1 \\ 1 & 0 & 0 & 0 & 1 & 0 & 0 & 0 \\ 0 & 0 & 0 & 0 & 0 & 1 & 0 & 0 \\ 0 & 0 & 0 & 0 & 0 & 0 & 1 & 0 \\ 0 & 0 & 0 & 0 & 0 & 0 & 0 & 1 \end{pmatrix}. \tag{A35}$$
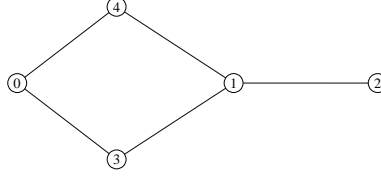
FIG. 2: Graph for a quantum code that is locally Clifford equivalent to the Leung et al. [[4,1]]-code.

To verify that Q is indeed a local Clifford operation, we observe that it exhibits the required block-diagonal structure and satisfies the relation $Q^{\mathrm{T}} P Q = P$ with

$$P \stackrel{\text{def}}{=} \begin{pmatrix} 0 & I_{4\times4} \\ I_{4\times4} & 0 \end{pmatrix}. \tag{A36}$$

Finally, it is fairly simple to use the graphical quantum error correction conditions presented in the SW-work and verify that the $[[4,1]]$ code with associated coincidence matrix in Eq. (A31) is a 1-error detecting quantum code.

3. The $[[5,1,3]]$ stabilizer code

The codespace of the perfect five-qubit stabilizer code is spanned by the following codewords [50, 51],

$$|0_L\rangle \stackrel{\text{def}}{=} \frac{1}{4} \left[\begin{array}{l} |00000\rangle + |11000\rangle + |01100\rangle + |00110\rangle + |00011\rangle + |10001\rangle - |01010\rangle - |00101\rangle + \\ - |10010\rangle - |01001\rangle - |10100\rangle - |11110\rangle - |01111\rangle - |10111\rangle - |11011\rangle - |11101\rangle \end{array} \right], \tag{A37}$$

and,

$$|1_L\rangle \stackrel{\text{def}}{=} \frac{1}{4} \left[\begin{array}{l} |11111\rangle + |00111\rangle + |10011\rangle + |11001\rangle + |11100\rangle + |01110\rangle - |10101\rangle - |11010\rangle + \\ - |01101\rangle - |10110\rangle - |01011\rangle - |00001\rangle - |10000\rangle - |01000\rangle - |00100\rangle - |00010\rangle \end{array} \right]. \tag{A38}$$

Furthermore, the four stabilizer generators of the code are given by,

$$g_1 \stackrel{\text{def}}{=} X^1 Z^2 Z^3 X^4, \; g_2 \stackrel{\text{def}}{=} X^2 Z^3 Z^4 X^5, \; g_3 \stackrel{\text{def}}{=} X^1 X^3 Z^4 Z^5 \text{ and, } g_4 \stackrel{\text{def}}{=} Z^1 X^2 X^4 Z^5. \tag{A39}$$

A suitable choice of logical operations reads,

$$\bar{X} \stackrel{\text{def}}{=} X^1 X^2 X^3 X^4 X^5 \text{ and, } \bar{Z} \stackrel{\text{def}}{=} Z^1 Z^2 Z^3 Z^4 Z^5. \tag{A40}$$

We observe that the codespace of the $[[5,1,3]]$ code can be equally well-described by the following set of orthonormal codewords,

$$|0'_L\rangle \stackrel{\text{def}}{=} \frac{|0_L\rangle + |1_L\rangle}{\sqrt{2}} \text{ and, } |1'_L\rangle \stackrel{\text{def}}{=} \frac{|0_L\rangle - |1_L\rangle}{\sqrt{2}}, \tag{A41}$$

with unchanged stabilizer and new logical operations given by,

$$\bar{Z}' = \bar{X} \stackrel{\text{def}}{=} X^1 X^2 X^3 X^4 X^5 \text{ and, } \bar{X}' = \bar{Z} \stackrel{\text{def}}{=} Z^1 Z^2 Z^3 Z^4 Z^5. \tag{A42}$$

The codeword stabilizer $\mathcal{S}_{\text{CWS}}$ of the CWS code that realizes the five-qubit code spanned by the codewords $|0'_L\rangle$ and $|1'_L\rangle$ reads,

$$\mathcal{S}_{\text{CWS}} \stackrel{\text{def}}{=} \langle g_1, g_2, g_3, g_4, \bar{Z}' \rangle = \langle X^1 Z^2 Z^3 X^4, \, X^2 Z^3 Z^4 X^5, \, X^1 X^3 Z^4 Z^5, \, Z^1 X^2 X^4 Z^5, \, X^1 X^2 X^3 X^4 X^5 \rangle. \tag{A43}$$
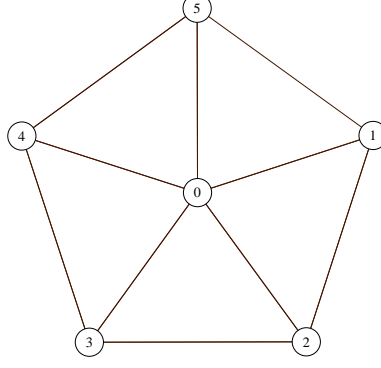
FIG. 3: Graph for a quantum code that is locally Clifford equivalent to the perfect [[5,1,3]]-code.

The codeword stabilizer matrix $\mathcal{H}_{\mathcal{S}_{\mathrm{CWS}}}$ associated with $\mathcal{S}_{\mathrm{CWS}}$ is given by,

$$\mathcal{H}_{\mathcal{S}_{\mathrm{CWS}}} \overset{\mathrm{def}}{=} (Z\,|\,X) = \left(\begin{array}{ccccc|ccccc} 0 & 1 & 1 & 0 & 0 & 1 & 0 & 0 & 1 & 0 \\ 0 & 0 & 1 & 1 & 0 & 0 & 1 & 0 & 0 & 1 \\ 0 & 0 & 0 & 1 & 1 & 1 & 0 & 1 & 0 & 0 \\ 1 & 0 & 0 & 0 & 1 & 0 & 1 & 0 & 1 & 0 \\ 0 & 0 & 0 & 0 & 0 & 1 & 1 & 1 & 1 & 1 \end{array} \right). \tag{A44}$$

We observe $\det X \neq 0$. Thus, using the VdN-work, the 5×5 adjacency matrix Γ becomes,

$$\Gamma \overset{\mathrm{def}}{=} Z^{\mathrm{T}} \cdot \left(X^{\mathrm{T}}\right)^{-1} = \left(\begin{array}{ccccc} 0 & 1 & 0 & 0 & 1 \\ 1 & 0 & 1 & 0 & 0 \\ 0 & 1 & 0 & 1 & 0 \\ 0 & 0 & 1 & 0 & 1 \\ 1 & 0 & 0 & 1 & 0 \end{array} \right). \tag{A45}$$

Therefore, applying now the S-work, the 6×6 symmetric coincidence matrix $\Xi_{[[5,1,3]]}$ characterizing the graph with both input and output vertices is given by,

$$\Xi_{[[5,1,3]]} \overset{\mathrm{def}}{=} \left(\begin{array}{cccccc} 0 & 1 & 1 & 1 & 1 & 1 \\ 1 & 0 & 1 & 0 & 0 & 1 \\ 1 & 1 & 0 & 1 & 0 & 0 \\ 1 & 0 & 1 & 0 & 1 & 0 \\ 1 & 0 & 0 & 1 & 0 & 1 \\ 1 & 1 & 0 & 0 & 1 & 0 \end{array} \right). \tag{A46}$$

In order to show that the pentagon graph with five output vertices and one input vertex with coincidence matrix $\Xi_{[[5,1,3]]}$ realizes a 1-error correcting code, it is required to apply the graph-theoretic error detection (correction) conditions of the SW-work to $\binom{5}{2} = 10$ two-error configurations E_k with $k \in \{1,..., 10\}$. These two-error configurations read,

$$E_1 \overset{\mathrm{def}}{=} \{0,\,1,\,2\},\ E_2 \overset{\mathrm{def}}{=} \{0,\,1,\,3\},\ E_3 \overset{\mathrm{def}}{=} \{0,\,1,\,4\},\ E_4 \overset{\mathrm{def}}{=} \{0,\,1,\,5\},\ E_5 \overset{\mathrm{def}}{=} \{0,\,2,\,3\},$$

$$E_6 \overset{\mathrm{def}}{=} \{0,\,2,\,4\},\ E_7 \overset{\mathrm{def}}{=} \{0,\,2,\,5\},\ E_8 \overset{\mathrm{def}}{=} \{0,\,3,\,4\},\ E_9 \overset{\mathrm{def}}{=} \{0,\,3,\,5\},\ E_{10} \overset{\mathrm{def}}{=} \{0,\,4,\,5\}. \tag{A47}$$

For instance, the application of the SW-theorem to the error configuration $E_1 = \{0,\,1,\,2\}$ leads to the following set of relations,

$$d_0 + d_2 = 0,\ d_0 = 0 \text{ and},\ d_0 + d_1 = 0. \tag{A48}$$

Solving this set of equations, we arrive at $d_0 = d_1 = d_2 = 0$. According to the SW-theorem, this implies that the the error configuration $E_1 = \{0, 1, 2\}$ is a detectable error-configuration. In other words, the detectability of E_1 is linked to the non-singularity of the following 3×3 submatrix of the 6×6 coincidence matrix,

$$E_1 \overset{\text{def}}{=} \{0, 1, 2\} \leftrightarrow \begin{cases} d_0 + d_2 = 0 \\ d_0 = 0 \\ d_0 + d_1 = 0 \end{cases} \leftrightarrow \det \begin{pmatrix} 1 & 0 & 1 \\ 1 & 0 & 0 \\ 1 & 1 & 0 \end{pmatrix} \neq 0. \tag{A49}$$

Following this line of reasoning, it turns out that the remaining nine error configurations in Eq. (A47) are detectable as well. The detectability of arbitrary error configurations with two nontrivial error operators leads to the conclusion that the graph realizes a 1-error correcting code.

4. The $[[6, 1, 3]]$ stabilizer codes

Calderbank et *al.* discovered two distinct six-qubit quantum degenerate codes which encode one logical qubit into six physical qubits [20]. The first of these codes was discovered by trivially extending the perfect five-qubit code and the other one through an exhaustive search of the encoding space.

a. Trivial case

The first (trivial) degenerate six-qubit code that we consider can be obtained from the $[[5, 1, 3]]$ code by appending an ancilla qubit to the five-qubit code. Thus, we add a new qubit and a new stabilizer generator which is X for the new qubit [22]. The other four stabilizer generators from the five-qubit code are tensored with the identity on the new qubit to form the generators of the new code. To be explicit, the codespace of this six-qubit code is spanned by the following two orthonormal codewords,

$$|0'_L\rangle \overset{\text{def}}{=} |0_L\rangle \otimes |+\rangle_6 \text{ and, } |1'_L\rangle \overset{\text{def}}{=} |1_L\rangle \otimes |+\rangle_6, \tag{A50}$$

where $|0_L\rangle$ and $|1_L\rangle$ are defined in Eqs. (A37) and (A38), respectively. Following the point of view adopted for the five-qubit code, let us choose a codespace for the six-qubit code spanned by the new orthonormal codewords given by,

$$\left|0''_L\right\rangle \overset{\text{def}}{=} \frac{|0'_L\rangle + |1'_L\rangle}{\sqrt{2}} \text{ and, } \left|1''_L\right\rangle \overset{\text{def}}{=} \frac{|0'_L\rangle - |1'_L\rangle}{\sqrt{2}}. \tag{A51}$$

The five stabilizer generators of the code with codespace spanned by $\left|0''_L\right\rangle$ and $\left|1''_L\right\rangle$ read,

$$g_1 \overset{\text{def}}{=} X^1 Z^2 Z^3 X^4, \; g_2 \overset{\text{def}}{=} X^2 Z^3 Z^4 X^5, \; g_3 \overset{\text{def}}{=} X^1 X^3 Z^4 Z^5, \; g_4 \overset{\text{def}}{=} Z^1 X^2 X^4 Z^5 \text{ and, } g_5 \overset{\text{def}}{=} X^6. \tag{A52}$$

A suitable choice of logical operations on $\left|0''_L\right\rangle$ and $\left|1''_L\right\rangle$ is provided by,

$$\bar{X} \overset{\text{def}}{=} Z^1 Z^2 Z^3 Z^4 Z^5 \text{ and, } \bar{Z} \overset{\text{def}}{=} X^1 X^2 X^3 X^4 X^5. \tag{A53}$$

We remark that $\bar{X}$ and $\bar{Z}$ anticommute, and that each commutes with all the five stabilizer generators in Eq. (A52). The codeword stabilizer $\mathcal{S}_{\text{CWS}}$ of the CWS code that realizes the six-qubit code spanned by the codewords $\left|0''_L\right\rangle$ and $\left|1''_L\right\rangle$ reads,

$$\mathcal{S}_{\text{CWS}} \overset{\text{def}}{=} \langle g_1, g_2, g_3, g_4, g_5, \bar{Z} \rangle = \langle X^1 Z^2 Z^3 X^4, X^2 Z^3 Z^4 X^5, X^1 X^3 Z^4 Z^5, Z^1 X^2 X^4 Z^5, X^6, X^1 X^2 X^3 X^4 X^5 \rangle. \tag{A54}$$

The codeword stabilizer matrix $\mathcal{H}_{\mathcal{S}_{\text{CWS}}}$ associated with $\mathcal{S}_{\text{CWS}}$ is given by,

$$\mathcal{H}_{\mathcal{S}_{\text{CWS}}} \overset{\text{def}}{=} (Z \,|\, X) = \left(\begin{array}{cccccc|cccccc} 0 & 1 & 1 & 0 & 0 & 0 & 1 & 0 & 0 & 1 & 0 & 0 \\ 0 & 0 & 1 & 1 & 0 & 0 & 0 & 1 & 0 & 0 & 1 & 0 \\ 0 & 0 & 0 & 1 & 1 & 0 & 1 & 0 & 1 & 0 & 0 & 0 \\ 1 & 0 & 0 & 0 & 1 & 0 & 0 & 1 & 0 & 1 & 0 & 0 \\ 0 & 0 & 0 & 0 & 0 & 0 & 0 & 0 & 0 & 0 & 0 & 1 \\ 0 & 0 & 0 & 0 & 0 & 0 & 1 & 1 & 1 & 1 & 1 & 0 \end{array} \right). \tag{A55}$$
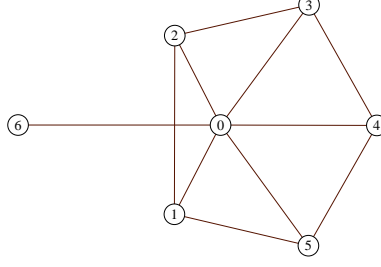
FIG. 4: Graph for a quantum code that is locally Clifford equivalent to the trivial [[6,1,3]]-code.

We observe $\det X \neq 0$. Thus, using the VdN-work, the 6×6 adjacency matrix Γ becomes,

$$\Gamma \overset{\text{def}}{=} Z^{\mathrm{T}} \cdot \left(X^{\mathrm{T}}\right)^{-1} = \begin{pmatrix} 0 & 1 & 0 & 0 & 1 & 0 \\ 1 & 0 & 1 & 0 & 0 & 0 \\ 0 & 1 & 0 & 1 & 0 & 0 \\ 0 & 0 & 1 & 0 & 1 & 0 \\ 1 & 0 & 0 & 1 & 0 & 0 \\ 0 & 0 & 0 & 0 & 0 & 0 \end{pmatrix}. \tag{A56}$$

Therefore, applying now the S-work, the 7×7 symmetric coincidence matrix $\Xi_{[[6,1,3]]}^{\text{trivial}}$ characterizing the graph with both input and output vertices reads,

$$\Xi_{[[6,1,3]]}^{\text{trivial}} \overset{\text{def}}{=} \begin{pmatrix} 0 & 1 & 1 & 1 & 1 & 1 & 1 \\ 1 & 0 & 1 & 0 & 0 & 1 & 0 \\ 1 & 1 & 0 & 1 & 0 & 0 & 0 \\ 1 & 0 & 1 & 0 & 1 & 0 & 0 \\ 1 & 0 & 0 & 1 & 0 & 1 & 0 \\ 1 & 1 & 0 & 0 & 1 & 0 & 0 \\ 1 & 0 & 0 & 0 & 0 & 0 & 0 \end{pmatrix}. \tag{A57}$$

In order to show that the graph with six output vertices and one input vertex with coincidence matrix $\Xi_{[[6,1,3]]}^{\text{trivial}}$ realizes a 1-error correcting degenerate code, we have to apply the graph-theoretic error detection (correction) conditions of the SW-work to $\binom{6}{2} = 15$ error configurations E_k with $k \in \{1,..., 15\}$. It can be verified that any of the ten error configurations $E_k \overset{\text{def}}{=} \{0, e, e'\}$ with e, $e' \neq 6$ satisfy the strong version of the graph-theoretic error detection conditions. In addition, the five two-error configurations E_k with an error $e = 6$ only satisfy the weak form of the graph-theoretic error detection conditions. This fact is consistent with the finding that concerns degenerate codes presented in the SW-work.

b. Nontrivial case

The second example of a six-qubit degenerate code provided by Calderbank et al. is a nontrivial six-qubit code [20], which, according to Calderbank et al., in unique up to equivalence. The example that we consider was indeed introduced by Bilal et al. in [52]. They state that since their example is not reducible to the trivial six-qubit code because every one of its qubits is entangled with the others, their code is equivalent to the (second) nontrivial six-qubit code according to the arguments of Calderbank et al. The codespace of this nontrivial six-qubit code is spanned by the codewords $|0_L\rangle$ and $|1_L\rangle$ defined as [52],

$$|0_L\rangle \overset{\text{def}}{=} \frac{1}{\sqrt{8}} \left[|000000\rangle - |100111\rangle + |001111\rangle - |101000\rangle - |010010\rangle + |110101\rangle + |011101\rangle - |111010\rangle \right], \tag{A58}$$

and,

$$|1_L\rangle \overset{\text{def}}{=} \frac{1}{\sqrt{8}} \left[|001010\rangle + |101101\rangle + |000101\rangle + |1000010\rangle - |011000\rangle - |111111\rangle + |010111\rangle + |110000\rangle \right], \tag{A59}$$

respectively. The five stabilizer generators for this code are given by,

$$g_1 \stackrel{\text{def}}{=} Y^1 Z^3 X^4 X^5 Y^6, \; g_2 \stackrel{\text{def}}{=} Z^1 X^2 X^5 Z^6, \; g_3 \stackrel{\text{def}}{=} Z^2 X^3 X^4 X^5 X^6, \; g_4 \stackrel{\text{def}}{=} Z^4 Z^6, \; g_5 \stackrel{\text{def}}{=} Z^1 Z^2 Z^3 Z^5. \tag{A60}$$

A suitable choice for the logical operations reads,

$$\bar{X} \stackrel{\text{def}}{=} Z^1 X^3 X^5 \text{ and, } \bar{Z} \stackrel{\text{def}}{=} Z^2 Z^5 Z^6. \tag{A61}$$

In what follows, we shall consider the codespace spanned by the orthonormal codewords

$$|0'_L\rangle \stackrel{\text{def}}{=} \frac{|0_L\rangle + |1_L\rangle}{\sqrt{2}} \text{ and, } |1'_L\rangle \stackrel{\text{def}}{=} \frac{|0_L\rangle - |1_L\rangle}{\sqrt{2}}. \tag{A62}$$

This way, the codeword stabilizer $\mathcal{S}_{\text{CWS}}$ of the CWS code that realizes the six-qubit code with a codespace spanned by $|0'_L\rangle$ and $|1'_L\rangle$ is given by,

$$\mathcal{S}_{\text{CWS}} \stackrel{\text{def}}{=} \langle g_1, \, g_2, \, g_3, \, g_4, \, g_5, \, \bar{Z}' \rangle, \tag{A63}$$

with $\bar{Z}' \equiv \bar{X} \stackrel{\text{def}}{=} Z^1 X^3 X^5$. Therefore, $\mathcal{S}_{\text{CWS}}$ becomes,

$$\mathcal{S}_{\text{CWS}} \stackrel{\text{def}}{=} \langle Y^1 Z^3 X^4 X^5 Y^6, \, Z^1 X^2 X^5 Z^6, \, Z^2 X^3 X^4 X^5 X^6, \, Z^4 Z^6, \, Z^1 Z^2 Z^3 Z^5, \, Z^1 X^3 X^5 \rangle. \tag{A64}$$

Observe that $\mathcal{S}_{\text{CWS}}$ is locally Clifford equivalent to $\mathcal{S}'_{\text{CWS}}$ with $\mathcal{S}'_{\text{CWS}} \stackrel{\text{def}}{=} U \mathcal{S}_{\text{CWS}} U^\dagger$ and $U \stackrel{\text{def}}{=} H^1 H^4$. Therefore, we obtain,

$$\mathcal{S}'_{\text{CWS}} = \langle Y^1 Z^3 Z^4 X^5 Y^6, \, X^1 X^2 X^5 Z^6, \, Z^2 X^3 Z^4 X^5 X^6, \, X^4 Z^6, \, X^1 Z^2 Z^3 Z^5, \, X^1 X^3 X^5 \rangle. \tag{A65}$$

The codeword stabilizer matrix $\mathcal{H}_{\mathcal{S}'_{\text{CWS}}}$ associated with $\mathcal{S}'_{\text{CWS}}$ reads,

$$\mathcal{H}_{\mathcal{S}'_{\text{CWS}}} \stackrel{\text{def}}{=} (Z' \, | \, X') = \left(\begin{array}{cccccc|cccccc} 1 & 0 & 1 & 1 & 0 & 1 & 1 & 0 & 0 & 0 & 1 & 1 \\ 0 & 0 & 0 & 0 & 0 & 1 & 1 & 1 & 0 & 0 & 1 & 0 \\ 0 & 1 & 0 & 1 & 0 & 0 & 0 & 0 & 1 & 0 & 1 & 1 \\ 0 & 0 & 0 & 0 & 0 & 1 & 0 & 0 & 0 & 1 & 0 & 0 \\ 0 & 1 & 1 & 0 & 1 & 0 & 1 & 0 & 0 & 0 & 0 & 0 \\ 0 & 0 & 0 & 0 & 0 & 0 & 1 & 0 & 1 & 0 & 1 & 0 \end{array}\right). \tag{A66}$$

We observe that $\det X'^{\text{T}} \neq 0$ and, applying the VdN-work, the symmetric adjacency matrix Γ becomes,

$$\Gamma \stackrel{\text{def}}{=} Z'^{\text{T}} \cdot \left(X'^{\text{T}}\right)^{-1} = \left(\begin{array}{cccccc} 0 & 1 & 1 & 0 & 1 & 0 \\ 1 & 0 & 0 & 0 & 1 & 0 \\ 1 & 0 & 0 & 0 & 1 & 1 \\ 0 & 0 & 0 & 0 & 0 & 1 \\ 1 & 1 & 1 & 0 & 0 & 1 \\ 0 & 0 & 1 & 1 & 1 & 0 \end{array}\right). \tag{A67}$$

Therefore, applying now the S-work, the 7×7 symmetric coincidence matrix $\Xi^{\text{nontrivial}}_{[[6,1,3]]}$ characterizing the graph with both input and output vertices is given by,

$$\Xi^{\text{nontrivial}}_{[[6,1,3]]} \stackrel{\text{def}}{=} \left(\begin{array}{ccccccc} 0 & 1 & 0 & 1 & 0 & 1 & 0 \\ 1 & 0 & 1 & 1 & 0 & 1 & 0 \\ 0 & 1 & 0 & 0 & 0 & 1 & 0 \\ 1 & 1 & 0 & 0 & 0 & 1 & 1 \\ 0 & 0 & 0 & 0 & 0 & 0 & 1 \\ 1 & 1 & 1 & 1 & 0 & 0 & 1 \\ 0 & 0 & 0 & 1 & 1 & 1 & 0 \end{array}\right). \tag{A68}$$

In order to show that the graph with six output vertices and one input vertex with coincidence matrix $\Xi^{\text{nontrivial}}_{[[6,1,3]]}$ realizes a 1-error correcting (degenerate) code, we have to apply the graph-theoretic error detection (correction) conditions of the SW-work to $\binom{6}{2} = 15$ two-error configurations E_k with $k \in \{1,..., 15\}$. It can be checked that the only problematic error configuration is $E_k \stackrel{\text{def}}{=} \{0, e, e'\}$ with $e = 4$, $e' = 6$. The only undetectable nontrivial error is represented by $X^4 Z^6$. However, this error operator belongs to the stabilizer of the code and therefore it will have no impact on the encoded quantum state. Thus, the code considered has indeed distance $d = 3$. Furthermore, since a quantum stabilizer code with distance d is a degenerate code if and only if its stabilizer has an element of weight less than d (excluding the identity element), our code with $d = 3$ and a stabilizer element of weight-2 is indeed a degenerate code.
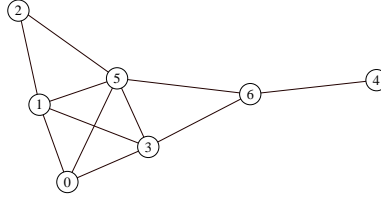
FIG. 5: Graph for a quantum code that is locally Clifford equivalent to the nontrivial [[6,1,3]]-code.

5. The CSS $[[7,1,3]]$ stabilizer code

The codespace of the CSS seven-qubit stabilizer code is spanned by the following codewords [53, 54],

$$|0_L\rangle \stackrel{\text{def}}{=} \frac{1}{\left(\sqrt{2}\right)^3} \left[\begin{array}{l} |0000000\rangle + |0110011\rangle + |1010101\rangle + |1100110\rangle + \\ + |0001111\rangle + |0111100\rangle + |1011010\rangle + |1101001\rangle \end{array} \right], \tag{A69}$$

and,

$$|1_L\rangle \stackrel{\text{def}}{=} \frac{1}{\left(\sqrt{2}\right)^3} \left[\begin{array}{l} |1111111\rangle + |1001100\rangle + |0101010\rangle + |0011001\rangle + \\ + |1110000\rangle + |1000011\rangle + |0100101\rangle + |0010110\rangle \end{array} \right]. \tag{A70}$$

Furthermore, the six stabilizer generators of the code are given by

$$g_1 \stackrel{\text{def}}{=} X^4 X^5 X^6 X^7, \ g_2 \stackrel{\text{def}}{=} X^2 X^3 X^6 X^7, \ g_3 \stackrel{\text{def}}{=} X^1 X^3 X^5 X^7, \ g_4 \stackrel{\text{def}}{=} Z^4 Z^5 Z^6 Z^7, \ g_5 \stackrel{\text{def}}{=} Z^2 Z^3 Z^6 Z^7, \ g_6 \stackrel{\text{def}}{=} Z^1 Z^3 Z^5 Z^7. \tag{A71}$$

A suitable choice of logical operations reads,

$$\bar{X} \stackrel{\text{def}}{=} X^1 X^2 X^3 \text{ and, } \bar{Z} \stackrel{\text{def}}{=} Z^1 Z^2 Z^3. \tag{A72}$$

We observe that the codespace of the CSS code can be equally well-described by the following set of orthonormal codewords,

$$|0'_L\rangle \stackrel{\text{def}}{=} \frac{|0_L\rangle + |1_L\rangle}{\sqrt{2}} \text{ and, } |1'_L\rangle \stackrel{\text{def}}{=} \frac{|0_L\rangle - |1_L\rangle}{\sqrt{2}}, \tag{A73}$$

with unchanged stabilizer and new logical operations given by,

$$\bar{Z}' = \bar{X} \stackrel{\text{def}}{=} X^1 X^2 X^3 \text{ and, } \bar{X}' = \bar{Z} \stackrel{\text{def}}{=} Z^1 Z^2 Z^3. \tag{A74}$$

The codeword stabilizer $\mathcal{S}_{\text{CWS}}$ of the CWS code that realizes the seven-qubit code spanned by the codewords $|0'_L\rangle$ and $|1'_L\rangle$ reads,

$$\mathcal{S}_{\text{CWS}} \stackrel{\text{def}}{=} \left\langle g_1, \, g_2, \, g_3, \, g_4, \, g_5, \, g_6, \, \bar{Z}' \right\rangle, \tag{A75}$$

that is,

$$\mathcal{S}_{\text{CWS}} = \left\langle X^4 X^5 X^6 X^7, \, X^2 X^3 X^6 X^7, \, X^1 X^3 X^5 X^7, \, Z^4 Z^5 Z^6 Z^7, \, Z^2 Z^3 Z^6 Z^7, \, Z^1 Z^3 Z^5 Z^7, \, X^1 X^2 X^3 \right\rangle. \tag{A76}$$

Observe that $\mathcal{S}_{\text{CWS}}$ is local Clifford equivalent to $\mathcal{S}'_{\text{CWS}}$ with $\mathcal{S}'_{\text{CWS}} \stackrel{\text{def}}{=} U \mathcal{S}_{\text{CWS}} U^\dagger$ and $U \stackrel{\text{def}}{=} H^1 H^2 H^4$. Therefore, $\mathcal{S}'_{\text{CWS}}$ is given by,

$$\mathcal{S}'_{\text{CWS}} = \left\langle Z^4 X^5 X^6 X^7, \, Z^2 X^3 X^6 X^7, \, Z^1 X^3 X^5 X^7, \, X^4 Z^5 Z^6 Z^7, \, X^2 Z^3 Z^6 Z^7, \, X^1 Z^3 Z^5 Z^7, \, Z^1 Z^2 X^3 \right\rangle. \tag{A77}$$
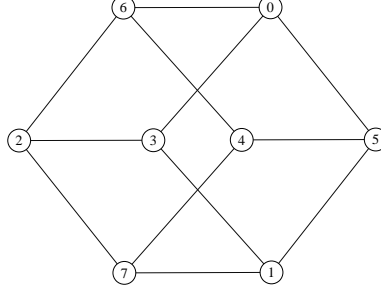
FIG. 6: Graph for a quantum code that is locally Clifford equivalent to the CSS [[7,1,3]]-code.

The codeword stabilizer matrix $\mathcal{H}_{\mathcal{S}'_{\text{CWS}}}$ associated with $\mathcal{S}'_{\text{CWS}}$ reads,

$$\mathcal{H}_{\mathcal{S}'_{\text{CWS}}} \overset{\text{def}}{=} (Z' \,|\, X') = \left(\begin{array}{ccccccc|ccccccc} 0 & 0 & 0 & 1 & 0 & 0 & 0 & 0 & 0 & 0 & 0 & 1 & 1 & 1 \\ 0 & 1 & 0 & 0 & 0 & 0 & 0 & 0 & 0 & 1 & 0 & 0 & 1 & 1 \\ 1 & 0 & 0 & 0 & 0 & 0 & 0 & 0 & 0 & 1 & 0 & 1 & 0 & 1 \\ 0 & 0 & 0 & 0 & 1 & 1 & 1 & 0 & 0 & 0 & 1 & 0 & 0 & 0 \\ 0 & 0 & 1 & 0 & 0 & 1 & 1 & 0 & 1 & 0 & 0 & 0 & 0 & 0 \\ 0 & 0 & 1 & 0 & 1 & 0 & 1 & 1 & 0 & 0 & 0 & 0 & 0 & 0 \\ 1 & 1 & 0 & 0 & 0 & 0 & 0 & 0 & 0 & 1 & 0 & 0 & 0 & 0 \end{array}\right). \tag{A78}$$

We observe $\det X' \neq 0$. Thus, using the VdN-work, the 7×7 adjacency matrix Γ reads,

$$\Gamma \overset{\text{def}}{=} Z'^{\text{T}} \cdot \left(X'^{\text{T}}\right)^{-1} = \left(\begin{array}{ccccccc} 0 & 0 & 1 & 0 & 1 & 0 & 1 \\ 0 & 0 & 1 & 0 & 0 & 1 & 1 \\ 1 & 1 & 0 & 0 & 0 & 0 & 0 \\ 0 & 0 & 0 & 0 & 1 & 1 & 1 \\ 1 & 0 & 0 & 1 & 0 & 0 & 0 \\ 0 & 1 & 0 & 1 & 0 & 0 & 0 \\ 1 & 1 & 0 & 1 & 0 & 0 & 0 \end{array}\right). \tag{A79}$$

Therefore, applying now the S-work, the 8×8 symmetric coincidence matrix $\Xi_{\text{CSS-}[[7,13]]}$ characterizing the graph with both input and output vertices becomes,

$$\Xi_{\text{CSS-}[[7,13]]} \overset{\text{def}}{=} \left(\begin{array}{cccccccc} 0 & 0 & 0 & 1 & 0 & 1 & 1 & 0 \\ 0 & 0 & 0 & 1 & 0 & 1 & 0 & 1 \\ 0 & 0 & 0 & 1 & 0 & 0 & 1 & 1 \\ 1 & 1 & 1 & 0 & 0 & 0 & 0 & 0 \\ 0 & 0 & 0 & 0 & 0 & 1 & 1 & 1 \\ 1 & 1 & 0 & 0 & 1 & 0 & 0 & 0 \\ 1 & 0 & 1 & 0 & 1 & 0 & 0 & 0 \\ 0 & 1 & 1 & 0 & 1 & 0 & 0 & 0 \end{array}\right). \tag{A80}$$

It is straightforward to show that the cube graph with seven output vertices and one input vertex with coincidence matrix $\Xi_{\text{CSS-}[[7,13]]}$ realizes a 1-error correcting code. Namely, all the $\binom{7}{2} = 21$ two-error configurations E_k with $k \in \{1, ..., 21\}$,

$$E_1 \overset{\text{def}}{=} \{0, 1, 2\},\, E_2 \overset{\text{def}}{=} \{0, 1, 3\},\, E_3 \overset{\text{def}}{=} \{0, 1, 4\},\, E_4 \overset{\text{def}}{=} \{0, 1, 5\},\, E_5 \overset{\text{def}}{=} \{0, 1, 6\},\, E_6 \overset{\text{def}}{=} \{0, 1, 7\},$$

$$E_7 \overset{\text{def}}{=} \{0, 2, 3\},\, E_8 \overset{\text{def}}{=} \{0, 2, 4\},\, E_9 \overset{\text{def}}{=} \{0, 2, 5\},\, E_{10} \overset{\text{def}}{=} \{0, 2, 6\},\, E_{11} \overset{\text{def}}{=} \{0, 2, 7\},\, E_{12} \overset{\text{def}}{=} \{0, 3, 4\},$$

$$E_{13} \overset{\text{def}}{=} \{0, 3, 5\},\, E_{14} \overset{\text{def}}{=} \{0, 3, 6\},\, E_{15} \overset{\text{def}}{=} \{0, 3, 7\},\, E_{16} \overset{\text{def}}{=} \{0, 4, 5\},\, E_{17} \overset{\text{def}}{=} \{0, 4, 6\},$$

$$E_{18} \overset{\text{def}}{=} \{0, 4, 7\},\, E_{19} \overset{\text{def}}{=} \{0, 5, 6\},\, E_{20} \overset{\text{def}}{=} \{0, 5, 7\},\, E_{21} \overset{\text{def}}{=} \{0, 6, 7\}, \tag{A81}$$

satisfy the strong version of the graph-theoretic error detection (correction) conditions of the SW-work in agreement with the fact that the code is nondegenerate.

6. The Shor $[[9, 1, 3]]$ stabilizer code

a. First case

When realized as a CWS quantum code, the Shor nine-qubit code [55] is characterized by the codeword stabilizer $\mathcal{S}_{\mathrm{CWS}}$ given by,

$$\mathcal{S}_{\mathrm{CWS}} \overset{\mathrm{def}}{=} \left\langle g_1, g_2, g_3, g_4, g_5, g_6, g_7, g_8, \bar{Z} \right\rangle, \tag{A82}$$

with codeword stabilizer generators given by,

$$g_1 \overset{\mathrm{def}}{=} Z^1 Z^2,\; g_2 \overset{\mathrm{def}}{=} Z^1 Z^3,\; g_3 \overset{\mathrm{def}}{=} Z^4 Z^5,\; g_4 \overset{\mathrm{def}}{=} Z^4 Z^6,\; g_5 \overset{\mathrm{def}}{=} Z^7 Z^8,\; g_6 \overset{\mathrm{def}}{=} Z^7 Z^9,$$

$$g_7 \overset{\mathrm{def}}{=} X^1 X^2 X^3 X^4 X^5 X^6,\; g_8 \overset{\mathrm{def}}{=} X^1 X^2 X^3 X^7 X^8 X^9,\; \bar{Z} \overset{\mathrm{def}}{=} X^1 X^2 X^3 X^4 X^5 X^6 X^7 X^8 X^9. \tag{A83}$$

What is the graph that realizes the Shor code? The codeword stabilizer matrix $\mathcal{H}_{\mathcal{S}_{\mathrm{CWS}}}$ corresponding to $\mathcal{S}_{\mathrm{CWS}}$ in Eq. (A82) can be formally written as,

$$\mathcal{H}_{\mathcal{S}_{\mathrm{CWS}}} \overset{\mathrm{def}}{=} (Z \,|\, X) = \left(\begin{array}{ccccccccc|ccccccccc} 1 & 1 & 0 & 0 & 0 & 0 & 0 & 0 & 0 & 0 & 0 & 0 & 0 & 0 & 0 & 0 & 0 & 0 \\ 1 & 0 & 1 & 0 & 0 & 0 & 0 & 0 & 0 & 0 & 0 & 0 & 0 & 0 & 0 & 0 & 0 & 0 \\ 0 & 0 & 0 & 1 & 1 & 0 & 0 & 0 & 0 & 0 & 0 & 0 & 0 & 0 & 0 & 0 & 0 & 0 \\ 0 & 0 & 0 & 1 & 0 & 1 & 0 & 0 & 0 & 0 & 0 & 0 & 0 & 0 & 0 & 0 & 0 & 0 \\ 0 & 0 & 0 & 0 & 0 & 0 & 1 & 1 & 0 & 0 & 0 & 0 & 0 & 0 & 0 & 0 & 0 & 0 \\ 0 & 0 & 0 & 0 & 0 & 0 & 1 & 0 & 1 & 0 & 0 & 0 & 0 & 0 & 0 & 0 & 0 & 0 \\ 0 & 0 & 0 & 0 & 0 & 0 & 0 & 0 & 0 & 1 & 1 & 1 & 1 & 1 & 1 & 0 & 0 & 0 \\ 0 & 0 & 0 & 0 & 0 & 0 & 0 & 0 & 0 & 1 & 1 & 1 & 0 & 0 & 0 & 1 & 1 & 1 \\ 0 & 0 & 0 & 0 & 0 & 0 & 0 & 0 & 0 & 1 & 1 & 1 & 1 & 1 & 1 & 1 & 1 & 1 \end{array} \right). \tag{A84}$$

Since X^{T} is not invertible, the algorithmic procedure introduced in the VdN-work cannot be applied. However, we notice that the codeword stabilizer $\mathcal{S}_{\mathrm{CWS}}$ in Eq. (A82) is locally Clifford equivalent to $\mathcal{S}'_{\mathrm{CWS}}$ defined by,

$$\mathcal{S}'_{\mathrm{CWS}} \overset{\mathrm{def}}{=} U \mathcal{S}_{\mathrm{CWS}} U^\dagger \text{ with, } U \overset{\mathrm{def}}{=} I^1 \otimes H^2 \otimes H^3 \otimes I^4 \otimes H^5 \otimes H^6 \otimes I^7 \otimes H^8 \otimes H^9. \tag{A85}$$

Using Eqs. (A82) and (A85), it follows that

$$\mathcal{S}'_{\mathrm{CWS}} \overset{\mathrm{def}}{=} \left\langle g'_1, g'_2, g'_3, g'_4, g'_5, g'_6, g'_7, g'_8, \bar{Z}' \right\rangle, \tag{A86}$$

with,

$$g'_1 \overset{\mathrm{def}}{=} Z^1 X^2,\; g'_2 \overset{\mathrm{def}}{=} Z^1 X^3,\; g'_3 \overset{\mathrm{def}}{=} Z^4 X^5,\; g'_4 \overset{\mathrm{def}}{=} Z^4 X^6,\; g'_5 \overset{\mathrm{def}}{=} Z^7 X^8,\; g'_6 \overset{\mathrm{def}}{=} Z^7 X^9,$$

$$g'_7 \overset{\mathrm{def}}{=} X^1 Z^2 Z^3 X^4 Z^5 Z^6,\; g'_8 \overset{\mathrm{def}}{=} X^1 Z^2 Z^3 X^7 Z^8 Z^9,\; \bar{Z}' \overset{\mathrm{def}}{=} X^1 Z^2 Z^3 X^4 Z^5 Z^6 X^7 Z^8 Z^9. \tag{A87}$$

We observe that the the codeword stabilizer matrix $\mathcal{H}_{\mathcal{S}'_{\mathrm{CWS}}}$ corresponding to $\mathcal{S}'_{\mathrm{CWS}}$ becomes,

$$\mathcal{H}_{\mathcal{S}'_{\mathrm{CWS}}} \overset{\mathrm{def}}{=} (Z' \,|\, X') = \left(\begin{array}{ccccccccc|ccccccccc} 1 & 0 & 0 & 0 & 0 & 0 & 0 & 0 & 0 & 0 & 1 & 0 & 0 & 0 & 0 & 0 & 0 & 0 \\ 1 & 0 & 0 & 0 & 0 & 0 & 0 & 0 & 0 & 0 & 0 & 1 & 0 & 0 & 0 & 0 & 0 & 0 \\ 0 & 0 & 0 & 1 & 0 & 0 & 0 & 0 & 0 & 0 & 0 & 0 & 0 & 1 & 0 & 0 & 0 & 0 \\ 0 & 0 & 0 & 1 & 0 & 0 & 0 & 0 & 0 & 0 & 0 & 0 & 0 & 0 & 1 & 0 & 0 & 0 \\ 0 & 0 & 0 & 0 & 0 & 0 & 1 & 0 & 0 & 0 & 0 & 0 & 0 & 0 & 0 & 1 & 0 & 0 \\ 0 & 0 & 0 & 0 & 0 & 0 & 1 & 0 & 0 & 0 & 0 & 0 & 0 & 0 & 0 & 0 & 0 & 1 \\ 0 & 1 & 1 & 0 & 1 & 1 & 0 & 0 & 0 & 1 & 0 & 0 & 1 & 0 & 0 & 0 & 0 & 0 \\ 0 & 1 & 1 & 0 & 0 & 0 & 0 & 1 & 1 & 1 & 0 & 0 & 0 & 0 & 0 & 1 & 0 & 0 \\ 0 & 1 & 1 & 0 & 1 & 1 & 0 & 1 & 1 & 1 & 0 & 0 & 1 & 0 & 0 & 1 & 0 & 0 \end{array} \right). \tag{A88}$$

FIG. 7: First example of a graph for a quantum code that is locally Clifford equivalent to the Shor [[9,1,3]]-code.

Omitting further details and applying the VdN-work, the symmetric 9×9 adjacency matrix Γ for the Shor code becomes,

$$\Gamma \overset{\text{def}}{=} Z'^{\text{T}} \cdot \left(X'^{\text{T}}\right)^{-1} = \begin{pmatrix} 0 & 1 & 1 & 0 & 0 & 0 & 0 & 0 & 0 \\ 1 & 0 & 0 & 0 & 0 & 0 & 0 & 0 & 0 \\ 1 & 0 & 0 & 0 & 0 & 0 & 0 & 0 & 0 \\ 0 & 0 & 0 & 0 & 1 & 1 & 0 & 0 & 0 \\ 0 & 0 & 0 & 1 & 0 & 0 & 0 & 0 & 0 \\ 0 & 0 & 0 & 1 & 0 & 0 & 0 & 0 & 0 \\ 0 & 0 & 0 & 0 & 0 & 0 & 0 & 1 & 1 \\ 0 & 0 & 0 & 0 & 0 & 0 & 1 & 0 & 0 \\ 0 & 0 & 0 & 0 & 0 & 0 & 1 & 0 & 0 \end{pmatrix}. \tag{A89}$$

Finally, applying the S-work, the 10×10 symmetric coincidence matrix $\Xi_{[[9,1,3]]}$ characterizing the graph with both input and output vertices reads,

$$\Xi_{[[9,1,3]]} \overset{\text{def}}{=} \begin{pmatrix} 0 & 0 & 1 & 1 & 0 & 1 & 1 & 0 & 1 & 1 \\ 0 & 0 & 1 & 1 & 0 & 0 & 0 & 0 & 0 & 0 \\ 1 & 1 & 0 & 0 & 0 & 0 & 0 & 0 & 0 & 0 \\ 1 & 1 & 0 & 0 & 0 & 0 & 0 & 0 & 0 & 0 \\ 0 & 0 & 0 & 0 & 0 & 1 & 1 & 0 & 0 & 0 \\ 1 & 0 & 0 & 0 & 1 & 0 & 0 & 0 & 0 & 0 \\ 1 & 0 & 0 & 0 & 1 & 0 & 0 & 0 & 0 & 0 \\ 0 & 0 & 0 & 0 & 0 & 0 & 0 & 0 & 1 & 1 \\ 1 & 0 & 0 & 0 & 0 & 0 & 0 & 1 & 0 & 0 \\ 1 & 0 & 0 & 0 & 0 & 0 & 0 & 1 & 0 & 0 \end{pmatrix}. \tag{A90}$$

In what follows, we shall consider an alternative path leading to a graph for the nine-qubit stabilizer code. Finally, we shall discuss the error-correcting capability of the code in graph-theoretic terms as originally advocated in the SW-work.

b. Second case

Being within the CWS framework, consider a graph with nine vertices characterized by the following canonical codeword stabilizer,

$$\mathcal{S}_{\text{CWS}} \overset{\text{def}}{=} \langle g_1, \, g_2, \, g_3, \, g_4, \, g_5, \, g_6, \, g_7, \, g_8, \, g_9 \rangle, \tag{A91}$$

with,

$$g_1 \stackrel{\text{def}}{=} X^1 Z^2 Z^3 Z^4 Z^5, \ g_2 \stackrel{\text{def}}{=} Z^1 X^2, \ g_3 \stackrel{\text{def}}{=} Z^1 X^3, \ g_4 \stackrel{\text{def}}{=} Z^1 X^4 Z^5 Z^6 Z^7, \ g_5 \stackrel{\text{def}}{=} Z^4 X^5, \ g_6 \stackrel{\text{def}}{=} Z^4 X^6,$$

$$g_7 \stackrel{\text{def}}{=} Z^1 Z^4 X^7 Z^8 Z^9, \ g_8 \stackrel{\text{def}}{=} Z^7 X^8, \ g_9 \equiv \bar{Z} \stackrel{\text{def}}{=} Z^7 X^9. \tag{A92}$$

The 9×9 adjacency matrix Γ for this graph is given by,

$$\Gamma \stackrel{\text{def}}{=} \begin{pmatrix} 0 & 1 & 1 & 1 & 0 & 0 & 1 & 0 & 0 \\ 1 & 0 & 0 & 0 & 0 & 0 & 0 & 0 & 0 \\ 1 & 0 & 0 & 0 & 0 & 0 & 0 & 0 & 0 \\ 1 & 0 & 0 & 0 & 1 & 1 & 1 & 0 & 0 \\ 0 & 0 & 0 & 1 & 0 & 0 & 0 & 0 & 0 \\ 0 & 0 & 0 & 1 & 0 & 0 & 0 & 0 & 0 \\ 1 & 0 & 0 & 1 & 0 & 0 & 0 & 1 & 1 \\ 0 & 0 & 0 & 0 & 0 & 0 & 1 & 0 & 0 \\ 0 & 0 & 0 & 0 & 0 & 0 & 1 & 0 & 0 \end{pmatrix}. \tag{A93}$$

Applying the S-work, the 10×10 symmetric coincidence matrix $\Xi'_{[[9,1,3]]}$ characterizing the graph with both input and output vertices becomes,

$$\Xi'_{[[9,1,3]]} \stackrel{\text{def}}{=} \begin{pmatrix} 0 & 0 & 1 & 1 & 0 & 1 & 1 & 0 & 1 & 1 \\ 0 & 0 & 1 & 1 & 1 & 0 & 0 & 1 & 0 & 0 \\ 1 & 1 & 0 & 0 & 0 & 0 & 0 & 0 & 0 & 0 \\ 1 & 1 & 0 & 0 & 0 & 0 & 0 & 0 & 0 & 0 \\ 0 & 1 & 0 & 0 & 0 & 1 & 1 & 1 & 0 & 0 \\ 1 & 0 & 0 & 0 & 1 & 0 & 0 & 0 & 0 & 0 \\ 1 & 0 & 0 & 0 & 1 & 0 & 0 & 0 & 0 & 0 \\ 0 & 1 & 0 & 0 & 1 & 0 & 0 & 0 & 1 & 1 \\ 1 & 0 & 0 & 0 & 0 & 0 & 0 & 1 & 0 & 0 \\ 1 & 0 & 0 & 0 & 0 & 0 & 0 & 1 & 0 & 0 \end{pmatrix}. \tag{A94}$$

Does the graph associated with the adjacency matrix in Eq. (A93) realize the Shor nine-qubit code? If we show that $\mathcal{S}_{\text{CWS}}$ in Eq. (A91) is locally Clifford equivalent to a new stabilizer $\mathcal{S}'_{\text{CWS}}$ from which we can construct a graph that realizes the Shor code, then we can reply with an affirmative answer. Observe that $\mathcal{S}_{\text{CWS}}$ in Eq. (A91) is locally Clifford equivalent to $\mathcal{S}'_{\text{CWS}}$ defined as,

$$\mathcal{S}'_{\text{CWS}} \stackrel{\text{def}}{=} U \mathcal{S}_{\text{CWS}} U^\dagger \text{ with, } U \stackrel{\text{def}}{=} P^1 \otimes H^2 \otimes H^3 \otimes P^4 \otimes H^5 \otimes H^6 \otimes P^7 \otimes H^8 \otimes H^9. \tag{A95}$$

Using Eqs. (A91) and (A95), it follows that

$$\mathcal{S}'_{\text{CWS}} \stackrel{\text{def}}{=} \langle g'_1, \, g'_2, \, g'_3, \, g'_4, \, g'_5, \, g'_6, \, g'_7, \, g'_8, \, \bar{Z}' \rangle, \tag{A96}$$

with,

$$g'_1 \stackrel{\text{def}}{=} Z^1 X^2, \ g'_2 \stackrel{\text{def}}{=} Z^1 X^3, \ g'_3 \stackrel{\text{def}}{=} Z^4 X^5, \ g'_4 \stackrel{\text{def}}{=} Z^4 X^6, \ g'_5 \stackrel{\text{def}}{=} Z^7 X^8, \ g'_6 \stackrel{\text{def}}{=} Z^7 X^9,$$

$$g'_7 \stackrel{\text{def}}{=} Y^1 Z^2 Z^3 Y^4 Z^5 Z^6, \ g'_8 \stackrel{\text{def}}{=} Y^1 Z^2 Z^3 Y^7 Z^8 Z^9, \ \bar{Z}' \stackrel{\text{def}}{=} Y^1 Z^2 Z^3 Y^4 Z^5 Z^6 Y^7 Z^8 Z^9. \tag{A97}$$

We observe that the the codeword stabilizer matrix $\mathcal{H}_{\mathcal{S}'_{\text{CWS}}}$ corresponding to $\mathcal{S}'_{\text{CWS}}$ becomes,

$$\mathcal{H}_{\mathcal{S}'_{\text{CWS}}} \stackrel{\text{def}}{=} \left(\begin{array}{ccccccccc|ccccccccc} 1 & 0 & 0 & 0 & 0 & 0 & 0 & 0 & 0 & 0 & 1 & 0 & 0 & 0 & 0 & 0 & 0 & 0 \\ 1 & 0 & 0 & 0 & 0 & 0 & 0 & 0 & 0 & 0 & 0 & 1 & 0 & 0 & 0 & 0 & 0 & 0 \\ 0 & 0 & 0 & 1 & 0 & 0 & 0 & 0 & 0 & 0 & 0 & 0 & 0 & 1 & 0 & 0 & 0 & 0 \\ 0 & 0 & 0 & 1 & 0 & 0 & 0 & 0 & 0 & 0 & 0 & 0 & 0 & 0 & 1 & 0 & 0 & 0 \\ 0 & 0 & 0 & 0 & 0 & 0 & 1 & 0 & 0 & 0 & 0 & 0 & 0 & 0 & 0 & 1 & 0 & 0 \\ 0 & 0 & 0 & 0 & 0 & 0 & 1 & 0 & 0 & 0 & 0 & 0 & 0 & 0 & 0 & 0 & 0 & 1 \\ 1 & 1 & 1 & 1 & 1 & 1 & 0 & 0 & 0 & 1 & 0 & 0 & 1 & 0 & 0 & 0 & 0 & 0 \\ 1 & 1 & 1 & 0 & 0 & 0 & 1 & 1 & 1 & 1 & 0 & 0 & 0 & 0 & 0 & 1 & 0 & 0 \\ 1 & 1 & 1 & 1 & 1 & 1 & 1 & 1 & 1 & 1 & 0 & 0 & 1 & 0 & 0 & 1 & 0 & 0 \end{array} \right). \tag{A98}$$
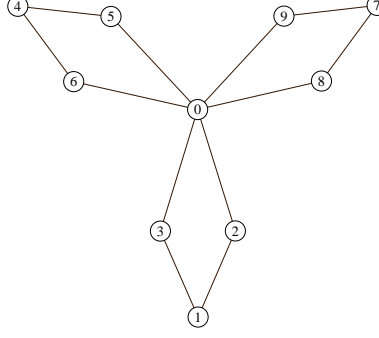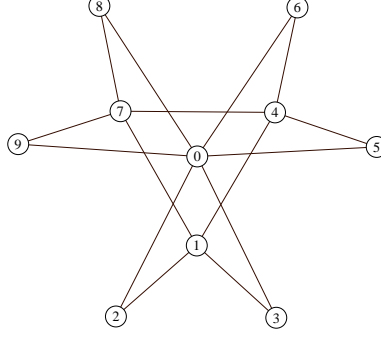
FIG. 8: Second example of a graph for a quantum code that is locally Clifford equivalent to the Shor [[9,1,3]]-code.

Omitting further details and applying the VdN-work, the 9×9 symmetric adjacency matrix Γ associated with the new graph reads,

$$
\Gamma \overset{\text{def}}{=}
\begin{pmatrix}
0 & 1 & 1 & 0 & 0 & 0 & 0 & 0 & 0 \\
1 & 0 & 0 & 0 & 0 & 0 & 0 & 0 & 0 \\
1 & 0 & 0 & 0 & 0 & 0 & 0 & 0 & 0 \\
0 & 0 & 0 & 0 & 1 & 1 & 0 & 0 & 0 \\
0 & 0 & 0 & 1 & 0 & 0 & 0 & 0 & 0 \\
0 & 0 & 0 & 1 & 0 & 0 & 0 & 0 & 0 \\
0 & 0 & 0 & 0 & 0 & 0 & 0 & 1 & 1 \\
0 & 0 & 0 & 0 & 0 & 0 & 1 & 0 & 0 \\
0 & 0 & 0 & 0 & 0 & 0 & 1 & 0 & 0
\end{pmatrix}.
\tag{A99}
$$

Since the adjacency matrices in Eqs. (A89) and (A99) represent essentially the same graphs, we conclude that the graph with canonical stabilizer (A91) realizes the Shor code as well. In addition, we point out that among all the possible 36 two-element error configurations, 27 configurations satisfy the strong error correction condition, 3 satisfy the weak error correction condition and 6 do not satisfy neither of them but they are harmless as we shall show. The strongly correctable 27 configurations are given by,

$$
\{0, 1, 4\}, \ \{0, 1, 5\}, \ \{0, 1, 6\}, \ \{0, 1, 7\}, \ \{0, 1, 8\}, \ \{0, 1, 9\}, \ \{0, 2, 4\}, \ \{0, 2, 5\}, \ \{0, 2, 6\}, \ \{0, 2, 7\},
$$

$$
\{0, 2, 8\}, \ \{0, 2, 9\}, \ \{0, 3, 4\}, \ \{0, 3, 5\}, \ \{0, 3, 6\}, \ \{0, 3, 7\}, \ \{0, 3, 8\}, \ \{0, 3, 9\}, \ \{0, 4, 7\}, \ \{0, 4, 8\},
$$

$$
\{0, 4, 9\}, \ \{0, 5, 7\}, \ \{0, 5, 8\}, \ \{0, 5, 9\}, \ \{0, 6, 7\}, \ \{0, 6, 8\}, \ \{0, 6, 9\},
\tag{A100}
$$

while the weakly correctable 3 configurations read,

$$
\{0, 2, 3\}, \ \{0, 5, 6\}, \ \{0, 8, 9\}.
\tag{A101}
$$

Finally, the potentially dangerous 6 error configurations are,

$$
\{0, 1, 2\}, \ \{0, 1, 3\}, \ \{0, 4, 5\}, \ \{0, 4, 6\}, \ \{0, 7, 8\}, \ \{0, 7, 9\}.
\tag{A102}
$$

Each of the 6 two-error configurations in Eq. (A102) generates 9 weight-2 error operators for a total of 54 errors. It turns out that in each set of errors of cardinality 9, there is 1 weight-2 nondetectable nontrivial error. However, this single error operator belongs to the stabilizer $\mathcal{S}_{\text{stabilizer}}$ of the code and therefore it will have no impact on the encoded quantum state. Thus, the code considered has indeed distance $d = 3$. To be explicit, consider the set $\{0, 1, 2\}$. This sets generates the following 9 weight-2 error operators,

$$
X^1 X^2, \ X^1 Y^2, \ X^1 Z^2, \ Y^1 X^2, \ Y^1 Y^2, \ Y^1 Z^2, \ Z^1 X^2, \ Z^1 Y^2, \ Z^1 Z^2.
\tag{A103}
$$

The only nontrivial error with vanishing error syndrome is $Z^1 Z^2$ which, however, belongs to the stabilizer.

7. The $[[11, 1, 5]]$ stabilizer code

The smallest possible code protecting against two arbitrary errors maps one logical qubit into eleven physical qubits. The existence of such a code was proven in [20] while its stabilizer structure was constructed in [22]. When realized as a CWS code, the eleven-qubit quantum stabilizer code is characterized by the codeword stabilizer,

$$\mathcal{S}_{\mathrm{CWS}} \stackrel{\mathrm{def}}{=} \langle g_1, g_2, g_3, g_4, g_5, g_6, g_7, g_8, g_9, g_{10}, \bar{Z} \rangle, \tag{A104}$$

with [22],

$$g_1 \stackrel{\mathrm{def}}{=} Z^1 Z^2 Z^3 Z^4 Z^5 Z^6, \; g_2 \stackrel{\mathrm{def}}{=} X^1 X^2 X^3 X^4 X^5 X^6, \; g_3 \stackrel{\mathrm{def}}{=} Z^4 X^5 Y^6 Y^7 Y^8 Y^9 X^{10} Z^{11}, \; g_4 \stackrel{\mathrm{def}}{=} X^4 Y^5 Z^6 Z^7 Z^8 Z^9 Y^{10} X^{11},$$

$$g_5 \stackrel{\mathrm{def}}{=} Z^1 Y^2 X^3 Z^7 Y^8 X^9, \; g_6 \stackrel{\mathrm{def}}{=} X^1 Z^2 Y^3 X^7 Z^8 Y^9, \; g_7 \stackrel{\mathrm{def}}{=} Z^4 Y^5 X^6 X^7 Y^8 Z^9, \; g_8 \stackrel{\mathrm{def}}{=} X^4 Z^5 Y^6 Z^7 X^8 Y^9,$$

$$g_9 \stackrel{\mathrm{def}}{=} Z^1 X^2 Y^3 Z^7 Z^8 Z^9 X^{10} Y^{11}, \; g_{10} \stackrel{\mathrm{def}}{=} Y^1 Z^2 X^3 Y^7 Y^8 Y^9 Z^{10} X^{11}, \; \bar{Z} \stackrel{\mathrm{def}}{=} Z^7 Z^8 Z^9 Z^{10} Z^{11}. \tag{A105}$$

What is the graph that realizes such eleven-qubit code? The codeword stabilizer matrix $\mathcal{H}_{\mathcal{S}_{\mathrm{CWS}}}$ corresponding to $\mathcal{S}_{\mathrm{CWS}}$ in Eq. (A104) can be formally written as,

$$\mathcal{H}_{\mathcal{S}_{\mathrm{CWS}}} \stackrel{\mathrm{def}}{=} (Z \,|\, X) = \left(\begin{array}{ccccccccccc|ccccccccccc}
1 & 1 & 1 & 1 & 1 & 1 & 0 & 0 & 0 & 0 & 0 & 0 & 0 & 0 & 0 & 0 & 0 & 0 & 0 & 0 & 0 & 0 \\
0 & 0 & 0 & 0 & 0 & 0 & 0 & 0 & 0 & 0 & 0 & 1 & 1 & 1 & 1 & 1 & 1 & 0 & 0 & 0 & 0 & 0 \\
0 & 0 & 0 & 1 & 0 & 1 & 1 & 1 & 1 & 0 & 1 & 0 & 0 & 0 & 0 & 1 & 1 & 1 & 1 & 1 & 1 & 0 \\
0 & 0 & 0 & 0 & 1 & 1 & 1 & 1 & 1 & 1 & 0 & 0 & 0 & 0 & 1 & 1 & 0 & 0 & 0 & 0 & 1 & 1 \\
1 & 1 & 0 & 0 & 0 & 0 & 1 & 1 & 0 & 0 & 0 & 0 & 1 & 1 & 0 & 0 & 0 & 0 & 1 & 1 & 0 & 0 \\
0 & 1 & 1 & 0 & 0 & 0 & 0 & 1 & 1 & 0 & 0 & 1 & 0 & 1 & 0 & 0 & 0 & 1 & 0 & 1 & 0 & 0 \\
0 & 0 & 0 & 1 & 1 & 0 & 0 & 1 & 1 & 0 & 0 & 0 & 0 & 0 & 0 & 1 & 1 & 1 & 1 & 0 & 0 & 0 \\
0 & 0 & 0 & 0 & 1 & 1 & 1 & 0 & 1 & 0 & 0 & 0 & 0 & 0 & 1 & 0 & 1 & 0 & 1 & 1 & 0 & 0 \\
1 & 0 & 1 & 0 & 0 & 0 & 1 & 1 & 1 & 0 & 1 & 0 & 1 & 1 & 0 & 0 & 0 & 0 & 0 & 0 & 1 & 1 \\
1 & 1 & 0 & 0 & 0 & 0 & 1 & 1 & 1 & 1 & 0 & 1 & 0 & 1 & 0 & 0 & 0 & 1 & 1 & 1 & 0 & 1 \\
0 & 0 & 0 & 0 & 0 & 0 & 1 & 1 & 1 & 1 & 1 & 0 & 0 & 0 & 0 & 0 & 0 & 0 & 0 & 0 & 0 & 0
\end{array} \right). \tag{A106}$$

Since X^{T} is not invertible, the algorithmic procedure introduced in the VdN-work cannot be applied. However, we notice that the stabilizer $\mathcal{S}_{\mathrm{CWS}}$ in Eq. (A104) is locally Clifford equivalent to $\mathcal{S}'_{\mathrm{CWS}}$ defined by,

$$\mathcal{S}'_{\mathrm{CWS}} \stackrel{\mathrm{def}}{=} U \mathcal{S}_{\mathrm{CWS}} U^\dagger, \tag{A107}$$

where the unitary operator U is defined as,

$$U \stackrel{\mathrm{def}}{=} \left(H^1 P^1 H^1 \right) \otimes H^2 \otimes H^3 \otimes H^4 \otimes H^5 \otimes H^6 \otimes H^7 \otimes H^8 \otimes H^9 \otimes H^{10} \otimes \left(H^{11} P^{11} H^{11} \right). \tag{A108}$$

The operator U can be regarded as the composition of three unitary operators $U \stackrel{\mathrm{def}}{=} U_3 \circ U_2 \circ U_1$ with,

$$U_1 \stackrel{\mathrm{def}}{=} H^1 \otimes I^2 \otimes I^3 \otimes I^4 \otimes I^5 \otimes I^6 \otimes I^7 \otimes I^8 \otimes I^9 \otimes I^{10} \otimes H^{11},$$

$$U_2 \stackrel{\mathrm{def}}{=} P^1 \otimes I^2 \otimes I^3 \otimes I^4 \otimes I^5 \otimes I^6 \otimes I^7 \otimes I^8 \otimes I^9 \otimes I^{10} \otimes P^{11},$$

$$U_3 \stackrel{\mathrm{def}}{=} H^1 \otimes H^2 \otimes H^3 \otimes H^4 \otimes H^5 \otimes H^6 \otimes H^7 \otimes H^8 \otimes H^9 \otimes H^{10} \otimes H^{11}. \tag{A109}$$

Using Eqs. (A104) and (A108), it follows that

$$\mathcal{S}'_{\mathrm{CWS}} \stackrel{\mathrm{def}}{=} \langle g'_1, g'_2, g'_3, g'_4, g'_5, g'_6, g'_7, g'_8, g'_9, g'_{10}, \bar{Z}' \rangle, \tag{A110}$$
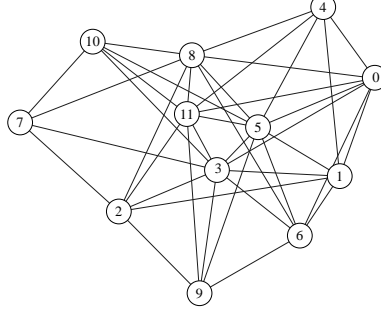
FIG. 9: Graph for a quantum code that is locally Clifford equivalent to the Gottesman [[11,1,5]]-code.

with,

$$g_1' \stackrel{\text{def}}{=} Y^1 X^2 X^3 X^4 X^5 X^6, \ g_2' \stackrel{\text{def}}{=} X^1 Z^2 Z^3 Z^4 Z^5 Z^6, \ g_3' \stackrel{\text{def}}{=} X^4 Z^5 Y^6 Y^7 Y^8 Y^9 Z^{10} Y^{11}, \ g_4' \stackrel{\text{def}}{=} Z^4 Y^5 X^6 X^7 X^8 X^9 Y^{10} X^{11},$$

$$g_5' \stackrel{\text{def}}{=} Y^1 Y^2 Z^3 X^7 Y^8 Z^9, \ g_6' \stackrel{\text{def}}{=} X^1 X^2 Y^3 Z^7 X^8 Y^9, \ g_7' \stackrel{\text{def}}{=} X^4 Y^5 Z^6 Z^7 Y^8 X^9, \ g_8' \stackrel{\text{def}}{=} Z^4 X^5 Y^6 X^7 Z^8 Y^9,$$

$$g_9' \stackrel{\text{def}}{=} Y^1 Z^2 Y^3 X^7 X^8 X^9 Z^{10} Z^{11}, \ g_{10}' \stackrel{\text{def}}{=} Z^1 X^2 Z^3 Y^7 Y^8 Y^9 X^{10} X^{11}, \ \bar{Z}' \stackrel{\text{def}}{=} X^7 X^8 X^9 X^{10} Y^{11}. \tag{A111}$$

We observe that the codeword stabilizer matrix $\mathcal{H}_{\mathcal{S}'_{\text{CWS}}}$ corresponding to $\mathcal{S}'_{\text{CWS}}$ becomes,

$$\mathcal{H}_{\mathcal{S}'_{\text{CWS}}} \stackrel{\text{def}}{=} (X'|Z') = \left(\begin{array}{ccccccccccc|ccccccccccc}
1 & 0 & 0 & 0 & 0 & 0 & 0 & 0 & 0 & 0 & 0 & 1 & 1 & 1 & 1 & 1 & 1 & 0 & 0 & 0 & 0 & 0 \\
0 & 1 & 1 & 1 & 1 & 1 & 0 & 0 & 0 & 0 & 0 & 1 & 0 & 0 & 0 & 0 & 0 & 0 & 0 & 0 & 0 & 0 \\
0 & 0 & 0 & 0 & 1 & 1 & 1 & 1 & 1 & 1 & 1 & 0 & 0 & 0 & 1 & 0 & 1 & 1 & 1 & 1 & 0 & 1 \\
0 & 0 & 0 & 1 & 1 & 0 & 0 & 0 & 0 & 1 & 0 & 0 & 0 & 0 & 0 & 1 & 1 & 1 & 1 & 1 & 1 & 1 \\
1 & 1 & 1 & 0 & 0 & 0 & 0 & 1 & 1 & 0 & 0 & 1 & 1 & 0 & 0 & 0 & 0 & 1 & 1 & 0 & 0 & 0 \\
0 & 0 & 1 & 0 & 0 & 0 & 1 & 0 & 1 & 0 & 0 & 1 & 1 & 1 & 0 & 0 & 0 & 0 & 1 & 1 & 0 & 0 \\
0 & 0 & 0 & 0 & 1 & 1 & 1 & 1 & 0 & 0 & 0 & 0 & 0 & 0 & 1 & 1 & 0 & 0 & 1 & 1 & 0 & 0 \\
0 & 0 & 0 & 1 & 0 & 1 & 0 & 1 & 1 & 0 & 0 & 0 & 0 & 0 & 0 & 1 & 1 & 1 & 0 & 1 & 0 & 0 \\
1 & 1 & 1 & 0 & 0 & 0 & 0 & 0 & 0 & 1 & 1 & 1 & 0 & 1 & 0 & 0 & 0 & 1 & 1 & 1 & 0 & 0 \\
1 & 0 & 1 & 0 & 0 & 0 & 1 & 1 & 1 & 0 & 0 & 0 & 1 & 0 & 0 & 0 & 0 & 1 & 1 & 1 & 1 & 1 \\
0 & 0 & 0 & 0 & 0 & 0 & 0 & 0 & 0 & 0 & 1 & 0 & 0 & 0 & 0 & 0 & 0 & 1 & 1 & 1 & 1 & 1
\end{array} \right). \tag{A112}$$

Omitting further details and applying the VdN-work, the 11×11 symmetric adjacency matrix Γ for the eleven-qubit code becomes,

$$\Gamma \stackrel{\text{def}}{=} \left(\begin{array}{ccccccccccc}
0 & 1 & 1 & 1 & 1 & 1 & 0 & 0 & 0 & 0 & 0 \\
1 & 0 & 1 & 0 & 0 & 0 & 1 & 1 & 1 & 0 & 1 \\
1 & 1 & 0 & 0 & 1 & 1 & 1 & 0 & 1 & 1 & 1 \\
1 & 0 & 0 & 0 & 1 & 0 & 0 & 1 & 0 & 0 & 1 \\
1 & 0 & 1 & 1 & 0 & 1 & 0 & 1 & 1 & 1 & 1 \\
1 & 0 & 1 & 0 & 1 & 0 & 0 & 1 & 1 & 0 & 0 \\
0 & 1 & 1 & 0 & 0 & 0 & 1 & 0 & 1 & 0 \\
0 & 1 & 0 & 1 & 1 & 1 & 1 & 0 & 0 & 1 & 1 \\
0 & 1 & 1 & 0 & 1 & 1 & 0 & 0 & 0 & 0 & 1 \\
0 & 0 & 1 & 0 & 1 & 0 & 1 & 1 & 0 & 0 & 1 \\
0 & 1 & 1 & 1 & 1 & 0 & 0 & 1 & 1 & 1 & 0
\end{array} \right). \tag{A113}$$

Employing the S-work, the 12×12 symmetric coincidence matrix $\Xi_{[[11,1,5]]}$ can be written as,

$$\Xi_{[[11,1,5]]} \overset{\text{def}}{=} \begin{pmatrix} 0 & a_1 & a_2 & a_3 & a_4 & a_5 & a_6 & a_7 & a_8 & a_9 & a_{10} & a_{11} \\ a_1 & 0 & 1 & 1 & 1 & 1 & 1 & 0 & 0 & 0 & 0 & 0 \\ a_2 & 1 & 0 & 1 & 0 & 0 & 0 & 1 & 1 & 1 & 0 & 1 \\ a_3 & 1 & 1 & 0 & 0 & 1 & 1 & 1 & 0 & 1 & 1 & 1 \\ a_4 & 1 & 0 & 0 & 0 & 1 & 0 & 0 & 1 & 0 & 0 & 1 \\ a_5 & 1 & 0 & 1 & 1 & 0 & 1 & 0 & 1 & 1 & 1 & 1 \\ a_6 & 1 & 0 & 1 & 0 & 1 & 0 & 0 & 1 & 1 & 0 & 0 \\ a_7 & 0 & 1 & 1 & 0 & 0 & 0 & 0 & 1 & 0 & 1 & 0 \\ a_8 & 0 & 1 & 0 & 1 & 1 & 1 & 1 & 0 & 0 & 1 & 1 \\ a_9 & 0 & 1 & 1 & 0 & 1 & 1 & 0 & 0 & 0 & 0 & 1 \\ a_{10} & 0 & 0 & 1 & 0 & 1 & 0 & 1 & 1 & 0 & 0 & 1 \\ a_{11} & 0 & 1 & 1 & 1 & 1 & 0 & 0 & 1 & 1 & 1 & 0 \end{pmatrix}, \tag{A114}$$

where the eleven matrix coefficients a_k with $k \in \{1,..., 11\}$ satisfy the following eleven constraints,

$$a_2 + a_3 + a_4 + a_5 + a_6 = 0,$$
$$a_1 + a_3 + a_7 + a_8 + a_9 + a_{11} = 0,$$
$$a_1 + a_2 + a_5 + a_6 + a_7 + a_9 + a_{10} + a_{11} = 0,$$
$$a_1 + a_5 + a_8 + a_{11} = 0,$$
$$a_1 + a_3 + a_4 + a_6 + a_8 + a_9 + a_{10} + a_{11} = 0,$$
$$a_1 + a_3 + a_5 + a_8 + a_9 = 0,$$
$$a_2 + a_3 + a_8 + a_{10} = 0,$$
$$a_2 + a_4 + a_5 + a_6 + a_7 + a_{10} + a_{11} = 0,$$
$$a_2 + a_3 + a_5 + a_6 + a_{11} = 0,$$
$$a_3 + a_5 + a_7 + a_8 + a_{11} = 0,$$
$$a_2 + a_3 + a_4 + a_5 + a_8 + a_9 + a_{10} = 0. \tag{A115}$$

It turns out that a suitable solution of the system of equations in (A115) reads,

$$\mathbf{a} = (a_1,\, a_2,\, a_3,\, a_4,\, a_5,\, a_6,\, a_7,\, a_8,\, a_9,\, a_{10},\, a_{11}) = (1,\, 0,\, 1,\, 1,\, 1,\, 1,\, 0,\, 1,\, 0,\, 0,\, 1)\,. \tag{A116}$$

Finally, the coincidence matrix $\Xi_{[[11,1,5]]}$ for a graph associated with the eleven-qubit code reads,

$$\Xi_{[[11,1,5]]} \overset{\text{def}}{=} \begin{pmatrix} 0 & 1 & 0 & 1 & 1 & 1 & 1 & 0 & 1 & 0 & 0 & 1 \\ 1 & 0 & 1 & 1 & 1 & 1 & 1 & 1 & 0 & 0 & 0 & 0 \\ 0 & 1 & 0 & 1 & 0 & 0 & 0 & 1 & 1 & 1 & 0 & 1 \\ 1 & 1 & 1 & 0 & 0 & 1 & 1 & 1 & 0 & 1 & 1 & 1 \\ 1 & 1 & 0 & 0 & 0 & 1 & 0 & 0 & 1 & 0 & 0 & 1 \\ 1 & 1 & 0 & 1 & 1 & 0 & 1 & 0 & 1 & 1 & 1 & 1 \\ 1 & 1 & 0 & 1 & 0 & 1 & 0 & 0 & 1 & 1 & 0 & 0 \\ 0 & 0 & 1 & 1 & 0 & 0 & 0 & 0 & 1 & 0 & 1 & 0 \\ 1 & 0 & 1 & 0 & 1 & 1 & 1 & 1 & 0 & 0 & 1 & 1 \\ 0 & 0 & 1 & 1 & 0 & 1 & 1 & 0 & 0 & 0 & 0 & 1 \\ 0 & 0 & 0 & 1 & 0 & 1 & 0 & 1 & 1 & 0 & 0 & 1 \\ 1 & 0 & 1 & 1 & 1 & 1 & 0 & 0 & 1 & 1 & 1 & 0 \end{pmatrix}. \tag{A117}$$

It is straightforward, though tedious, to check that all the $\binom{11}{2} = 330$ four-error configurations satisfy the graph-theoretic error detection conditions in their strong version in agreement with the SW-work for nondegenerate codes. However, we also remark that checking out 330 graphical error detection conditions is always better that checking out 529 Knill-Laflamme error correction conditions,

$$3^0 \binom{11}{0} + 3^1 \binom{11}{1} + 3^2 \binom{11}{2} = 529 > 330. \tag{A118}$$

In the next section, we shall consider few graphical constructions of stabilizer codes characterized by multi-qubit encoding operators.

Appendix B: Multi-qubit encoding

1. The $[[4, 2, 2]]$ stabilizer code

In what follows, we shall consider the graphical construction of two non-equivalent quantum stabilizer codes encoding two logical qubits into four physical qubits.

a. First case

The $[[4, 2, 2]]$ code is the simplest example of a class of $[[n-1, k+1, d-1]]$ codes that are derivable from pure (or, nondegenerate) codes $[[n, k, d]]$ with $n \geq 2$ (for more details, we refer to [20]) and is an explicit example of multi-qubit encoding. It is derivable from the perfect five-qubit code and can detect a single qubit error. The stabilizer generators of the code are defined by [21],

$$g_1 \overset{\text{def}}{=} X^1 Z^2 Z^3 X^4 \text{ and, } g_2 \overset{\text{def}}{=} Y^1 X^2 X^3 Y^4. \tag{B1}$$

Each encoded qubit i with $i \in \{1, 2\}$ has its own of logical operations $\bar{X}_i$ and $\bar{Z}_i$. A convenient choice is,

$$\bar{X}_1 \overset{\text{def}}{=} X^1 Y^3 Y^4, \ \bar{X}_2 \overset{\text{def}}{=} X^1 X^3 Z^4, \ \bar{Z}_1 \overset{\text{def}}{=} Y^1 Z^2 Y^3 \text{ and, } \bar{Z}_2 \overset{\text{def}}{=} X^2 Z^3 Z^4. \tag{B2}$$

The codeword stabilizer $\mathcal{S}_{\text{CWS}}$ associated with the CWS code that realizes this stabilizer code reads,

$$\mathcal{S}_{\text{CWS}} \overset{\text{def}}{=} \langle g_1, g_2, \bar{Z}_1, \bar{Z}_2 \rangle = \langle X^1 Z^2 Z^3 X^4, Y^1 X^2 X^3 Y^4, Y^1 Z^2 Y^3, X^2 Z^3 Z^4 \rangle. \tag{B3}$$

The codeword stabilizer matrix $\mathcal{H}_{\mathcal{S}_{\text{CWS}}}$ associated with $\mathcal{S}_{\text{CWS}}$ reads,

$$\mathcal{H}_{\mathcal{S}_{\text{CWS}}} \overset{\text{def}}{=} (Z \mid X) = \begin{pmatrix} 0 & 1 & 1 & 0 & | & 1 & 0 & 0 & 1 \\ 1 & 0 & 0 & 1 & | & 1 & 1 & 1 & 1 \\ 1 & 1 & 1 & 0 & | & 1 & 0 & 1 & 0 \\ 0 & 0 & 1 & 1 & | & 0 & 1 & 0 & 0 \end{pmatrix}. \tag{B4}$$

We observe $\det X \neq 0$. Thus, using the VdN-work, the 4×4 adjacency matrix Γ becomes,

$$\Gamma \overset{\text{def}}{=} \begin{pmatrix} 0 & 0 & 1 & 0 \\ 0 & 0 & 1 & 1 \\ 1 & 1 & 0 & 0 \\ 0 & 1 & 0 & 0 \end{pmatrix}. \tag{B5}$$

We remark that the graph with symmetric adjacency matrix Γ in Eq. (B5) is in the local unitary equivalence class of the square graph (see Figure 7 in [9]). Therefore, an alternative graph (with only output vertices) for our stabilizer code can be characterized by the alternative 4×4 symmetric adjacency matrix Γ',

$$\Gamma' \overset{\text{def}}{=} \begin{pmatrix} 0 & 1 & 0 & 1 \\ 1 & 0 & 1 & 0 \\ 0 & 1 & 0 & 1 \\ 1 & 0 & 1 & 0 \end{pmatrix}. \tag{B6}$$

Finally, applying the S-work and considering Γ', the 6×6 symmetric coincidence matrix $\Xi^{\text{Beigi}}_{[[4,2,2]]}$ characterizing the graph with both input and output vertices is given by,

$$\Xi^{\text{Beigi}}_{[[4,2,2]]} \overset{\text{def}}{=} \begin{pmatrix} 0 & 0 & 1 & 0 & 0 & 1 \\ 0 & 0 & 0 & 1 & 1 & 0 \\ 1 & 0 & 0 & 1 & 0 & 1 \\ 0 & 1 & 1 & 0 & 1 & 0 \\ 0 & 1 & 0 & 1 & 0 & 1 \\ 1 & 0 & 1 & 0 & 1 & 0 \end{pmatrix}. \tag{B7}$$

Using the SW-work, it is simple to verify that any graphical single-error configuration $\{0, 0', e\}$ with $e \in \{1, 2, 3, 4\}$ is detectable. Thus, the code detects any single-qubit error. As a final remark, we emphasize that the graph associated with $\Xi^{\text{Beigi}}_{[[4,2,2]]}$ is identical to the one appeared in [15].
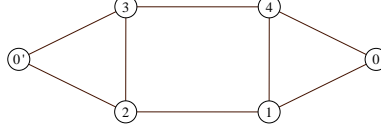
FIG. 10: Graph for a quantum code that is locally Clifford equivalent to the Beigi et al. [[4,2,2]]-code.

b. Second case

Let us consider a different $[[4, 2, 2]]$ stabilizer code with stabilizer generators defined by [21],

$$g_1 \stackrel{\text{def}}{=} X^1 X^2 X^3 X^4 \text{ and, } g_2 \stackrel{\text{def}}{=} Z^1 Z^2 Z^3 Z^4. \tag{B8}$$

Each encoded qubit i with $i \in \{1, 2\}$ has its own of logical operations $\bar{X}_i$ and $\bar{Z}_i$. A convenient choice is,

$$\bar{X}_1 \stackrel{\text{def}}{=} X^1 X^2, \ \bar{X}_2 \stackrel{\text{def}}{=} X^1 X^3, \ \bar{Z}_1 \stackrel{\text{def}}{=} Z^2 Z^4 \text{ and, } \bar{Z}_2 \stackrel{\text{def}}{=} Z^3 Z^4. \tag{B9}$$

The codeword stabilizer $\mathcal{S}_{\text{CWS}}$ associated with the CWS code that realizes this stabilizer code reads,

$$\mathcal{S}_{\text{CWS}} \stackrel{\text{def}}{=} \langle g_1, \, g_2, \, \bar{Z}_1, \, \bar{Z}_2 \, \rangle = \langle X^1 X^2 X^3 X^4, \, Z^1 Z^2 Z^3 Z^4, \, Z^2 Z^4, \, Z^3 Z^4 \, \rangle. \tag{B10}$$

The codeword stabilizer matrix $\mathcal{H}_{\mathcal{S}_{\text{CWS}}}$ associated with $\mathcal{S}_{\text{CWS}}$ reads,

$$\mathcal{H}_{\mathcal{S}_{\text{CWS}}} \stackrel{\text{def}}{=} (Z \, | \, X) = \begin{pmatrix} 0 & 0 & 0 & 0 & | & 1 & 1 & 1 & 1 \\ 1 & 1 & 1 & 1 & | & 0 & 0 & 0 & 0 \\ 0 & 1 & 0 & 1 & | & 0 & 0 & 0 & 0 \\ 0 & 0 & 1 & 1 & | & 0 & 0 & 0 & 0 \end{pmatrix}. \tag{B11}$$

We observe $\det X = 0$ and the VdN-work cannot be applied. However, we also notice that $\mathcal{S}_{\text{CWS}}$ is locally Clifford equivalent to $\mathcal{S}'_{\text{CWS}}$ with $\mathcal{S}'_{\text{CWS}} = U \mathcal{S}_{\text{CWS}} U^\dagger$ and $U \stackrel{\text{def}}{=} H^2 H^3 H^4$. Thus, $\mathcal{S}'_{\text{CWS}}$ becomes,

$$\mathcal{S}'_{\text{CWS}} \stackrel{\text{def}}{=} \langle g'_1, \, g'_2, \, \bar{Z}'_1, \, \bar{Z}'_2 \, \rangle = \langle X^1 Z^2 Z^3 Z^4, \, Z^1 X^2 X^3 X^4, \, X^2 X^4, \, X^3 X^4 \, \rangle. \tag{B12}$$

The codeword stabilizer matrix $\mathcal{H}_{\mathcal{S}'_{\text{CWS}}}$ associated with $\mathcal{S}'_{\text{CWS}}$ is given by,

$$\mathcal{H}_{\mathcal{S}'_{\text{CWS}}} \stackrel{\text{def}}{=} (Z' \, | \, X') = \begin{pmatrix} 0 & 1 & 1 & 1 & | & 1 & 0 & 0 & 0 \\ 1 & 0 & 0 & 0 & | & 0 & 1 & 1 & 1 \\ 0 & 0 & 0 & 0 & | & 0 & 1 & 0 & 1 \\ 0 & 0 & 0 & 0 & | & 0 & 0 & 1 & 1 \end{pmatrix}. \tag{B13}$$

We now have $\det X' \neq 0$. Therefore, using the VdN-work, the 4×4 adjacency matrix Γ becomes,

$$\Gamma \stackrel{\text{def}}{=} \begin{pmatrix} 0 & 1 & 1 & 1 \\ 1 & 0 & 0 & 0 \\ 1 & 0 & 0 & 0 \\ 1 & 0 & 0 & 0 \end{pmatrix}. \tag{B14}$$

Finally, applying the S-work and considering Γ in Eq. (B14), the 6×6 symmetric coincidence matrix $\Xi^{\text{Schlingemann}}_{[[4,2,2]]}$ characterizing the graph with both input and output vertices reads,

$$\Xi^{\text{Schlingemann}}_{[[4,2,2]]} \stackrel{\text{def}}{=} \begin{pmatrix} 0 & 0 & 0 & 1 & 1 & 0 \\ 0 & 0 & 0 & 0 & 1 & 1 \\ 0 & 0 & 0 & 1 & 1 & 1 \\ 1 & 0 & 1 & 0 & 0 & 0 \\ 1 & 1 & 1 & 0 & 0 & 0 \\ 0 & 1 & 1 & 0 & 0 & 0 \end{pmatrix}. \tag{B15}$$
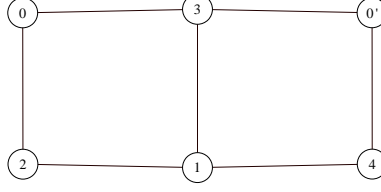
FIG. 11: Graph for a quantum code that is locally Clifford equivalent to the Schlingemann [[4,2,2]]-code.

Applying the SW-work, it is simple to verify that any graphical single-error configuration $\{0, 0', e\}$ with $e \in \{1, 2, 3, 4\}$ is detectable. Therefore, the code detects any single-qubit error. As a final remark, we emphasize that the graph associated with $\Xi^{\text{Schlingemann}}_{[[4,2,2]]}$ is identical to the one appeared in [6].

We stress that the stabilizer generated by the stabilizers in Eq. (B1) for the first code can be obtained from the stabilizer generated by the stabilizers in Eq. (B8) for the second code by applying a local unitary transformation $U \overset{\text{def}}{=} Q^1 H^2 H^3 Q^4$ where $Q \overset{\text{def}}{=} PHP$. However, the codeword stabilizer in Eq. (B3) cannot be obtained from the codeword stabilizer in Eq. (B10) via a local unitary transformation. This feature is consistent with the fact that graphs associated with adjacency matrices in Eqs. (B5) and (B14) are inequivalent. In other words, these two matrices characterize graphs that belong to different orbits [9].

2. The $[[8, 3, 3]]$ stabilizer code

The $[[8, 3, 3]]$ code is a special case of a class of $\left[\left[2^j, 2^j - j - 2, 3\right]\right]$ codes [56]. It encodes three logical qubits into eight physical qubits and corrects all single-qubit errors. The five stabilizer generators are given by [21],

$$g_1 \overset{\text{def}}{=} X^1 X^2 X^3 X^4 X^5 X^6 X^7 X^8, \; g_2 \overset{\text{def}}{=} Z^1 Z^2 Z^3 Z^4 Z^5 Z^6 Z^7 Z^8, \; g_3 \overset{\text{def}}{=} X^2 X^4 Y^5 Z^6 Y^7 Z^8,$$

$$g_4 \overset{\text{def}}{=} X^2 Z^3 Y^4 X^6 Z^7 Y^8, \; g_5 \overset{\text{def}}{=} Y^2 X^3 Z^4 X^5 Z^6 Y^8, \tag{B16}$$

and a suitable choice for the logical operations $\bar{X}_i$ and $\bar{Z}_i$ with $i \in \{1, 2, 3\}$ reads,

$$\bar{X}_1 \overset{\text{def}}{=} X^1 X^2 Z^6 Z^8, \; \bar{X}_2 \overset{\text{def}}{=} X^1 X^3 Z^4 Z^7, \; \bar{X}_3 \overset{\text{def}}{=} X^1 Z^4 X^5 Z^6, \; \bar{Z}_1 \overset{\text{def}}{=} Z^2 Z^4 Z^6 Z^8, \; \bar{Z}_2 \overset{\text{def}}{=} Z^3 Z^4 Z^7 Z^8, \; \bar{Z}_3 \overset{\text{def}}{=} Z^5 Z^6 Z^7 Z^8. \tag{B17}$$

The codeword stabilizer $\mathcal{S}_{\text{CWS}}$ of the CWS code that realizes this stabilizer code is given by,

$$\mathcal{S}_{\text{CWS}} \overset{\text{def}}{=} \langle g_1, g_2, g_3, g_4, g_5, \bar{Z}_1, \bar{Z}_2, \bar{Z}_3 \rangle. \tag{B18}$$

We observe that $\mathcal{S}_{\text{CWS}}$ is locally Clifford equivalent to $\mathcal{S}'_{\text{CWS}} \overset{\text{def}}{=} U \mathcal{S}_{\text{CWS}} U^\dagger$ with $U \overset{\text{def}}{=} H^1 H^2 H^3 H^5$. Therefore, $\mathcal{S}'_{\text{CWS}}$ reads,

$$\mathcal{S}'_{\text{CWS}} \overset{\text{def}}{=} \langle g'_1, g'_2, g'_3, g'_4, g'_5, \bar{Z}'_1, \bar{Z}'_2, \bar{Z}'_3 \rangle, \tag{B19}$$

with,

$$g'_1 \overset{\text{def}}{=} Z^1 Z^2 Z^3 X^4 Z^5 X^6 X^7 X^8, \; g'_2 \overset{\text{def}}{=} X^1 X^2 X^3 Z^4 X^5 Z^6 Z^7 Z^8, \; g'_3 \overset{\text{def}}{=} Z^2 X^4 Y^5 Z^6 Y^7 Z^8,$$

$$g'_4 \overset{\text{def}}{=} Z^2 X^3 Y^4 X^6 Z^7 Y^8, \; g'_5 \overset{\text{def}}{=} Y^2 Z^3 Z^4 Z^5 Z^6 Y^8, \tag{B20}$$

and,

$$\bar{Z}'_1 \overset{\text{def}}{=} X^2 Z^4 Z^6 Z^8, \; \bar{Z}'_2 \overset{\text{def}}{=} X^3 Z^4 Z^7 Z^8, \; \bar{Z}'_3 \overset{\text{def}}{=} X^5 Z^6 Z^7 Z^8. \tag{B21}$$
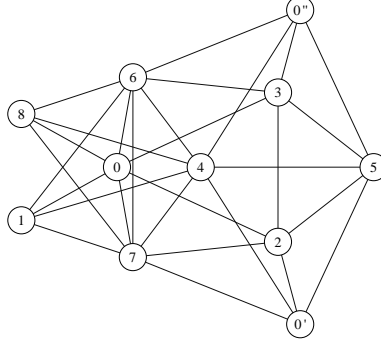
FIG. 12: Graph for a quantum code that is locally Clifford equivalent to the Gottesman [[8,3,3]]-code.

The codeword stabilizer matrix $\mathcal{H}_{\mathcal{S}'_{\mathrm{CWS}}}$ associated with $\mathcal{S}'_{\mathrm{CWS}}$ is given by,

$$
\mathcal{H}_{\mathcal{S}'_{\mathrm{CWS}}} \overset{\mathrm{def}}{=} (Z'|X') = \left(\begin{array}{cccccccc|cccccccc}
1 & 1 & 1 & 0 & 1 & 0 & 0 & 0 & 0 & 0 & 0 & 1 & 0 & 1 & 1 & 1 \\
0 & 0 & 0 & 1 & 0 & 1 & 1 & 1 & 1 & 1 & 1 & 0 & 1 & 0 & 0 & 0 \\
0 & 1 & 0 & 0 & 1 & 1 & 1 & 1 & 0 & 0 & 0 & 1 & 1 & 0 & 1 & 0 \\
0 & 1 & 0 & 1 & 0 & 0 & 1 & 1 & 0 & 0 & 1 & 1 & 0 & 1 & 0 & 1 \\
0 & 1 & 1 & 1 & 1 & 1 & 0 & 1 & 0 & 1 & 0 & 0 & 0 & 0 & 0 & 1 \\
0 & 0 & 0 & 1 & 0 & 1 & 0 & 1 & 0 & 1 & 0 & 0 & 0 & 0 & 0 & 0 \\
0 & 0 & 0 & 1 & 0 & 0 & 1 & 1 & 0 & 0 & 1 & 0 & 0 & 0 & 0 & 0 \\
0 & 0 & 0 & 0 & 0 & 1 & 1 & 1 & 0 & 0 & 0 & 0 & 1 & 0 & 0 & 0
\end{array}\right). \tag{B22}
$$

Since $\det X' \neq 0$, we can use the VdN-work and the 8×8 adjacency matrix Γ becomes,

$$
\Gamma \overset{\mathrm{def}}{=} Z'^{\mathrm{T}} \cdot \left(X'^{\mathrm{T}}\right)^{-1} = \left(\begin{array}{cccccccc}
0 & 0 & 0 & 1 & 0 & 1 & 1 & 0 \\
0 & 0 & 0 & 1 & 0 & 1 & 0 & 1 \\
0 & 0 & 0 & 1 & 0 & 0 & 1 & 1 \\
1 & 1 & 1 & 0 & 0 & 0 & 0 & 0 \\
0 & 0 & 0 & 0 & 0 & 1 & 1 & 1 \\
1 & 1 & 0 & 0 & 1 & 0 & 0 & 0 \\
1 & 0 & 1 & 0 & 1 & 0 & 0 & 0 \\
0 & 1 & 1 & 0 & 1 & 0 & 0 & 0
\end{array}\right). \tag{B23}
$$

We observe that the graph associated with the adjacency matrix Γ (with $\det \Gamma \neq 0$) in Eq. (B23) is the cube. Acting with a local complementation with respect to the vertex 1, Γ becomes Γ' (with $\det \Gamma' = 0$).

$$
\Gamma' \overset{\mathrm{def}}{=} \left(\begin{array}{cccccccc}
0 & 0 & 0 & 1 & 0 & 1 & 1 & 0 \\
0 & 0 & 1 & 0 & 1 & 0 & 1 & 0 \\
0 & 1 & 0 & 0 & 1 & 1 & 0 & 0 \\
1 & 0 & 0 & 0 & 1 & 1 & 1 & 1 \\
0 & 1 & 1 & 1 & 0 & 0 & 0 & 0 \\
1 & 0 & 1 & 1 & 0 & 0 & 1 & 1 \\
1 & 1 & 0 & 1 & 0 & 1 & 0 & 1 \\
0 & 0 & 0 & 1 & 0 & 1 & 1 & 0
\end{array}\right). \tag{B24}
$$

Finally, applying the S-work and considering Γ' in Eq. (B24), the 11×11 symmetric coincidence matrix $\Xi_{[[8,3,3]]}$

associated with the graph with both input and output vertices becomes,

$$\Xi_{[[8,3,3]]} \overset{\text{def}}{=} \begin{pmatrix} 0 & 0 & 0 & 1 & 1 & 1 & 0 & 0 & 1 & 1 & 1 \\ 0 & 0 & 0 & 0 & 1 & 0 & 1 & 1 & 0 & 1 & 0 \\ 0 & 0 & 0 & 0 & 0 & 1 & 1 & 1 & 1 & 0 & 0 \\ 1 & 0 & 0 & 0 & 0 & 0 & 1 & 0 & 1 & 1 & 0 \\ 1 & 1 & 0 & 0 & 0 & 1 & 0 & 1 & 0 & 1 & 0 \\ 1 & 0 & 1 & 0 & 1 & 0 & 0 & 1 & 1 & 0 & 0 \\ 0 & 1 & 1 & 1 & 0 & 0 & 0 & 1 & 1 & 1 & 1 \\ 0 & 1 & 1 & 0 & 1 & 1 & 1 & 0 & 0 & 0 & 0 \\ 1 & 0 & 1 & 1 & 0 & 1 & 1 & 0 & 0 & 1 & 1 \\ 1 & 1 & 0 & 1 & 1 & 0 & 1 & 0 & 1 & 0 & 1 \\ 1 & 0 & 0 & 0 & 0 & 0 & 1 & 0 & 1 & 1 & 0 \end{pmatrix}. \tag{B25}$$

Using the SW-work, it can be finally verified that any of the $\binom{8}{2}$ graphical two-error configuration $\{0, 0', 0'', e_1, e_2\}$ with $e_{1,2} \in \{1,..., 8\}$ is detectable. Thus, the code corrects any single-qubit error.